

THE CHEMISTRY OF CIS AND TRANS-(C₅H₅)W(CO)₂(PPh₃)SR:
DIMERIZATION AND INSERTION REACTIONS OF CS₂ AND SO₂ INTO

THE W-SR BOND

by

Bernadette Soo Lum

A thesis submitted to the
Faculty of Graduate Studies and Research
in partial fulfillment of the requirements for
the degree of Doctor of Philosophy.

Department of Chemistry
McGill University
Montréal, Québec,
Canada

January 1990



National Library
of Canada

Bibliothèque nationale
du Canada

Canadian Theses Service Service des thèses canadiennes

Ottawa, Canada
K1A 0N4

The author has granted an irrevocable non-exclusive licence allowing the National Library of Canada to reproduce, loan, distribute or sell copies of his/her thesis by any means and in any form or format, making this thesis available to interested persons.

The author retains ownership of the copyright in his/her thesis. Neither the thesis nor substantial extracts from it may be printed or otherwise reproduced without his/her permission.

L'auteur a accordé une licence irrévocable et non exclusive permettant à la Bibliothèque nationale du Canada de reproduire, prêter, distribuer ou vendre des copies de sa thèse de quelque manière et sous quelque forme que ce soit pour mettre des exemplaires de cette thèse à la disposition des personnes intéressées.

L'auteur conserve la propriété du droit d'auteur qui protège sa thèse. Ni la thèse ni des extraits substantiels de celle-ci ne doivent être imprimés ou autrement reproduits sans son autorisation.

ISBN 0-315-63678-5

**THE CHEMISTRY OF CIS AND TRANS-(C₅H₅)W(CO)₂(PPh₃)SR:
DIMERIZATION AND INSERTION REACTIONS OF CS₂ AND SO₂
INTO THE W-SR BOND**

Ph.D.

Bernadette Soo Lum

Chemistry

ABSTRACT

Treatment of CpW(CO)₂(PPh₃)H, (Cp = η⁵-cyclopentadienyl) with methyllithium and subsequently with RS-phth (R = CHMe₂, CH₂Ph, 4-C₆H₄Me, Ph and phth; phth = phthalimido), gave CpW(CO)₂(PPh₃)SR as a mixture of cis and trans isomers. Warming cis/trans-CpW(CO)₂(PPh₃)SCHMe₂ in THF gave the tetracarbonyl dimer [CpW(CO)₂(μ-SCHMe₂)]₂ with loss of PPh₃, while further reaction in refluxing THF gave the dicarbonyl dimer [CpW(CO)(μ-SCHMe₂)]₂. X-ray crystal structures were obtained for both dimers. The complexes, CpW(CO)₂(PPh₃)SR for R = CHMe₂, CH₂Ph and 4-C₆H₄Me reacted with CS₂ to give the thioxanthate complexes CpW(CO)₂S₂CSR wherein the CS₂ had inserted into the W-SR bond. The structure of CpW(CO)₂S₂CSCH₂Ph was determined. It was found that the cis isomer reacted more rapidly than the trans isomer and that the reaction was retarded by the presence of free PPh₃ or CO. The implications with respect to the mechanism of CS₂ insertion are discussed. The cis/trans CpW(CO)₂(PPh₃)SR complexes also reacted with SO₂ to form the SO₂ adduct complexes trans-CpW(CO)₂(PPh₃)S(SO₂)R. The reaction was monitored by ¹H NMR spectroscopy and rapid SO₂ exchange was indicated. Addition of free PPh₃ slowed the formation of the SO₂ product.

**LA CHIMIE DES COMPLEXES CIS ET TRANS DE $(C_5H_5)W(CO)_2(PPh_3)SR$:
RÉACTIONS DE DIMÉRISATION ET D'INSERTION DE CS_2 ET DE SO_2
DANS LA LIAISON W-SR**

Ph.D.

Bernadette Soo Lum

Chimie

RÉSUMÉ

Le traitement du complexe $CpW(CO)_2(PPh_3)H$ (où $Cp = \eta^5$ -cyclopentadiényle) avec le méthyllithium et ensuite avec le RS-phth (où $R = CHMe_2, CH_2Ph, Me-4-C_6H_4, Ph$ et phth; phth = phthalimido) a donné le mélange des isomères cis et trans du complexe $CpW(CO)_2(PPh_3)SR$. Le chauffage du mélange cis/trans du complexe $CpW(CO)_2(PPh_3)SCHMe_2$ en solution dans le THF donne le dimère tétracarbonylé $[CpW(CO)_2(\mu-SCHMe_2)]_2$ accompagné d'un dégagement de PPh_3 alors qu'un chauffage prolongé dans le THF à reflux a donné le dimère dicarbonylé $[CpW(CO)(\mu-SCHMe_2)]_2$. Les structures cristallographiques aux rayons-X de ces deux dimères furent déterminées. Les complexes $CpW(CO)_2(PPh_3)SR$, où $R = CHMe_2, CH_2Ph$ et $Me-4-C_6H_4$, ont réagi avec le CS_2 pour donner les complexes thioxanthates $CpW(CO)_2S_2CSR$ où le CS_2 fut inséré dans la liaison W-SR. La structure cristallographique du complexe $CpW(CO)_2S_2CSCH_2Ph$ a été déterminée. Il fut démontré que l'isomère cis réagit plus rapidement que l'isomère trans et que la réaction était ralentie par la présence de PPh_3 ou de CO libres. Les implications relatives au mécanisme de la réaction d'insertion de CS_2 sont discutées. Les complexes cis et trans de $CpW(CO)_2(PPh_3)SR$ ont également réagi avec le SO_2 pour former les produits d'addition trans- $CpW(CO)_2(PPh_3)S(SO_2)R$. Ces réactions furent suivies par spectroscopie RMN- 1H et un échange rapide du SO_2 fut observé. L'ajout de PPh_3 libre ralentit la formation des produits d'addition de SO_2 .

ACKNOWLEDGMENTS

I would like to express my sincere thanks to my supervisor, Dr. Alan Shaver, for his direction and support during this project. His encouragement and extensive knowledge of sulfur chemistry has made the past four years an enjoyable learning experience.

To my fellow inhabitants of Room 435, past and present, I thank them for their friendship and helpful discussions; in particular, Stephen Morris for showing me how to use sulfur compounds properly (i.e. without clearing the building), Pierre-Yves Plouffe for proof-reading the entire manuscript and his constructive suggestions, Jacques Demers for his patience and help in showing me that the computer really is a wonderful invention and François Gauvin for translating the abstract and encouraging me to use what little French I knew. I also wish to express my appreciation to Hae Won Uhm, Steve Barnett and Nancy Kawai for proof-reading some of the chapters.

My thanks to Françoise Sauriol for her help with the low-temperature and phosphorus NMR experiments and to Brian Harkness and François St. Germain for measuring the photoacoustic IR spectra. I thank Spang Microanalytical Laboratories for providing unfailingly accurate determinations of the elemental analyses and for recording the mass spectra, I acknowledge Drs. Mamer, Osei-Twun and Finkenbine. For determining the crystal structures, I acknowledge Dr. Peter Bird and his students at Concordia University, and for showing me how to get those structures into my thesis, I thank Pierre and Dr. Jim Britten.

For financial support I acknowledge the Laboratory for Inorganic Materials at Concordia University.

Finally, I wish to express my deepest gratitude to my parents for their unending moral (and sometimes, financial) support, to my sisters, for all the mail and especially to Brian, for being there.

To my parents

and Brian

TABLE OF CONTENTS

	<u>Page</u>
ABSTRACT	i
RÉSUMÉ	ii
ACKNOWLEDGMENTS	iii
TABLE OF CONTENTS	v
LIST OF TABLES	vii
LIST OF FIGURES	ix
LIST OF ABBREVIATIONS	x
CHAPTER 1: General Introduction	1
The Synthesis of Transition Metal Thiolate Complexes	4
The Reactivity of Transition Metal Thiolate Complexes	9
The Nature of the Metal-Sulfur Bond	17
Statement of Project	23
References	24
CHAPTER 2: The Preparation of $(\eta^5\text{-C}_5\text{H}_5)\text{W}(\text{CO})_2(\text{PPh}_3)\text{SR}$ (R = CHMe ₂ , CH ₂ Ph , 4-C ₆ H ₄ Me , Ph , phthalimido)	
Introduction	31
Results and Discussion	35
General Experimental	43
Experimental	47
References	57
CHAPTER 3: The Preparation of $[(\eta^5\text{-C}_5\text{H}_5)\text{W}(\text{CO})_2\text{SCHMe}_2]_2$ and $[(\eta^5\text{-C}_5\text{H}_5)\text{W}(\text{CO})\text{SCHMe}_2]_2$	
Introduction	60
Results and Discussion	64
Experimental	79
References	83

TABLE OF CONTENTS (cont'd)

	<u>Page</u>
CHAPTER 4: The Preparation of the Thioxanthate Complexes ($\eta^5\text{-C}_5\text{H}_5$)W(CO) ₂ S ₂ CSR (R = CHMe ₂ , CH ₂ Ph , 4-C ₆ H ₄ Me)	
Introduction	86
Results and Discussion	90
Experimental	106
References	114
CHAPTER 5: The Preparation of ($\eta^5\text{-C}_5\text{H}_5$)W(CO) ₂ (PPh ₃)S(SO ₂)R (R = CHMe ₂ , CH ₂ Ph , 4-C ₆ H ₄ Me)	
Introduction	121
Results and Discussion	132
Experimental	144
References	146
CONTRIBUTIONS TO ORIGINAL KNOWLEDGE	151
APPENDIX A: The Crystallographic Data, Positional and Anisotropic Parameters for [($\eta^5\text{-C}_5\text{H}_5$)W(CO) ₂ SCHMe ₂], [($\eta^5\text{-C}_5\text{H}_5$)W(CO)SCHMe ₂] and ($\eta^5\text{-C}_5\text{H}_5$)W(CO) ₂ S ₂ CSCH ₂ Ph	152
APPENDIX B: Data Sets for Figures 4.2 and 4.3; First Order Plots of the Reaction Between ($\eta^5\text{-C}_5\text{H}_5$)W(CO) ₂ (PPh ₃)SR and CS ₂ to Give ($\eta^5\text{-C}_5\text{H}_5$)W(CO) ₂ S ₂ CSR	163

LIST OF TABLES

		<u>Page</u>
Table 2.1	^1H NMR data for $\text{CpW}(\text{CO})_2(\text{PPh}_3)\text{SR}$ and $\text{CpW}(\text{CO})_2(\text{PPh}_3)\text{E}$ (E = H, CH_2Ph)	37
Table 3.1	^1H NMR and IR data for $[\text{CpW}(\text{CO})_2\text{SCHMe}_2]_2$ and $[\text{CpW}(\text{CO})\text{SCHMe}_2]_2$	66
Table 3.2	Bond distances and angles of $[\text{CpW}(\text{CO})_2\text{SCHMe}_2]_2$	77
Table 3.3	Bond distances and angles of $[\text{CpW}(\text{CO})\text{SCHMe}_2]_2$	78
Table 3.4	Comparison of ^1H NMR and IR data of $[\text{CpW}(\text{CO})_x\text{S}-4-\text{C}_6\text{H}_4\text{Me}]_2$ (x = 1,2)	75
Table 4.1	^1H NMR, IR and UV/Vis data for $\text{CpW}(\text{CO})_2(\text{PPh}_3)\text{SH}$ and $\text{CpW}(\text{CO})_2\text{S}_2\text{CSR}$	91
Table 4.2	Bond distances of $\text{CpW}(\text{CO})_2\text{S}_2\text{CSCH}_2\text{Ph}$	104
Table 4.3	Bond angles of $\text{CpW}(\text{CO})_2\text{S}_2\text{CSCH}_2\text{Ph}$	105
Table 5.1	Diagnostic $\nu(\text{SO})$ frequencies of relevant SO_2 coordination geometries in metal complexes	123
Table 5.2	^1H NMR and IR data for $\text{CpW}(\text{CO})_2(\text{PPh}_3)\text{S}(\text{SO}_2)\text{SR}$	133
Table A.1	Crystallographic data for $[\text{CpW}(\text{CO})_2\text{SCHMe}_2]_2$	154
Table A.2	Positional and isotropic thermal parameters for $[\text{CpW}(\text{CO})_2\text{SCHMe}_2]_2$	155
Table A.3	Anisotropic thermal parameters for $[\text{CpW}(\text{CO})_2\text{SCHMe}_2]_2$	156
Table A.4	Crystallographic data for $[\text{CpW}(\text{CO})\text{SCHMe}_2]_2$	157
Table A.5	Positional and isotropic thermal parameters for $[\text{CpW}(\text{CO})\text{SCHMe}_2]_2$	158

LIST OF TABLES (cont'd)

	<u>Page</u>
Table A.6	Anisotropic thermal parameters for $[\text{CpW}(\text{CO})\text{SCHMe}_2]_2$ 159
Table A.7	Crystallographic data for $\text{CpW}(\text{CO})_2\text{S}_2\text{CSCH}_2\text{Ph}$ 160
Table A.8	Positional and isotropic thermal parameters for $\text{CpW}(\text{CO})_2\text{S}_2\text{CSCH}_2\text{Ph}$ 161
Table A.9	Anisotropic thermal parameters for $\text{CpW}(\text{CO})_2\text{S}_2\text{CSCH}_2\text{Ph}$ 162
Table B.1	Data for curves A-C in Figure 4.2: first order plots of the reaction of $\text{CpW}(\text{CO})_2(\text{PPh}_3)\text{SR}$ with 0.25, 0.15 and 0.05 mL of CS_2 164
Table B.2	Data for curves A-C in Figure 4.3: first order plots of the reaction of $\text{CpW}(\text{CO})_2(\text{PPh}_3)\text{SR}$ with 0.25 mL CS_2 and 0, 3.25 and 7.00 equivalents of PPh_3 165

LIST OF FIGURES

	<u>Page</u>
Figure 3.1 Conformational isomers for dimers containing the fragment [CpM(μ -SR)] ₂ with a non-planar M ₂ S ₂ ring	61
Figure 3.2 Geometrical isomers for dimers containing the fragment [CpM(μ -SR)] ₂ with a planar M ₂ S ₂ ring	62
Figure 3.3 ORTEP view of [CpW(CO) ₂ SCHMe ₂] ₂	67
Figure 3.4 ORTEP view of [CpW(CO)SCHMe ₂] ₂	69
Figure 4.1 ORTEP view of CpW(CO) ₂ S ₂ CSCH ₂ Ph	93
Figure 4.2 Effect of CS ₂ concentration on the reaction of CpW(CO) ₂ (PPh ₃)SR with CS ₂	94
Figure 4.3 Effect of excess PPh ₃ on the reaction of CpW(CO) ₂ (PPh ₃)SR with CS ₂	95
Figure 5.1 The reaction of CpW(CO) ₂ (PPh ₃)SCH ₂ Ph with increasing volumes of added SO ₂ to give CpW(CO) ₂ (PPh ₃)S(SO ₂)CH ₂ Ph, monitored by ¹ H NMR spectroscopy	135
Figure 5.2 The ¹ H NMR spectra of CpW(CO) ₂ (PPh ₃)SCHMe ₂ immediately after SO ₂ treatment and one hour later	137
Figure 5.3 The ¹ H NMR spectra of CpW(CO) ₂ (PPh ₃)SCHMe ₂ in the presence of 5 equivalents of PPh ₃ immediately after SO ₂ treatment, 1.25 and 24 hours later	138

LIST OF ABBREVIATIONS

Å	ångström (1 ångström = 10^{-10} m)
avg	average
br	broad
<i>n</i> Bu	(CH ₂) ₃ CH ₃ , normal butyl
bpy	2,2'-bipyridine
CMe ₃	C(CH ₃) ₃ , tertiary-butyl, <i>t</i> -Bu
CHMe ₂	CH(CH ₃) ₂ , isopropyl
CH ₂ Ph	CH ₂ C ₆ H ₅ , benzyl, phenylmethyl
4-C ₆ H ₄ Me	4-C ₆ H ₄ CH ₃ , <i>p</i> -tolyl, 4-methylphenyl
CI	chemical ionization
cm ⁻¹	wavenumbers
Cp	η ⁵ -C ₅ H ₅ , η ⁵ -cyclopentadienyl
Cp*	η ⁵ -C ₅ Me ₅
dec	decomposed
ε _o	molar absorption coefficient (L·moles ⁻¹ ·cm ⁻¹)
EI	electron impact
en	H ₂ NCH ₂ CH ₂ NH ₂ , ethylenediamine
EtOH	CH ₃ CH ₂ OH, ethanol
eV	electron volts
FAB	Fast Atom Bombardment
FTIR	fourier-transform infrared
HFBA	heptafluorobuteric acid
Hz	Hertz
IP	ionization potential

LIST OF ABBREVIATIONS (cont'd)

IR	infrared
m	medium
Me	CH ₃ , methyl
MeOH	CH ₃ OH, methanol
mult	multiplet
NBA	nitrobenzyl alcohol
nm	nanometer (1 nm = 10 ⁻⁹ metres)
NMR	nuclear magnetic resonance
np ₃	N(CH ₂ CH ₂ PPh ₂) ₃
PAS	photoacoustic spectroscopy
pdmt	pyridine-2,6-dimethane thiolato
Ph	C ₆ H ₅ , phenyl
phth	NC(O)C(O)C ₆ H ₂ , phthalimido
ppm	parts per million
PPN ⁺	Ph ₃ P=N ⁺ =PPh ₃ , bis(triphenylphosphine)iminium
qt	quartet
rel. int.	relative intensity
s	strong
sh	sharp
sing	singlet
THF	tetrahydrofuran
tpp	Ph(CH ₂ CH ₂ CH ₂ PPh ₂) ₂
UV-Vis	ultraviolet-visible
w	weak

CHAPTER 1

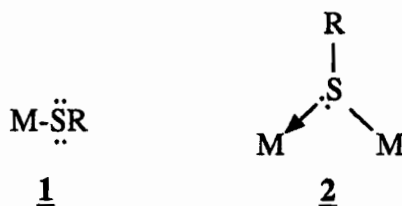
General Introduction

The thiolato ligand, RS^- , possesses a well-known high affinity for metal ions (1,2). In fact, the affinity of thiols for the mercuric ion, Hg^{2+} , led Klason (1) to coin the name "mercaptan" for mercury complexes of the type, $\text{Hg}(\text{SR})_2$. The propensity of the thiolato ligand for binding to metal ions extends throughout the periodic table, but is especially notable for the transition metals (1-15).

The ligand, RS^- , possesses an electronic structure and reactivity comparable, to some extent, to those of the halo (F^- , Cl^- , Br^- , I^-) ligands, and RS^- can often replace halide. In fact, RS^- is placed between F^- and Cl^- in the spectrochemical series (14):



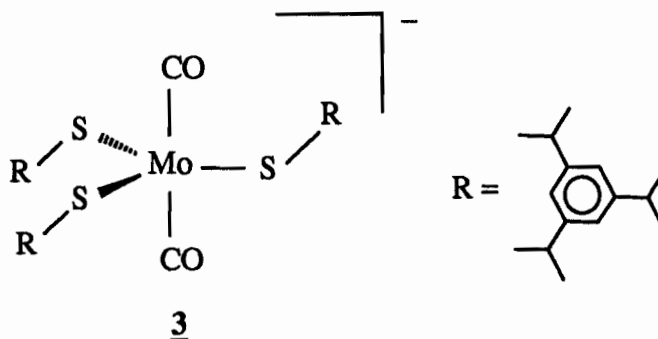
Like halo ligands (16), the thiolato ligand can act as either a terminal ligand (1), or as a μ_2 -bridging species (2) through the donation of a lone pair of electrons on the sulfur atom to another metal centre. Due to the strong tendency to act as a bridging ligand,



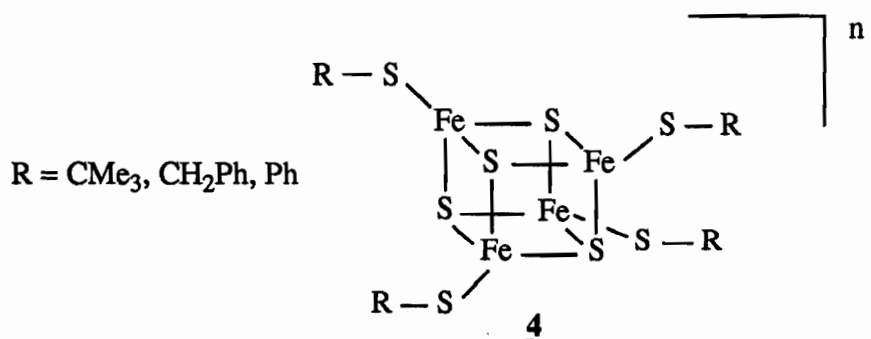
many transition metal thiolate complexes are dimers or higher order clusters and comparatively few monomeric compounds with terminal thiolato ligands have been prepared (3-13).

Complexes with monodentate thiolato groups have important biological

implications. Molybdenum (13,17,18), cadmium (13,19) and copper (13,19) complexes with sterically demanding thiolato ligands (13,20,21) such as 3 (18) are of interest as

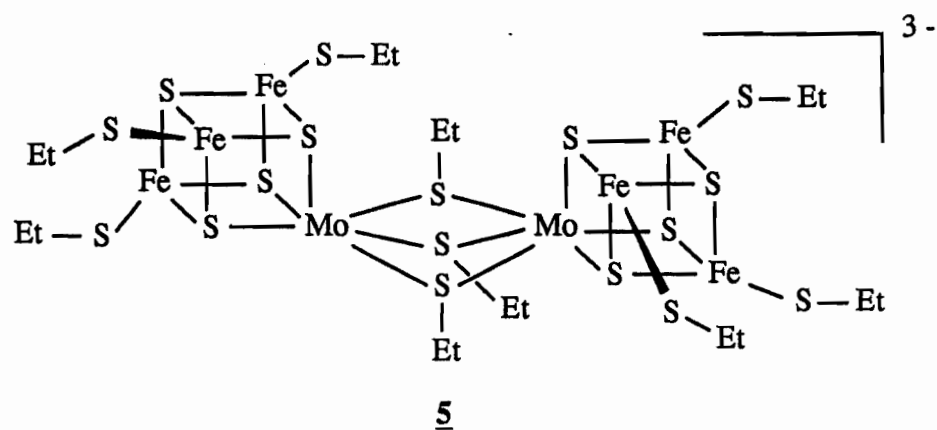


possible models for the active sites of nitrogenase enzymes (Mo oxidases) (22-24), metallothioneins (25,26), and "blue" copper proteins (27). The clusters, $[\text{Fe}_x\text{S}_x(\text{SR})_4]^{n-}$ ($x = 2, 4$; $n = 2, 3$; $\text{R} = \text{CMe}_3, \text{CH}_2\text{Ph}, \text{Ph}$) (4), are useful models for iron-sulfur proteins (24,28). Bridged thiolate complexes such as $[(\text{SEt})_3\text{Fe}_3\text{MoS}_4]_2(\mu\text{-SEt})_3]^{3-}$ (5) (29) are



excellent spectroscopic models for the Fe-Mo cofactor of nitrogenase.

A number of reviews (3-12) on metal complexes with sulfur ligands have appeared in the past but have rarely concentrated on transition metal complexes with thiolato ligands. A recent review by Blower and Dilworth (13) provides an excellent summary of this class of compounds but is restricted to those complexes in which the thiolato sulfur



comprises 50% of the coordinated ligands. This discussion will not be restricted by this criterion but will examine the modes of synthesis and general reactivity of transition metal thiolate complexes. An overview of the nature of the metal-thiolate bond will be included. In illustrating various points of interests in these discussions, most examples will be taken from Group VI (Cr, Mo, and W) transition metal chemistry where available since the research to be described later will concern tungsten thiolate complexes.

The Synthesis of Transition Metal Thiolate Complexes

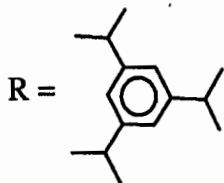
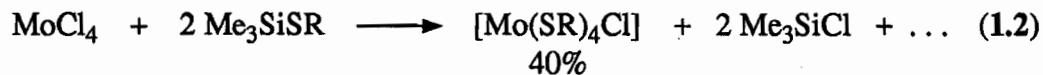
Several different synthetic methods used to incorporate the thiolato ligand in monomeric transition metal complexes (3-13) are outlined below.

1. The simplest and most direct approach involves the displacement of a ligand, X in M-X (M = transition metal; X = halide, hydride, or amine) by a thiolato group (M'SR; M' = cation) which is driven by the formation of an insoluble halide or volatile byproduct (M'X). Several different cations have been used as M'. Some are listed below with appropriate examples.

a) A common source of thiolato anions are alkali metal salts of thiols where M' = Li, Na, or K (3-13). The tetrakis-thiolate $[\text{Mo}(\text{SCMe}_3)_4]$ was prepared from MoCl_4 and LiSCMe_3 (Equation 1.1) (30).

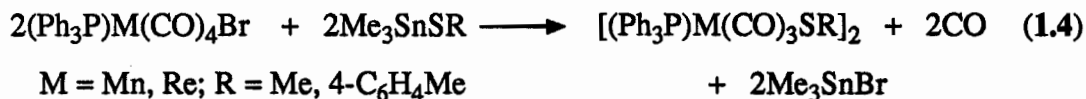


b) The trimethylsilyl group, Me_3Si (13,31), can effectively transfer the thiolato anion; $[\text{Mo}(\text{SR})_4\text{Cl}]$ was isolated in 40% yield from the reaction of MoCl_4 with Me_3SiSR (Equation 1.2). Further reaction with Na/Hg gave $[\text{Mo}(\text{SR})_4]$ (Equation 1.3) (31).

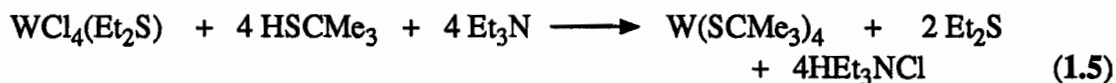


c) The use of trialkyltin, R_3Sn (13,32-34), as M' can also produce thiolate complexes but only dimeric species such as $[(\text{Ph}_3\text{P})\text{M}(\text{CO})_3\text{SR}]_2$, have been isolated thus

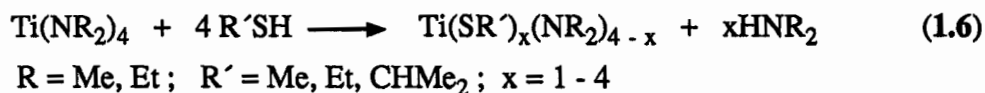
far from such reactions (Equation 1.4) (34).



d) The reaction of a thiol with a metal halide, often in the presence of a base such as NH_3 or Et_3N , can give a monomeric thiolate compound such as $\text{W}(\text{SCMe}_3)_4$ (13,35,36) as shown in Equation 1.5 (36).



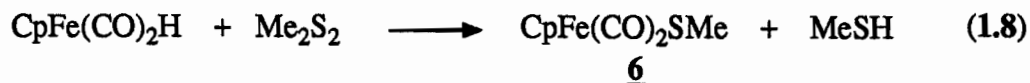
e) The reaction of a transition metal amide ($\text{X} = \text{NR}_2$) with thiols ($\text{M}' = \text{H}$) can produce thiolate complexes (13,37); $\text{Ti}(\text{NR}_2)_4$ reacted with $\text{R}'\text{SH}$ to give $\text{Ti}(\text{SR}')_x(\text{NR}_2)_{4-x}$ ($x = 1-4$) (Equation 1.6) (37).



f) Substitution reactions of a transition metal hydride ($\text{X} = \text{H}$) with thiols can also be effective in producing thiolate products (3-13,38,39); a reaction between $\text{M}(\text{CO})_5\text{H}$ ($\text{M} = \text{Mn, Re}$) and HSC_6F_5 gave $\text{M}(\text{CO})_5\text{SC}_6\text{F}_5$ (Equation 1.7) (39).

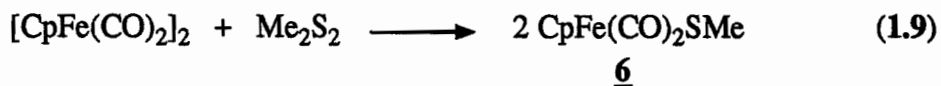


g) Likewise, a disulfide ($\text{M}' = \text{RS}^+$), Me_2S_2 , can react with a transition metal hydride such as $\text{CpFe}(\text{CO})_2\text{H}$ to form a thiolate product, $\text{CpFe}(\text{CO})_2\text{SMe}$ (6) (Equation 1.8) (38).



2. Another route to transition metal thiolates is via oxidative-addition.

a) Certain metal carbonyl complexes oxidatively add disulfides (3-13,38); CpFe(CO)₂SMe (**6**) was also prepared in this manner (Equation 1.9) (38).

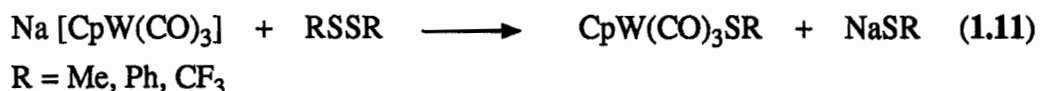


b) Thiols can oxidatively add to transition metal complexes as well (4); the reaction between Fe(CO)₂(NO)₂ and PhSH gave the dimer [Fe(NO)₂SPh]₂ (Equation 1.10) (40).

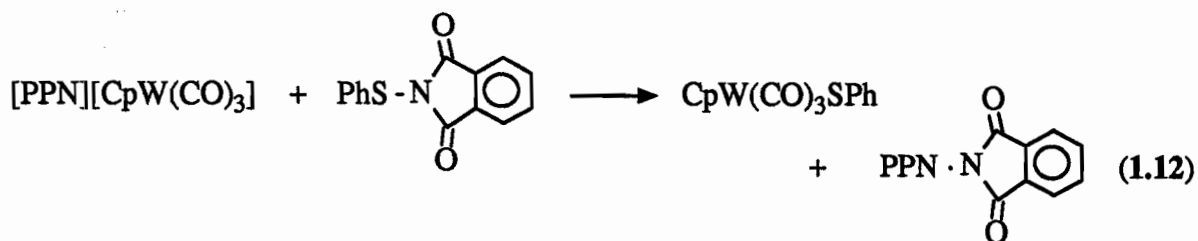


3. Recently, an approach to the synthesis of transition metal thiolates has been reported wherein an organometallic anion, M⁻, was treated with the cationic species, RS⁺ (41-48).

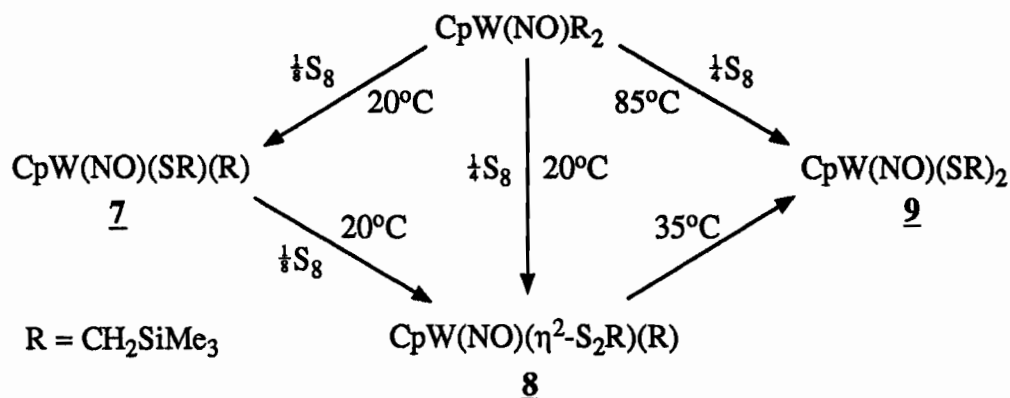
a) As shown in the reaction below, disulfides can be a source of RS⁺ as in the reaction of [CpW(CO)₃]⁻ to give CpW(CO)₃SR (Equation 1.11) (41).



b) The phthalimido sulfur transfer reagent, RS-phth (43) is a source of RS⁺ and the precipitation of an insoluble phthalimide salt provides a driving force for the reaction. The reaction of [PPN][CpW(CO)₃] (PPN = Ph₃P=N⁺=PPh₃) with PhS-phth gave CpW(CO)₃SPh (Equation 1.12) (42).

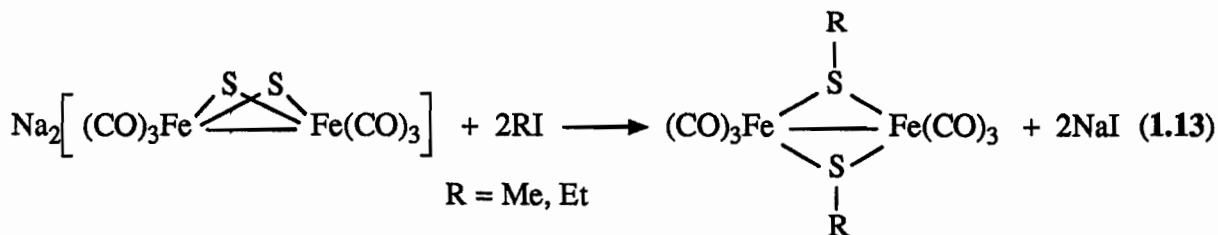


4. Recent reports of insertion of elemental sulfur into metal-alkyl bonds demonstrate yet another pathway for the formation of monomeric transition metal thiolate complexes. The complex $\text{CpW}(\text{NO})\text{R}_2$ elegantly inserted sulfur in a sequential manner to give $\text{CpW}(\text{NO})(\text{SR})(\text{R})$ (**7**) and $\text{CpW}(\text{NO})(\eta^2\text{-S}_2\text{R})(\text{R})$ (**8**), which when heated gave the bithiolate product $\text{CpW}(\text{NO})(\text{SR})_2$ (**9**) (49) as shown in Scheme 1.1.

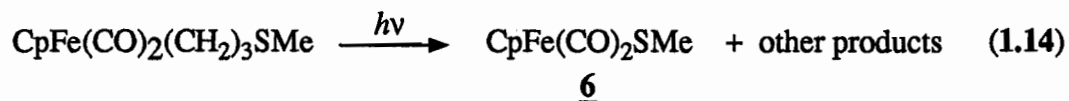


Scheme 1.1

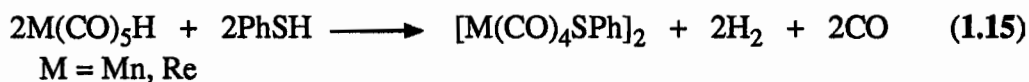
5. A less common mode of transition metal thiolate synthesis is the alkylation of a metal sulfide with an alkyl halide (RX). The preparation of a monomeric complex has not been reported yet but reaction of the bridged transition metal sulfide $\text{Na}_2[(\text{CO})_3\text{Fe}(\mu\text{-S})_2]$ with RI gave the thiolate shown in Equation 1.13 (50,51).



6. Although $\text{CpFe}(\text{CO})_2\text{SMe}$ **6** has been prepared by other routes mentioned above, it was first identified as one of a number of products from the irradiation of $\text{CpFe}(\text{CO})_2(\text{CH}_2)_x\text{SMe}$ ($x = 2,3$) (Equation 1.14) (52,53). To our knowledge, this is the only example of a transition metal thiolate complex prepared by this method.



While it appears that transition metal thiolate complexes are easily prepared, the tendency for these complexes to dimerize complicates the synthesis of monomeric thiolate products. To avoid dimerization, sterically demanding R groups, as in Equation 1.3, have been employed effectively to give monomeric thiolates (13,18,20,21,31). Another approach has been the use of strongly electron-withdrawing groups such as C_6F_5 , which reduce the donor ability of the sulfur atom. This strategy has produced the monomeric thiolate $\text{M(CO)}_5\text{SC}_6\text{F}_5$ ($\text{M} = \text{Mn, Re}$) (Equation 1.6), whereas the same reaction performed for $\text{R} = \text{C}_6\text{H}_5$ (Ph), gave the *dimer*, $[\text{M(CO)}_4\text{SPh}]_2$, (Equation 1.15) (39).



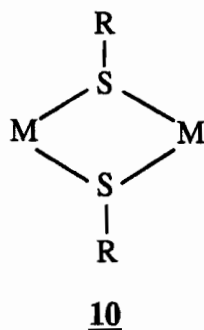
The Reactivity of Transition Metal Thiolate Complexes

Transition metal thiolate monomeric complexes are a highly reactive class of compounds giving a variety of products. These include polynuclear complexes containing bridging thiolato ligands, metal sulfides resulting from the cleavage of the S-C bond of the metal thiolate, redox products with the elimination of free disulfide and complexes arising from the reaction with electrophiles. Some examples of this chemistry is outlined below.

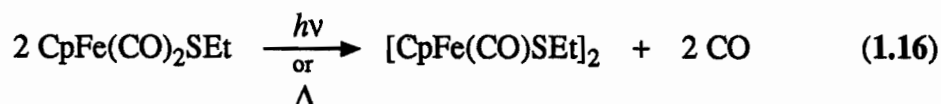
A. The Thiolato Ligand as a Bridging Ligand

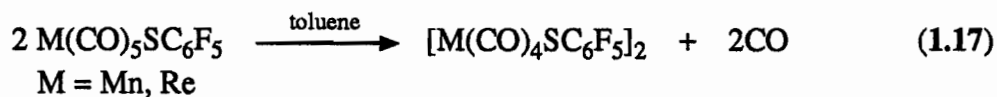
The most common reaction of monomeric transition metal thiolates is aggregation to give μ_2 - and μ_3 -bridged polynuclear thiolate complexes (7,12,13), often with the displacement of another ligand.

1. Dimeric thiolate complexes usually containing two thiolato bridges (10) are

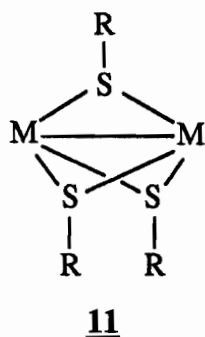


numerous and are often formed during reactions intended to give monomeric thiolates. Irradiating or mildly heating transition metal thiolate monomers in solution often gives μ_2 -SR dimers (3-13) as shown by Equations 1.16 (54,55) and 1.17 (39).

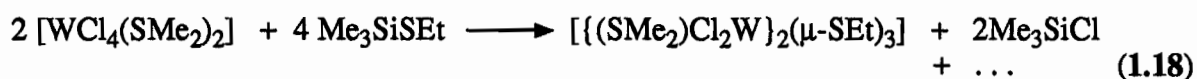




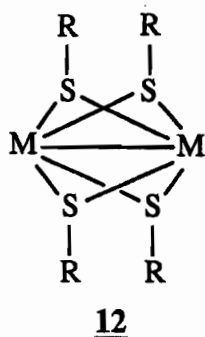
2. Complexes with three μ_2 -SR bridges (**11**) are known and often contain a metal-metal bond (*13*). These complexes are formed under similar conditions to those



with two thiolato bridges. For example, $[(\text{SMe}_2)\text{Cl}_2\text{W}]_2(\mu\text{-SEt})_3$ was produced from $[\text{WCl}_4(\text{SMe}_2)_2]$ and Me_3SiSEt , a reaction that was expected to give the monomer $[\text{W}(\text{SEt})_2\text{Cl}_2(\text{SMe}_2)_2]$, (Equation 1.18) (*56*).



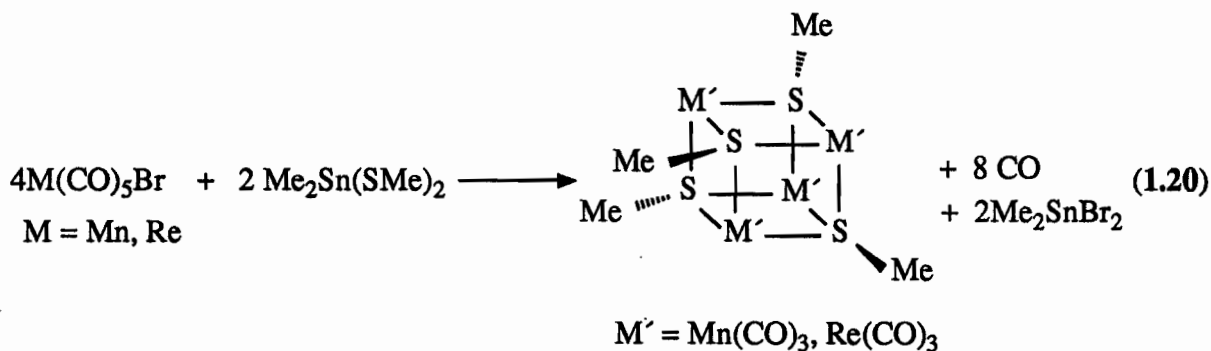
3. A few complexes with four thiolato bridges (**12**) are known; almost all have



π -cyclopentadienyl or π -arene terminal ligands (*13*). The path to these complexes is usually the oxidative addition of a disulfide or thiol to a complex as in the preparation of $[\text{Cp}_2\text{V}_2(\text{SMe})_4]$ Equation 1.19 (*57*).



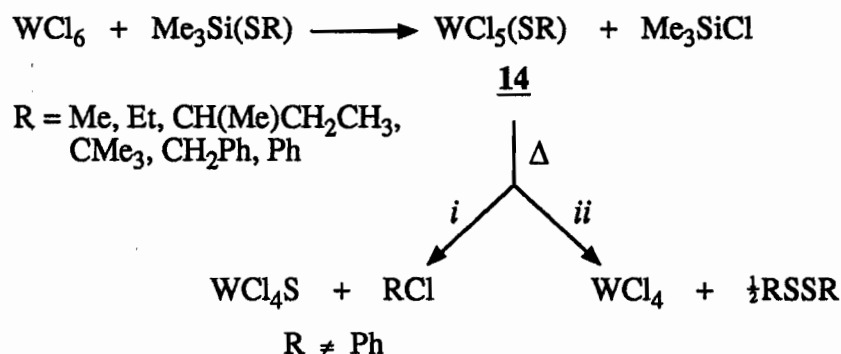
4. Given that the thiolato ligand possesses three lone pairs of electrons, it may theoretically coordinate to three metal centres and indeed, examples of μ_3 -SR bridges have been observed in several cluster compounds (13). The Fe-Mo-S aggregate, $[\{(\text{SEt})_3\text{Fe}_3\text{MoS}_4\}_2(\mu\text{-SEt})_3]^{3-}$ (5), shown previously, is one example. Other examples are the tetranuclear species, $[\text{M}(\text{SMe})(\text{CO})_3]_4$ ($\text{M} = \text{Mn}, \text{Re}$) (13) (55,58-60), prepared by the reaction of $[\text{M}(\text{CO})_5\text{Br}]$ with $\text{Me}_2\text{Sn}(\text{SMe})_2$ (Equation 1.20). The rhenium complex was identified by x-ray crystallography as a cubane structure where the sulfur atoms occupy alternate corners of the cube and are coordinated to three neighbouring Re atoms (60).



13

B. Cleavage of the S-C Bond in Thiolate Complexes

Transition metal thiolate complexes can also undergo cleavage of the sulfur-carbon bond which can hamper the preparation of monomeric thiolates (3,4,7,10-13,61-63). For example, WCl_5SR (14) was isolated and characterized only when $\text{R} = \text{Me}$ and Ph (Scheme 1.2) (62). For other R groups, 14 underwent (i) heterolytic S-C bond cleavage



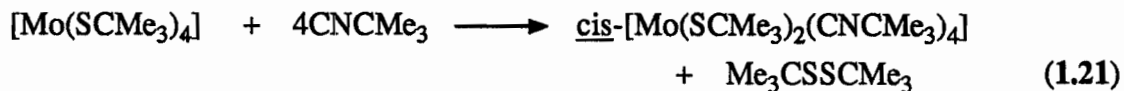
Scheme 1.2

to give RCl and/or (ii) decomposed via reductive elimination to give free RSSR.

C. Redox Chemistry of Thiolato Ligands

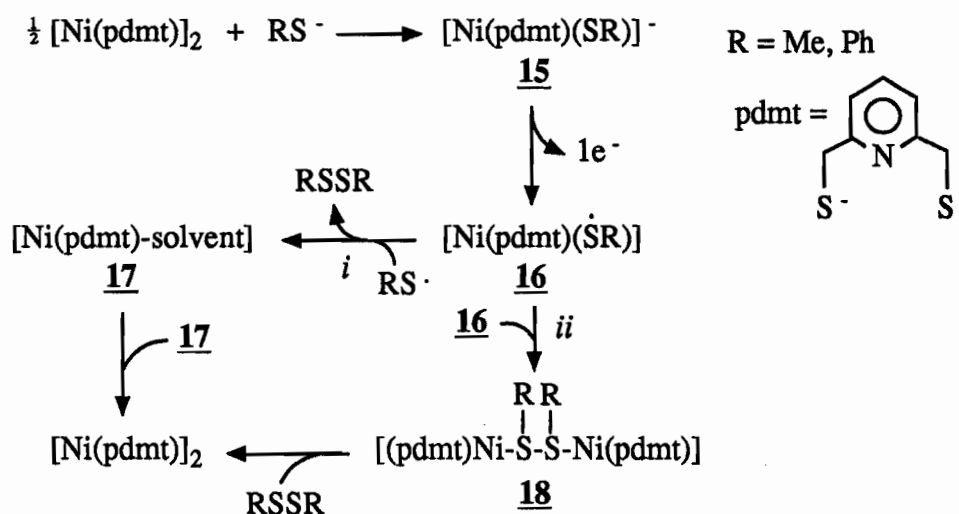
Thiolato ligands bonded to transition metals can exhibit redox chemistry (7,13,15) which can be classified into two basic reactions: 1) sulfur-sulfur bond formation to give free disulfide with concomitant reduction of the metal or some external oxidant (64-66), and 2) oxidation at sulfur to give M-S(O)_x-R complexes (x = 1,2) (67,68).

1. a) Examples of disulfide formation and reduction of the metal are shown in reaction (ii) of Scheme 1.2 and below where reaction of the Mo(IV) complex, [Mo(SCMe₃)₄], with tertiary butyl isocyanide gave tertiary butyl disulfide and the Mo(II) product [Mo(SCMe₃)₂(CNCMe₃)₄] (Equation 1.21) (64).



b) Electrochemical oxidation of [Ni(pdmt)SR]⁻ (pdmt = pyridine-2,6-dimethane thiolato; R = Me, Ph) (15) gave the disulfide, RSSR, as presented in Scheme 1.3 (65). After a one electron transfer to give a coordinated thynyl radical complex, 16, two

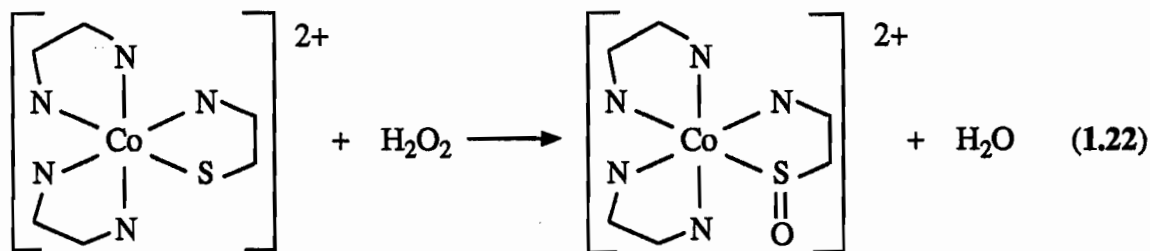
plausible pathways have been proposed for the formation of disulfide. Reaction (i) depicts the dissociation of coordinated RS^\cdot to afford disulfide with the production of the solvated monomer 17. Coupling with a second molecule of 17 gives the observed $[Ni(pdmt)]_2$ dimer. Alternatively, reaction (ii) proposes that two thynyl radical complexes (16) could combine and form the dimeric species (18). Dissociation of $RSSR$ and recombination yields $[Ni(pdmt)]_2$. Studies of the electrochemistry of transition metal



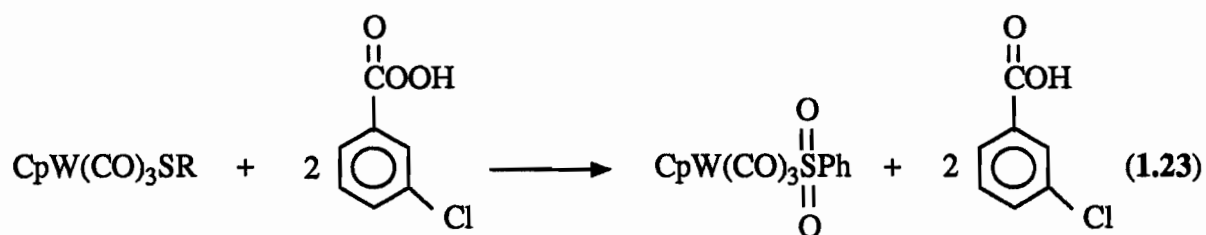
Scheme 1.3

thiolate complexes have shown that thiolato ligands are very efficient mediators of electron transfer (7,13,65,66) and may be important in the redox processes of thiolato-containing enzymes such as iron-sulfur proteins (28), nitrogenase (22-24) and hydrogenases (69).

2. A second type of redox reaction of coordinated thiolato ligands is the oxidation at the sulfur atom to give $M-S(O)_xR$ ($x = 1,2$), which can occur via the treatment with an oxidant such as hydrogen peroxide. The complex $[(en)_2Co(SCH_2CH_2NH)]^{2+}$ ($en =$ ethylenediamine) reacts with H_2O_2 to give $[(en)_2Co(S(O)CH_2CH_2NH)]^{2+}$ (Equation 1.22) (68,70). The formation of a metal sulfinate complex $CpW(CO)_3S(O)_2Ph$ by the



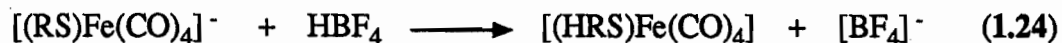
treatment of $\text{CpW}(\text{CO})_3\text{SPh}$ with metachloroperbenzoic acid is represented in Equation 1.23 (67).



D. Reactions of Thiolate Complexes with Electrophiles

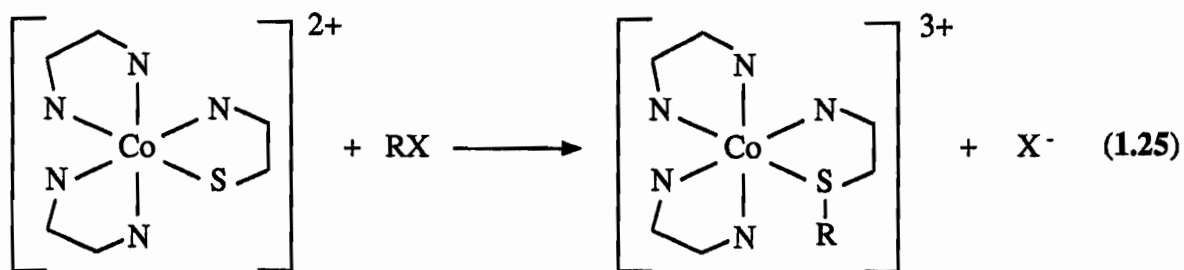
Transition metal thiolate complexes are vulnerable to electrophilic attack at the sulfur atom. This reactivity is based mainly on the availability of the lone pairs of electrons on the sulfur atom and can result in the protonation, alkylation or coordination of a thiolato ligand at sulfur (7,13,70-73). Other reactions include the insertion of small electrophiles such as CS_2 (35,74-81), $\text{RC}\equiv\text{CR}$ (82-85) or carbenes (86) into the metal-sulfur bond.

1. a) An example of protonation at the sulfur atom is the treatment of $[(\text{RS})\text{Fe}(\text{CO})_4]^-$ with HBF_4 to give $[(\text{HRS})\text{Fe}(\text{CO})_4]$ (Equation 1.24) (71).



b) Alkylation at S occurs upon treatment of $[(\text{en})_2\text{Co}(\text{SCH}_2\text{CH}_2\text{NH})]^{2+}$ with an

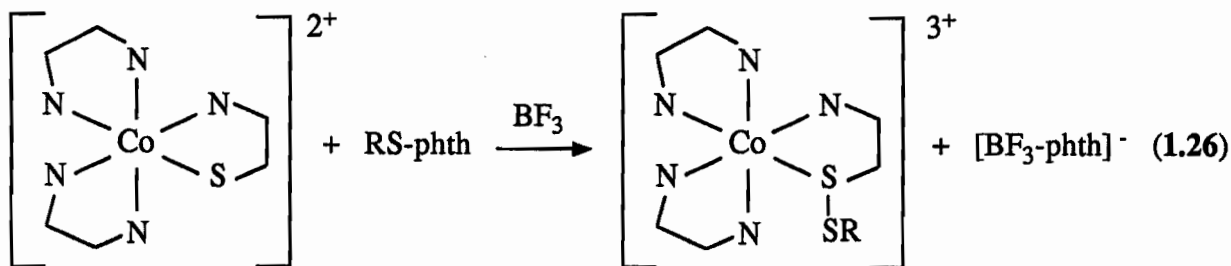
alkyl halide, RX (Equation 1.25) (72).



R = Me, Et, CH₂Ph, CH₂-4-C₆H₄F, CH₂-4-C₆H₄Me

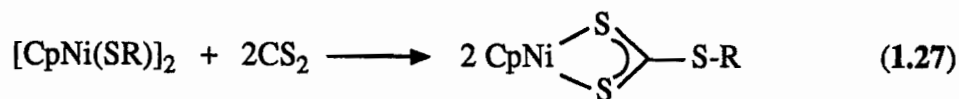
X = Cl, Br, I

c) Treatment of [(en)₂Co(SCH₂CH₂NH)]²⁺ with RS-phth (R = Me, Et, CHMe₂, CMe₃, Ph) in the presence of BF₃ gave a coordinated disulfide product [(en)₂Co{S(SR)CH₂CH₂NH}]³⁺ (Equation 1.26) (73).



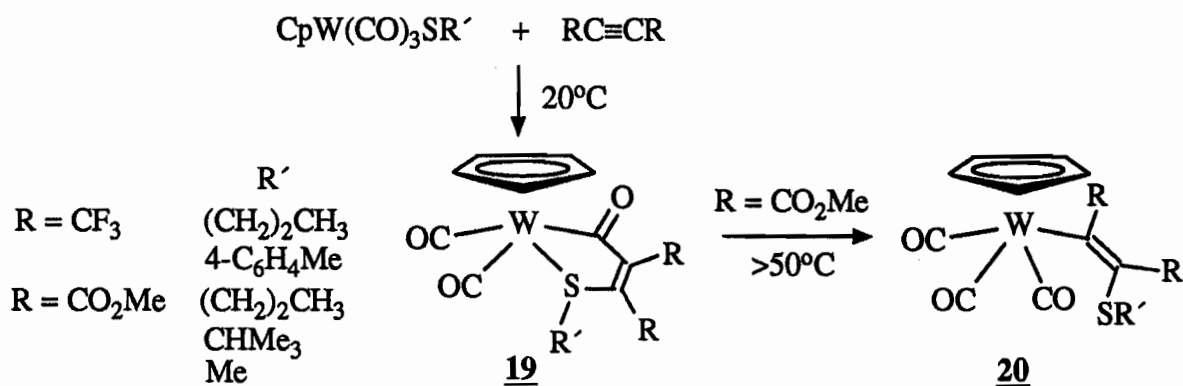
R = Me, Et, CHMe₂, CMe₃, Ph

2. a) The electrophilic attack by CS₂ on the sulfur atom of a thiolato ligand can lead to insertion into the M-S bond. This forms a bidentate trithiocarbonato or thioxanthato ligand (74-81), [S₂CSR]⁻. Accordingly, [CpNi(SR)]₂ (R = Me, Et, Ph) reacted with CS₂ to give [CpNi(S₂CSR)] as shown by Equation 1.27 (74).



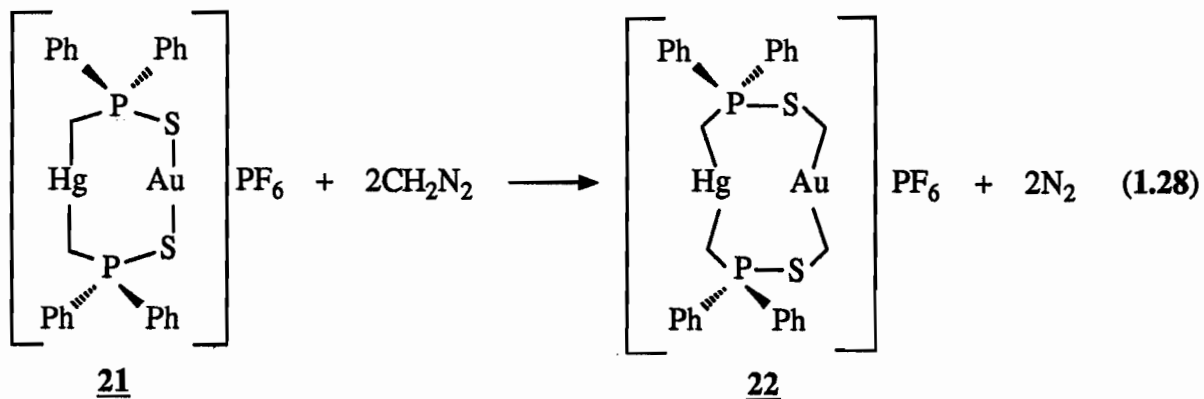
b) Alkynes, RC≡CR (R = CF₃, CO₂Me), insert into the metal-sulfur bond of certain iron and tungsten thiolates (82-85) to give complexes such as **19** and **20** (Scheme

1.4) (83).



Scheme 1.4

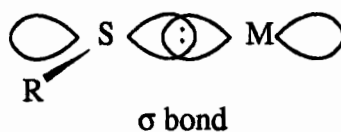
c) Most recently, a reaction between $[\text{HgAu}(\text{SPPPh}_2\text{CH}_2)_2]\text{PF}_6$ (**21**) and CH_2N_2 was reported as the first example of a carbene insertion into a metal-sulfur bond (Equation 1.28) (86). One molecule of CH_2N_2 inserts into each of the two Au-S bonds to give **22**; the structure was confirmed by x-ray crystallography.



The Nature of the Metal-Sulfur Bond

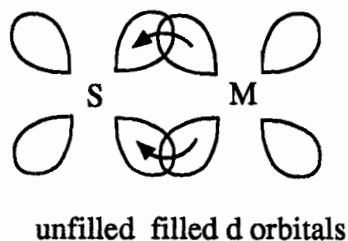
In the numerous reactions of transition metal thiolates, it is apparent that the reactivity of these complexes is often concentrated at the thiolato ligand, either at the sulfur atom itself or the metal-sulfur bond. Therefore, the nature of the metal-sulfur bond is of interest in order to better understand the chemistry of thiolate complexes.

The primary interaction between the transition metal and the sulfur atom is through the overlap of valence electrons in p orbitals of proper symmetry and orientations to form a σ bond as in 23 (7,87). Previously, a secondary interaction was thought to occur



23

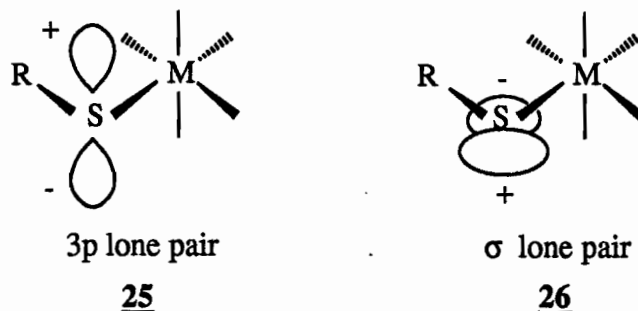
via the π -complexation of low-lying empty d orbitals on the sulfur atom and filled metal d orbitals as in 24 (8,88). However, more recent (7,87) molecular orbital calculations on



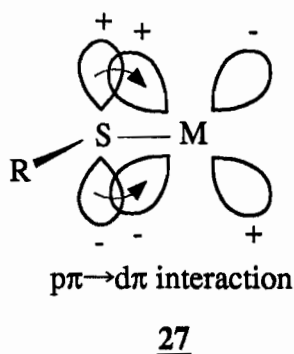
24

molecules containing thioether ligands ($M-SR_2$) did not detect important d-orbital interactions. Since then it has been shown that the coordinated RS^- ligand can act as a $p\pi \rightarrow d\pi$ donor through the two inequivalent 3p lone pair orbitals on the sulfur atom (64,89-92). The better donor is the higher energy pure 3p lone pair orthogonal to the

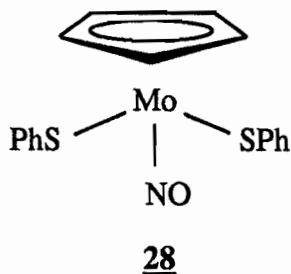
M-S-R plane depicted by 25. The poorer donor is the lower lying σ lone pair in the



M-S-R plane as in 26. One of these lone pair orbitals can overlap with empty metal d orbitals if both orbitals are in proper orientations for $p\pi-d\pi$ interaction as in 27. This

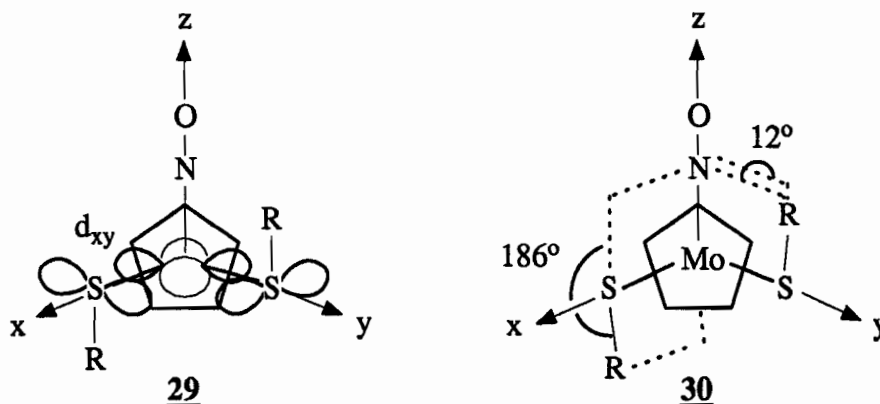


$p\pi-d\pi$ bonding interaction can contribute to the stability of mononuclear coordinatively unsaturated 16 electron molybdenum complexes (64,89,91) and 5-coordinate 14 electron ruthenium compounds (90,92). The x-ray crystal structure of $\text{CpMo}(\text{NO})(\text{SPh})_2$ (28) (91)



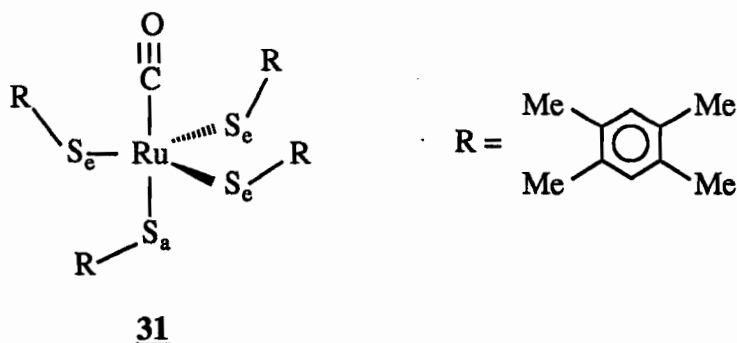
revealed this species to be a monomeric 16 electron complex, not a dimer as might be expected (21,93). The Mo-S distances of 2.34Å (avg) were unusually short. Typical

Mo-S distances range from 2.33 to 2.55 Å, with the shorter distances associated with Mo in high oxidation states. According to molecular orbital calculations, the unusual stability of **28** is due to the $p\pi-d\pi$ bonding interaction between a filled thiolato sulfur lone pair, that was chiefly 3p in character, and the empty $4d_{xy}$ molybdenum orbital as shown in **29**.



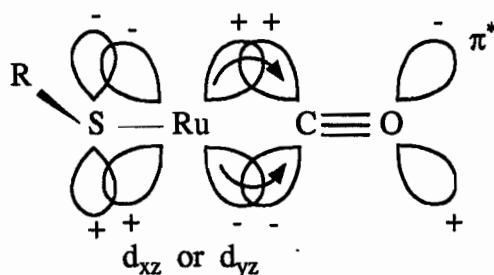
These calculations correlated with the structural data since torsional angles of 0° and 180° for R-S-Mo-N would place the sulfur 3p lone pairs in the xy plane and those observed were 12° and 186° as in **30**.

The ruthenium compound, $\text{Ru}(\text{S}-2,3,5,6\text{-C}_6\text{H-Me}_4)_4(\text{CO})$ (**31**) (90), is another example of how thiolato ligands stabilize a coordinatively unsaturated compound, even



to the extent of permitting the binding of a π acceptor ligand like CO to a metal atom in a formally high oxidation state (94). This was rationalized by a bonding scheme in which

there was significant donation of electron density from the sulfur ligands to the metal. Firstly, the four d-electrons of Ru(IV) were proposed to fill the d_{xz} and d_{yz} metal orbitals and engage in back donation to CO. The electron density of these *filled* metal d orbitals may be enhanced by the overlap of electron density from the σ lone pair orbital (26) of the equatorial sulfur atoms (S_e) and both the σ (26) and 3p lone pair (25) orbitals on the axial sulfur atom (S_a), thus augmenting the back-bonding to CO as shown in 32. Secondly, a $p\pi$ - $d\pi$ interaction occurs when the 3p lone pair on the S_e atoms donate into

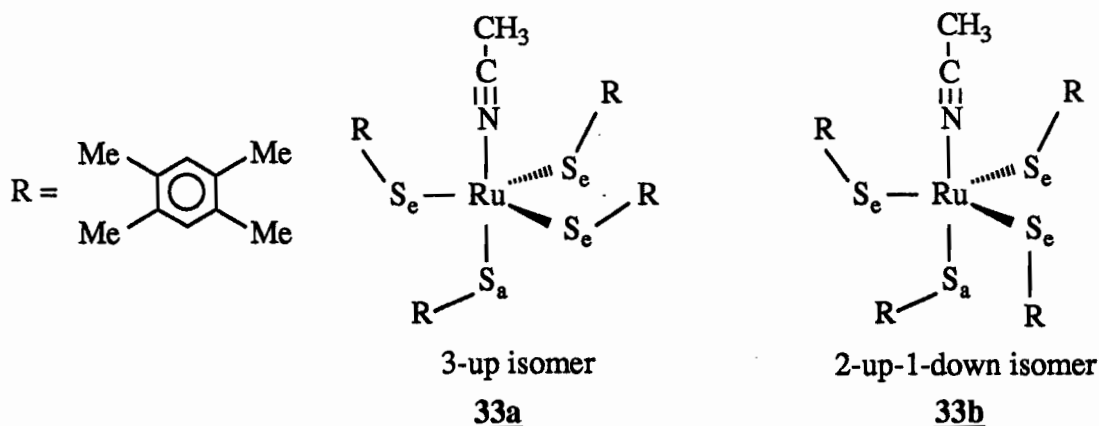


overlap of S lone pair orbitals,
augmenting CO back-bonding by metal orbitals

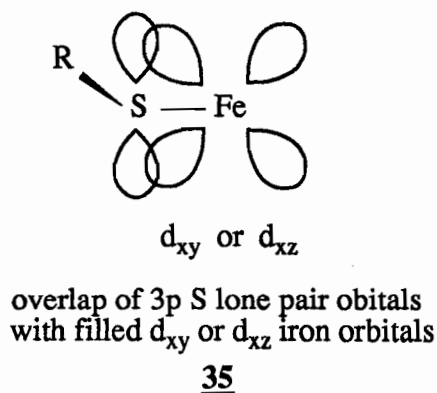
32

the *empty* $d_{x^2-y^2}$ and d_{xy} metal orbitals as in 27. This was reflected in the short Ru- S_e distances which averaged 2.213(7)Å compared to the longer Ru- S_a distance of 2.409(3)Å. A partial barrier to rotation of the Ru- S_e bond was suggested by the variable temperature ^1H NMR spectra of a similar compound, Ru(S-2,3,5,6- $\text{C}_6\text{H-Me}_4$) $_4$ (CH_3CN) (33) (92). It was concluded that the two isomers, the 3-up (33a) and the 2-up-1-down (33b) species, were present in solution from the appearance of two resonances due to the CH_3CN ligand in the room temperature spectrum. However, given the large bulk of the thiolato ligands, steric hindrance might also cause or contribute to the slow rotation about the Ru-S bond.

While the above examples show the stabilizing effect of thiolato ligands, a study on a normal, coordinatively saturated, 18 electron species, $\text{CpFe}(\text{CO})_2\text{SR}$ ($\text{R} =$



4-C₆H₄-Z; Z = OMe, H, Cl, CF₃, NO₂) (34), revealed an anti-bonding interaction between the metal and the thiolato ligand, resulting in an overall destabilizing effect (95). Molecular orbital calculations predicted that the formally occupied d_{xz} and the d_{xy} iron orbitals would overlap with the sulfur 3p lone pair orbital (25). This filled-filled $\pi\pi$ - $d\pi$ interaction shown in 35, resulted in a destabilized anti-bonding combination that



was the highest occupied molecular orbital and principally 3p in character.

The reaction of CpFe(CO)₂SR (34) with an alkyl iodide (R'I) gave [CpFe(CO)₂(SRR')I] (Equation 1.29). Kinetic studies of this reaction revealed that the rate of the reaction increased as the Z substituent became more electron-donating (OMe > H > Cl > CF₃ > NO₂). Therefore, as more electron density is placed on the sulfur 3p



orbital as in these complexes, this destabilizing effect of filled-filled $d\pi$ - $p\pi$ interaction is manifested by the increased nucleophilicity of the sulfur atom.

Comparison of the study of the coordinatively saturated $\text{CpFe}(\text{CO})_2\text{SR}$ (**34**) and those of the previous two complexes, $\text{CpMo}(\text{NO})(\text{SPh})_2$ (**28**) and $\text{Ru}(\text{S-2,3,5,6-C}_6\text{H-Me}_4)_4(\text{CO})$ (**31**) reveals that the two different effects observed, destabilizing in the former and stabilizing in the latter, are not contradictory but are rather, *complementary*. The stabilizing effect exhibited by **28** and **31** arose from the overlap of lone pair orbitals on the sulfur with the empty metal d orbitals to give a *filled-unfilled* $p\pi$ - $d\pi$ bonding interaction. On the other hand, if the metal d orbitals were filled, as in **34**, this overlap resulted in a destabilized *filled-filled* $p\pi$ - $d\pi$ anti-bonding interaction. Further, increased nucleophilicity at the sulfur atom of **34** was observed when the electron density in the S lone pair orbitals was increased by the use of electron-donating R groups. The destabilizing effect of the $p\pi$ - $d\pi$ antibonding interaction may account for much of the rich chemistry observed for coordinatively saturated, 18 electron transition metal thiolate complexes.

Statement of Project:

As part of other studies on the polysulfano tungsten complexes, $\text{CpW}(\text{CO})_3\text{S}_x\text{R}$ ($x = 1-3$), the triphenylphosphine substituted thiolate complexes, $\text{CpW}(\text{CO})_2(\text{PPh}_3)\text{SR}$, were required. The work presented here reports the preparation of the desired complexes by a mild and general route, commencing with the treatment of $\text{CpW}(\text{CO})_2(\text{PPh}_3)\text{H}$ with methyllithium. This deprotonation reaction is also investigated. It was found that the presence of PPh_3 rendered $\text{CpW}(\text{CO})_2(\text{PPh}_3)\text{SR}$ susceptible to further reactivity and the reactions of $\text{CpW}(\text{CO})_2(\text{PPh}_3)\text{SR}$ with electrophiles such as CS_2 and SO_2 are investigated and described. The starting thiolate complexes also dimerize, to give $[\text{CpW}(\text{CO})_x\text{SR}]_2$ ($x = 1,2$; $\text{R} = \text{CHMe}_2$). The x-ray crystal structures for each are the first determined for the tungsten derivatives for this class of dimeric compounds.

References

1. Klason, P. *Ber.* **1887**, *20*, 3407.
2. Wertheim, E. *J. Am. Chem. Soc.* **1929**, *51*, 3661.
3. Lindoy, L.F. *Coord. Chem. Rev.* **1969**, *4*, 41.
4. Abel, E.; Crosse, B.C. *Organomet. Chem. Rev.* **1967**, *2*, 443.
5. Bradley, D.C.; Fisher, K.J. in "Med. Tech. Publ. Co. Int. Rev. Sci.: Inorg. Chem. Ser. One"; Sharp, D.W.A., Ed.; Butterworth: London, 1972; Vol. 5, p 65.
6. McAuliffe, C.A.; Murray, S.G. *Inorg. Chim. Acta Rev.* **1972**, *6*, 103.
7. Kuehn, C.G.; Isied, S.S. *Prog. Inorg. Chem.* **1981**, *27*, 153.
8. Mehrotra, R.C.; Gupta, V.D.; Sukhani, D. *Inorg. Chem. Acta Rev.* **1968**, *2*, 111.
9. Murray, S.G.; Hartley, F.R. *Chem. Rev.* **1981**, *81*, 365.
10. Livingstone, S.E. *Q. Rev. Chem. Soc.* **1965**, *19*, 386.
11. Vergamini, P.J.; Kubas, G.J. *Prog. Inorg. Chem.* **1977**, *21*, 261.
12. Dance, I.G. *Polyhedron* **1986**, *5*, 1037.
13. Blower, P.J.; Dilworth, J.R. *Coord. Chem. Rev.* **1987**, *76*, 121.
14. Jørgensen, C.K. *Inorg. Chim. Acta Rev.* **1968**, *2*, 65.
15. Müller, A.; Diemann, E. in "Comprehensive Coordination Chemistry"; Wilkinson, G., Ed.; Pergamon Press: Oxford, 1987; Vol. 2, p 515.
16. a) Hodgson, D.J. *Prog. Inorg. Chem.* **1975**, *19*, 173.
b) Seppelt, K. *Angew. Chem. Int. Ed.* **1979**, *18*, 186.
c) Cotton, F.A.; Wilkinson, G. "Advanced Inorganic Chemistry, A Comprehensive Text", 4th ed.; Wiley Interscience: New York, 1980; Chap. 4, p 191.

17. Bishop, P.T.; Dilworth, J.R.; Hughes, D.L. *J. Chem. Soc. Dalton Trans.* **1988**, 2535.
18. Dilworth, J.R.; Hutchinson, J.; Zubieta, J.A. *J. Chem. Soc. Chem. Commun.* **1983**, 1034.
19. Block, E.; Gernon, M.; Kang, H.; Ofori-Okai, G.; Zubieta, J.A. *Inorg. Chem.* **1989**, 28, 1263 and references therein.
20. Blower, P.J.; Dilworth, J.R.; Hutchinson, J.P.; Zubieta, J.A. *J. Chem. Soc. Dalton Trans.* **1985**, 1533.
21. Dilworth, J.R. in "Sulfur - Its Significance for Chemistry in the Geo-, Bio-, and Cosmosphere and Technology"; Müller, A., Krebs, B., Eds.; Elsevier: Amsterdam, 1984; p 141.
22. Steifel, E.I. *Prog. Inorg. Chem.* **1977**, 22, 1.
23. Coucouvanis, D. *Acc. Chem. Res.* **1981**, 14, 201.
24. Holm, R.H. *Chem. Soc. Rev.* **1981**, 10, 455.
25. Dean, P.A.; Vittal, J.J.; Trattner, M.H. *Inorg. Chem.* **1987**, 26, 4245.
26. Swenson, D.; Baenziger, N.C.; Coucouvanis, D. *J. Am. Chem. Soc.* **1978**, 100, 1932.
27. Colman, P.M.; Freeman, H.C.; Guss, J.M.; Murata, M.; Norris, V.A.; Ramshaw, J.A.M.; Venkatappa, M.P. *Nature*, **1978**, 272, 319.
28. Holm, R.H. *Acc. Chem. Res.* **1977**, 10, 427.
29. Wolff, T.E.; Berg, J.M.; Hodgson, K.O.; Frankel, R.B.; Holm, R.H. *J. Am. Chem. Soc.* **1979**, 101, 4140.
30. Otsuka, S.; Kamata, M.; Hirotsu, K.; Higuchi, T. *J. Am. Chem. Soc.* **1981**, 103, 3011.
31. Roland, E.; Walborsky, E.C.; Dewan, J.C.; Schrock, R.R. *J. Am. Chem. Soc.* **1985**, 107, 5795.

32. Treichel, P.M.; Tegen, M.H. *J. Organomet. Chem.* **1988**, 358, 339.
33. a) Treichel, P.M.; Tegen, M.H. *Inorg. Synth.* **1989**, 25, 114.
b) Treichel, P.M.; Tegen, M.H. *Ibid* **1989**, 25, 115.
34. Abel, E.W.; Atkins, A.M.; Crosse, B.C.; Hutson, G.V. *J. Chem. Soc. (A)* **1968**, 687.
35. Havlin, R.; Knox, G.R. *Z. Naturforsch.* **1966**, 21b, 1108.
36. Listemann, M.L.; Dewan, J.C.; Schrock, R.R. *J. Am. Chem. Soc.* **1985**, 107, 7207.
37. Bradley, D.C.; Hammersley, P.A. *J. Chem. Soc. (A)* **1967**, 1894.
38. King, R.B. *J. Am. Chem. Soc.* **1963**, 85, 1587.
39. Osborne, A.G.; Stone, F.G.A. *J. Chem. Soc. (A)* **1966**, 1143.
40. Hieber, W.; Beck, W. *Z. Anorg. Chem.* **1960**, 305, 274.
41. Treichel, P.M.; Nakagaki, P.C. *Organometallics*, **1986**, 5, 711.
42. Treichel, P.M.; Nakagaki, P.C.; Haller, K.J. *J. Organomet. Chem.* **1987**, 327, 327.
43. a) Harpp, D.N.; Ash, D.K.; Back, T.G.; Gleason, J.G.; Orwig, B.A.; van Horn, W.F.; Snyder, J.P. *Tetrahedron Lett.* **1970**, 3551.
b) Boustany, K.S.; Sullivan, A.B. *Tetrahedron Lett.* **1970**, 3547.
c) Harpp, D.N.; Ash, D.K. *Int. J. Sulfur Chem., Part A* **1971**, 1, 21.
d) Behforouz M.; Kerwood, J.E. *J. Org. Chem.* **1969**, 34, 51.
e) Abe, Y.; Nakabayashi, T.; Tsurugu, J. *Bull. Chem. Soc. Jpn.* **1973**, 46, 1898.
44. Nosco, D.L.; Elder, R.C.; Deutsch, E. *Inorg. Chem.* **1980**, 19, 2545.
45. Shaver, A.; Hartgerink, J.; Lai, R.D.; Bird, P.; Ansari, N. *Organometallics*, **1983**, 2, 938.
46. Shaver, A.; Hartgerink, J. *Can. J. Chem.* **1987**, 65, 1190.
47. Shaver, A.; Lai, R.D. *Inorg. Chem.* **1988**, 27, 4664.

48. Morris, S.A. Ph.D Thesis, McGill University, 1987, p 104.
49. a) Legzdins, P.; Sánchez, L. *J. Am. Chem. Soc.* **1985**, *107*, 5525.
b) Evans, S.V.; Legzdins, P.; Rettig, S.J.; Sánchez, L.; Trotter, J.
Organometallics, **1987**, *6*, 10.
c) Legzdins, P.; Rettig, S.J.; Sánchez, L. *Organometallics*, **1988**, *7*, 2394.
50. Seyferth, D.; Henderson, R.S.; Song, L.-C. *Organometallics*, **1982**, *1*, 125.
51. Seyferth, D.; Womack, G.B. *J. Am. Chem. Soc.* **1982**, *104*, 6839.
52. a) King, R.B.; Bisnette, M.B. *Inorg. Chem.* **1965**, *4*, 482.
b) King, R.B.; Bisnette, M.B. *Ibid* **1965**, *4*, 486.
53. King, R.B.; Bissonette, M.B. *J. Am. Chem. Soc.* **1964**, *86*, 1267.
54. Ahmad, M.; Bruce, R.; Knox, G.R. *J. Organomet. Chem.* **1966**, *6*, 1.
55. a) Ahmad, M.; Bruce, R.; Knox, G.R. *Z. Naturforsch.* **1966**, *21b*, 289.
b) Ahmad, M.; Knox, G.R.; Preston, F.J.; Reed, R.I. *J. Chem. Soc. Chem. Commun.* **1967**, 138.
56. Boorman, P.M.; Patel, V.D.; Kerr, K.A.; Coddling, P.W.; Van Roey, P. *Inorg. Chem.* **1980**, *19*, 3508.
57. Holm, R.H.; King, R.B.; Stone, F.G.A. *Inorg. Chem.* **1963**, *2*, 219.
58. Duncan, W.E.; Ott, E.; Reid, E.E. *Ind. Eng. Chem.* **1931**, *23*, 381.
59. Braterman, P.S. *J. Chem. Soc. Chem. Commun.* **1968**, 91.
60. Abel, E.W.; Harrison, W.; McLean, R.A.N.; Marsh, W.C.; Trotter, J.T. *J. Chem. Soc. Chem. Commun.* **1967**, 138.
61. Blower, P.J.; Dilworth, J.R.; Hutchinson, J.P.; Zubieta, J.A. *Inorg. Chim. Acta* **1982**, *65*, L225.
62. Boorman, P.M.; O'Dell, B.D. *J. Chem. Soc. Dalton Trans.* **1980**, 257.
63. Satchell, D.P.N. *Chem. Soc. Rev.* **1977**, *6*, 345.
64. Kamata, M.; Hirotsu, K.; Higuchi, T.; Tatsumi, K.; Hoffmann, R.; Yoshida,

- T.; Otsuka, S. *J. Am. Chem. Soc.* **1981**, *103*, 5772.
65. Krüger, H.J.; Holm, R.H. *Inorg. Chem.* **1989**, *28*, 1148.
66. Kotz, J.C.; Vining, W.; Coco, W.; Rosen, R.; Dias, A.R.; Garcia, M.H. *Organometallics*, **1983**, *2*, 68.
67. Weinmann, D.J.; Abrahamson, H.B. *Inorg. Chem.* **1987**, *26*, 3034.
68. Adzamlı, I.K.; Libson, K.; Lydon, J.D.; Elder, R.C.; Deutsch, E. *Inorg. Chem.* **1979**, *18*, 303.
69. a) Hausinger, R.P. *Microbiol. Rev.* **1987**, *51*, 22.
b) Cammack, R. *Adv. Inorg. Chem.* **1988**, *32*, 297.
70. Adzamlı, I.K.; Nosco, D.L.; Deutsch, E. *J. Inorg. Nucl. Chem.* **1980**, *42*, 1364.
71. Darensbourg, M.Y.; Liaw, W.-F.; Riordan, C.G. *J. Am. Chem. Soc.* **1989**, *111*, 8051.
72. Elder, R.C.; Kennard, G.J.; Payne, M.D.; Deutsch, E. *Inorg. Chem.* **1978**, *17*, 1296.
73. Nosco, D.L.; Elder, R.C.; Deutsch, E. *Inorg. Chem.* **1980**, *19*, 2545.
74. Sato, F.; Iida, K.; Sato, M. *J. Organomet. Chem.* **1972**, *39*, 197.
75. Bladon, P.; Bruce, R.; Knox, G.R. *J. Chem. Soc. Chem. Commun.* **1965**, 557.
76. Avdeef, A.; Facker, J.P., Jr. *J. Coord. Chem.* **1975**, *4*, 211.
77. Chadha, R.K.; Kumar, R.; Tuck, D.G. *Polyhedron*, **1988**, *7*, 1121.
78. Gattow, G.; Behrendt, W. in "Topics in Sulfur Chemistry"; Senning, A., Ed.; Georg Thieme: Stuttgart, West Germany, 1977; Vol. 2, pp 178-190 and references therein.
79. Coucouvanis, D. *Prog. Inorg. Chem.* **1979**, *26*, 301.
80. Burns, R.P.; McCullough, F.P.; McAuliffe, C.A. *Adv. Inorg. Chem. Radiochem.* **1980**, *23*, 211.
81. Black, S.J.; Einstein, F.W.B.; Hayes, P.C.; Kumar, R.; Tuck, D.G. *Inorg.*

Chem. **1986**, *25*, 4181.

82. Davidson, J.L.; Carlton, L. *J. Chem. Soc. Chem. Commun.* **1984**, 964.
83. Carlton, L.; Davidson, J.L.; Shiralian, M. *J. Chem. Soc. Dalton Trans.* **1986**, 1577.
84. Ashby, M.T.; Enemark, J.H. *Organometallics*, **1987**, *6*, 1318.
85. Kubicki, M.M.; Kergoat, R.; Scordia, H.; Gomes de Lima, L.C.; Guerchais, J.E.; L'Haridon, P. *J. Organomet. Chem.* **1988**, *340*, 41.
86. Wang, S.; Fackler, J.P. Jr. *Organometallics*, **1989**, *8*, 1578.
87. a) Streitwieser, A.; Ewing, S.P. *J. Am. Chem. Soc.* **1975**, *97*, 190.
b) Streitwieser, A.; Williams, J.E. *Ibid* **1975**, *97*, 191.
88. Coates, G.E.; Whitcombe, R.A. *J. Chem. Soc.* **1956**, 3351.
89. Kamata, M.; Hirotsu, K.; Higuchi, T.; Kito, M.; Tatsumi, K.; Hoffmann, R.; Otsuka, S.; Yoshida, T. *Organometallics* **1982**, *1*, 227.
90. Millar, M.; O'Sullivan, T.; de Vries, N.; Koch, S.A. *J. Am. Chem. Soc.* **1985**, *107*, 3714.
91. Ashby, M.; Enemark, J. H. *J. Am. Chem. Soc.* **1986**, *108*, 730.
92. Millar, M.; Koch, S.A. *J. Am. Chem. Soc.* **1983**, *105*, 3362.
93. a) Lewis, D.F.; Lippard, S.J. *Inorg. Chem.* **1972**, *11*, 621.
b) Lewis, D.F.; Lippard, S.J. *J. Am. Chem. Soc.* **1975**, *97*, 2697.
c) Wood, T.E.; Deaton, J.C.; Corning, J.; Wild, R.E.; Walton, R.A. *Inorg. Chem.* **1980**, *19*, 2614 and references therein.
d) Chatt, J.; Pombeiro, A.J.L.; Richards, R.L. *J. Chem. Soc. Dalton Trans.* **1979**, 1585.
e) Brisdon, B.J.; Edwards, D.A.; Paddick, K.E.; Drew, M.G.B. *J. Chem. Soc. Dalton Trans.* **1980**, 1317.
f) Girolami, G.S.; Andersen, R.A. *J. Organomet. Chem.* **1979**, *26*, 302.

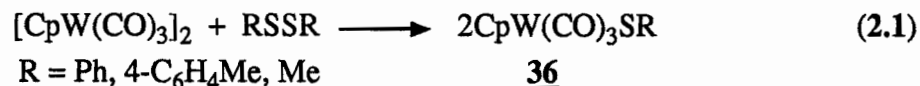
94. a) Griffith, W.P.; Pawson, D. *J. Chem. Soc. Dalton Trans.* **1973**, 1315.
b) Erler, B.S.; Dewan, J.C.; Lippard, S.J.; Tyler, D.R. *Inorg. Chem.* **1981**, *20*, 2719.
c) Crayston, J.A.; Almond, M.J.; Downs, A.J.; Poliakoff, M.; Turner, J.J. *Inorg. Chem.* **1984**, *23*, 3051.
d) La Monica, G.; Cenini, S. *J. Chem. Soc. Dalton Trans.* **1980**, 1145.
e) La Monica, G.; Cenini, S. *Inorg. Chim. Acta* **1978**, *29*, 183.
95. Ashby, M.T.; Enemark, J.H.; Lichtenberger, D.L. *Inorg. Chem.* **1988**, *27*, 191.

CHAPTER 2

The Preparation of $\text{CpW}(\text{CO})_2(\text{PPh}_3)\text{SR}$ ($\text{R} = \text{CHMe}_2, \text{CH}_2\text{Ph}, 4\text{-C}_6\text{H}_4\text{Me}, \text{Ph}, \text{phthalimido}$)

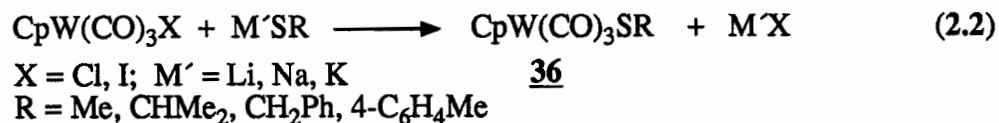
Introduction

The traditional preparative techniques used to synthesize cyclopentadienyl tungsten thiolate complexes can be separated into two classes. The first treats the tungsten carbonyl dimers, $[\text{CpW}(\text{CO})_3]_2$ (1), with organic disulfides, RSSR , to produce thiolate complexes, sometimes under UV or thermal conditions (Equation 2.1). However,

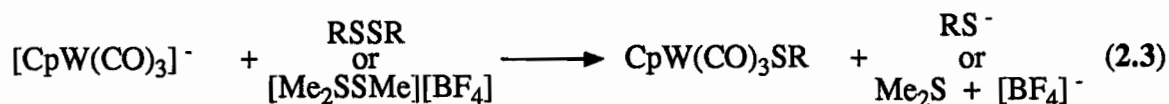


this method is susceptible to the presence of dimer impurities, $[\text{CpW}(\text{CO})_2\text{SR}]_2$. One publication (2) reported the synthesis of $\text{CpW}(\text{CO})_3\text{SR}$ ($\text{R} = \text{Ph}, 4\text{-C}_6\text{H}_4\text{Me}$) 36 by this route but also reported that the product goes on to give dimeric compounds under the same conditions. Earlier, Treichel *et al* (3) had reported using the same process to produce $[\text{CpW}(\text{CO})_2\text{SMe}]_2$ but this formulation was disputed by others (4) who claimed that the product was actually the monomer, $\text{CpW}(\text{CO})_3\text{SMe}$. These workers (4), however, gave no supporting evidence for their conclusion.

The other route to terminal thiolate tungsten complexes involves a metathetical reaction between a tungsten halide and the thiolato anion in the form of $\text{M}'\text{SR}$ (Equation 2.2) (5,6). The driving force for this reaction is the formation and precipitation of the salt, $\text{M}'\text{X}$.



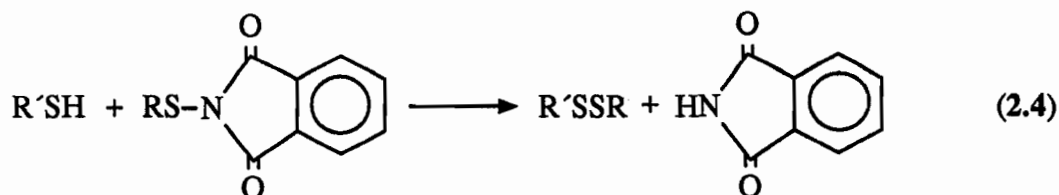
Recently, Treichel and Nakagaki have reported the preparation of tungsten thiolate complexes (36) by the reaction of $[\text{CpW(CO)}_3]^-$ and RSSR (R = Me, Ph, CF_3) or with $[\text{Me}_2\text{SSMe}]\text{BF}_4$ (Equation 2.3) (7). However, the reaction using MeSSMe is slow (~34



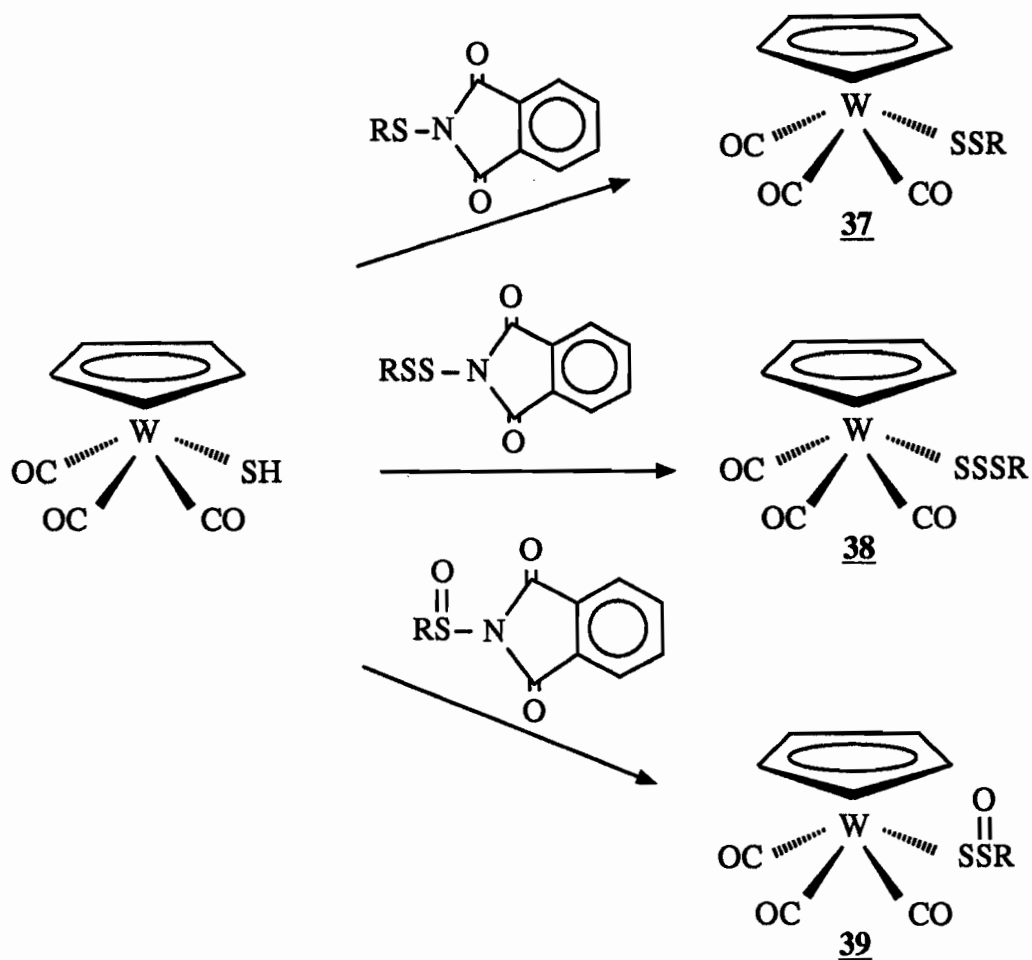
R = Me, CF_3 , Ph

hours) and any excess of $[\text{Me}_2\text{SSMe}]\text{BF}_4$ gives rise to a second reaction causing decomposition.

Another route to metal thiolate complexes has involved the sulfur transfer reagent, RS-phthalimide (RS-phth) (6,8-10). These reagents are well-known in organic chemistry as sources of "RS⁺" in conjunction with organic thiols to give unsymmetrical disulfides (Equation 2.4) (11,12). These thiophthalimide compounds were first used in

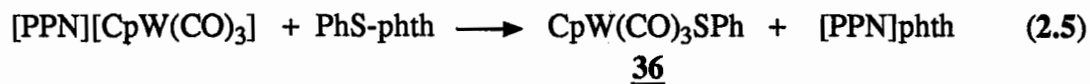


organometallic chemistry to give cobalt complexes with coordinated disulfides (Equation 1.26) (8). Tungsten disulfides (37), trisulfides (38) and thiosulphenyl (39) complexes were prepared from the appropriate sulfur transfer reagents and the metal thiol in an analogous reaction to Equation 2.4 (Scheme 2.1) (6,9). Treichel and coworkers (10) reacted these



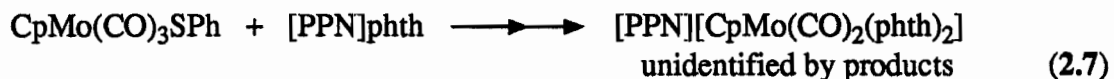
Scheme 2.1 The preparation of tungsten disulfides (**37**), trisulfides (**38**) and thiosulfonyl (**39**) complexes from phthalimido sulfur transfer reagents and $\text{CpW(CO)}_3\text{SH}$ (6,9).

sulfur transfer reagents with $[\text{CpW(CO)}_3]^-$ to prepare $\text{CpW(CO)}_3\text{SPh}$ (**36**) (Equation 2.5).



However, this method does not work well for other metal carbonyl anions. The byproduct, $[\text{PPN}]\text{phth}$, reacts with the thiolate product to give metal-phthalimide complexes. The reaction between $[\text{PPN}][\text{CpMo(CO)}_3]$ and PhS-phth gives $\text{CpMo(CO)}_3\text{SPh}$ which is rapidly converted to a species believed to be

[PPN][CpMo(CO)₂(phth)₂] (Equations 2.6 and 2.7).

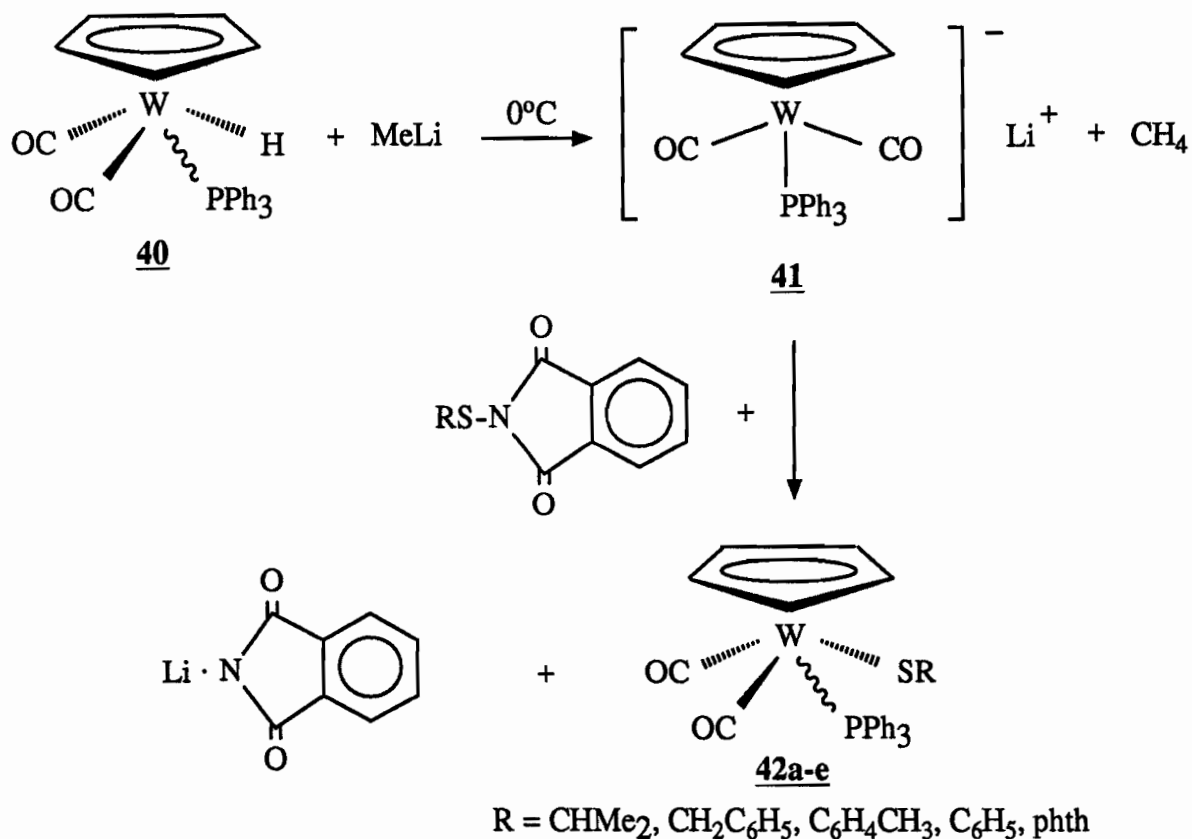


Abrahamson and Weinmann reported the synthesis of CpW(CO)₂(PPh₃)SR (R = Ph, 4-C₆H₄Me) from the photolysis of CpW(CO)₃SR (**36**) and PPh₃ in benzene but gave no yields (2). However, dimeric products may be a significant impurity by this method since the photolysis of **36** also yielded a complex mixture of these products. Both these reports (2,10) coincided with our preparation of the triphenylphosphine complexes, CpW(CO)₂(PPh₃)SR. Attempts to prepare CpW(CO)₂(PPh₃)SR using the metathetical reaction between CpW(CO)₂(PPh₃)Cl and LiSCHMe₂ did not work well, giving a mixture of product and starting materials. The complex CpW(CO)₂(PPh₃)H was known (14), and proton abstraction from the metal hydride with MeLi was likely to give an anionic species. Hence, it seemed reasonable that the anion, [CpW(CO)₂(PPh₃)]⁻ (15), treated with RS-phth would give CpW(CO)₂(PPh₃)SR.

Results and Discussion

A. Preparation of $\text{CpW}(\text{CO})_2(\text{PPh}_3)\text{SR}$

The preparation of the thiolate complexes, $\text{CpW}(\text{CO})_2(\text{PPh}_3)\text{SR}$ ($\text{R} = \text{CHMe}_2$, CH_2Ph , $4\text{-C}_6\text{H}_4\text{Me}$, Ph , phth) (**42a-e**), proceeded via the treatment of the anion, $[\text{CpW}(\text{CO})_2(\text{PPh}_3)]^-$, **41** with a solution of the appropriate sulfur transfer reagent, RS-phth (Scheme 2.2). The anion, **41**, was prepared *in situ* by treatment of $\text{CpW}(\text{CO})_2(\text{PPh}_3)\text{H}$, **40**, with MeLi at 0°C . The orange-yellow **42a-e** were isolated as



Scheme 2.2 The preparation of $\text{CpW}(\text{CO})_2(\text{PPh}_3)\text{SR}$ (**42**).

mixtures of cis (red-orange) and trans (yellow) isomers in good yield (50-70%). The isomers equilibrate in solution (trans:cis in CDCl_3 : 3.5 ± 0.3 , **42a**; 2.6 ± 0.2 , **42b**; 2.8 ± 0.2 , **42c**) and column chromatography yielded only samples that were rich in one isomer or the other.

The cis and trans isomers were, nevertheless, distinguishable by ^1H NMR (Table 2.1) and IR spectroscopy. In the cis isomer, the Cp ring protons appear as a sharp singlet in the NMR spectrum, whereas in the trans isomer these protons are coupled to the phosphorus atom and appear as a doublet, $J(\text{P-H}) = 2 \text{ Hz}$ (16). In the trans isomer of $\text{CpW}(\text{CO})_2(\text{PPh}_3)\text{SCHMe}_2$, one doublet is observed for the methyl groups since they are magnetically equivalent. However, in the cis isomer, the methyl groups are diastereotopic and appear as two doublets. Similarly, for the cis isomer of $\text{CpW}(\text{CO})_2(\text{PPh}_3)\text{SCH}_2\text{Ph}$, the methylene protons are diastereotopic and appear as an AB pattern.

The carbonyl stretching bands in the IR spectrum also distinguish a cis-rich from a trans-rich mixture. A strong symmetric stretch in the $1960\text{-}1930 \text{ cm}^{-1}$ region and a weak asymmetric stretch in the $1870\text{-}1850 \text{ cm}^{-1}$ range characterize a cis-rich solution. Trans-rich solutions exhibit an opposite $\nu(\text{CO})$ profile (16).

The obvious and traditional preparative routes (Scheme 2.3) to these thiolate complexes did not give products in good yield or the products were difficult to isolate. Since the reaction of $\text{CpW}(\text{CO})_3\text{X}$ ($\text{X} = \text{Cl}, \text{I}$) and RS^- is known (5,6) to give thiolate complexes (Equation 2.2), the reaction (i) between $\text{CpW}(\text{CO})_2(\text{PPh}_3)\text{Cl}$ and LiSCHMe_2 was attempted. Only a 50% conversion (observed by NMR) to the thiolate compound was obtained. Further, the starting material and product were inseparable by column chromatography. Attempts to prepare the derivative where $\text{R} = \text{H}$ (**42f**) by the reaction of the halide $\text{CpW}(\text{CO})_2(\text{PPh}_3)\text{X}$ ($\text{X} = \text{Cl}, \text{I}$) and NaSH were thwarted by the apparent lack of reactivity of the W-X bond, a surprising contrast to $\text{CpW}(\text{CO})_3\text{X}$.

Table 2.1 ^1H NMR^{a,b} Data for $\text{CpW}(\text{CO})_2(\text{PPh}_3)\text{SR}$ and $\text{CpW}(\text{CO})_2(\text{PPh}_3)\text{E}$ (E = H, CH_2Ph)

No.	Compound	isomer	C_5H_5	CHMe_2	CH_2Ph	CH_3	C_6H_x	W-H
<u>42a</u>	$\text{CpW}(\text{CO})_2(\text{PPh}_3)\text{SCHMe}_2$	cis trans	5.49 5.05 ^e	2.53 ^c 2.81 ^c		0.92, 0.11 ^d 1.31 ^d		
<u>42b</u>	$\text{CpW}(\text{CO})_2(\text{PPh}_3)\text{SCH}_2\text{Ph}$	cis trans	5.09 4.85 ^h		3.76, 3.42 ^f 3.64		7.26 ^g 7.26 ^g	
<u>42c</u>	$\text{CpW}(\text{CO})_2(\text{PPh}_3)\text{S-4-C}_6\text{H}_5\text{Me}$	cis trans	5.49 5.18 ^e			2.24 2.28	6.88, 7.09 ⁱ 7.00, 7.34 ^j	
<u>42d</u>	$\text{CpW}(\text{CO})_2(\text{PPh}_3)\text{SPh}$	cis trans	5.50 5.13 ^e				7.01 ^g 7.18 ^g	
<u>42e</u>	$\text{CpW}(\text{CO})_2(\text{PPh}_3)\text{Sphth}$	trans	5.39 ^e				7.60, 7.77 ^k	
<u>44</u>	$\text{CpW}(\text{CO})_2(\text{PPh}_3)\text{D}$ at -22.6°C	cis/trans { cis trans	5.01 5.19 4.97					-6.40 ^{l,m} -6.87 ^{n,m} -7.58 ^{o,m}
<u>45</u>	$\text{CpW}(\text{CO})_2(\text{PPh}_3)\text{CH}_2\text{Ph}$	trans	4.73 ^e		3.02 ^e		6.95, 7.14 ^p	

^a In CDCl_3 solution; reported in ppm. ^b Phenyl resonances of PPh_3 appeared in the range 7.38-7.44 ppm.

^c Septet, $J(\text{H-H}) = 6.6$ Hz. ^d Doublet, $J(\text{H-H}) = 6.6$ Hz. ^e Doublet, $J(\text{P-H}) = 2.0$ Hz.

^f Doublet, AB quartet, $\Delta\nu = 67$ Hz, $J(\text{H-H}) = 13.4$ Hz. ^g $x = 5$, multiplet. ^h Doublet, $J(\text{P-H}) = 2.2$ Hz.

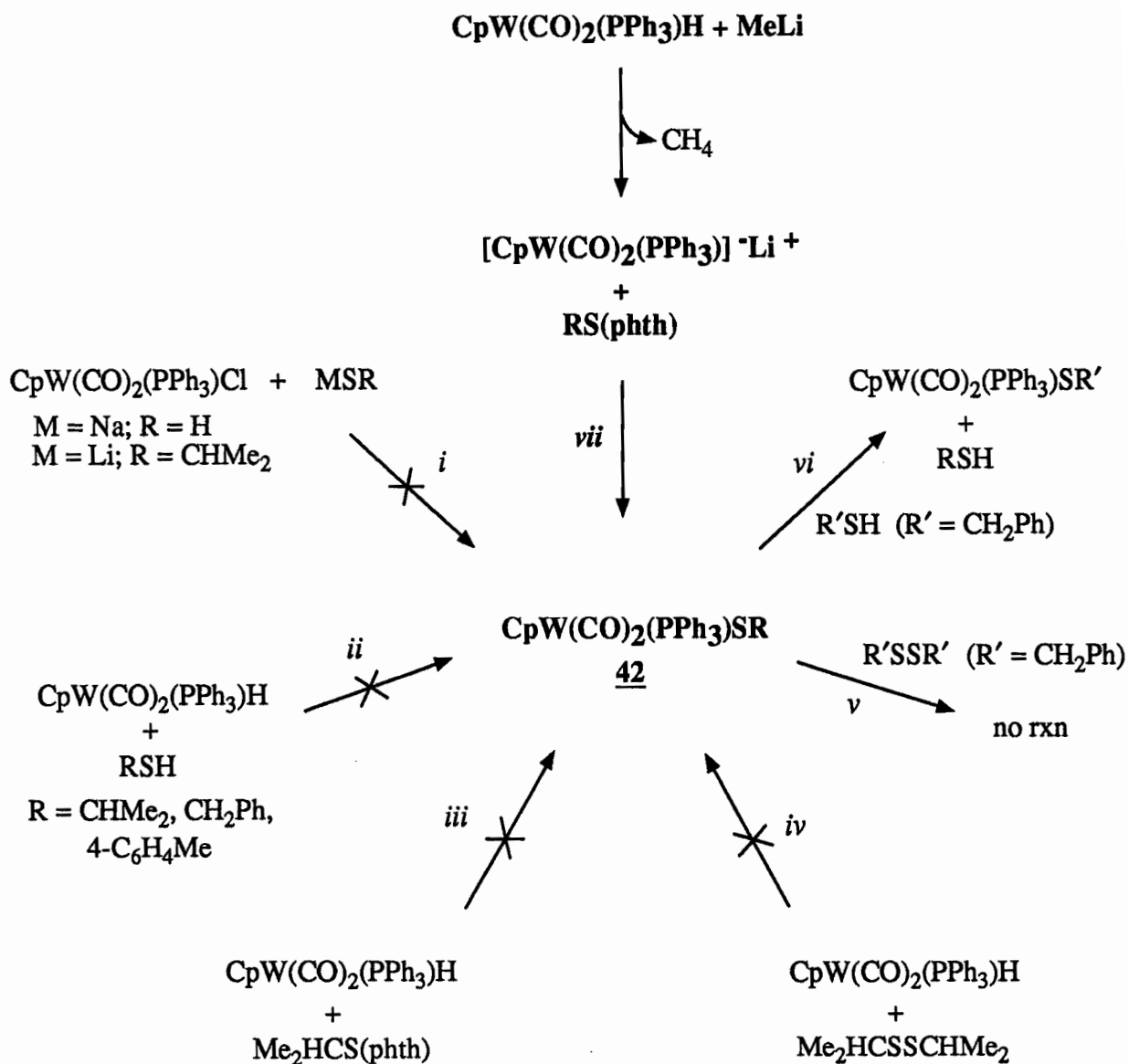
ⁱ $x = 4$, AB quartet, $\Delta\nu = 41$ Hz, $J(\text{H-H}) = 8$ Hz. ^j $x = 4$, AB quartet, $\Delta\nu = 69$ Hz, $J(\text{H-H}) = 8$ Hz.

^k $x = 4$, Doublet of multiplets. ^l Broad doublet.

^m For 100% W-H, integration Cp:H is 27.8:5.56; found, 27.8:2.0; 36%:64% W-H:W-D

ⁿ Doublet, $J(\text{P-H}) = 66$ Hz, $J(^{183}\text{W-H}) = 40$ Hz. ^o Doublet, $J(\text{P-H}) = 22$ Hz.

^p $x = 5$, Doublet of multiplets.



Scheme 2.3 The preparative routes to $\text{CpW}(\text{CO})_2(\text{PPh}_3)\text{SR}$.

Other attempts to prepare 42 included the treatment of 40 with the organic thiol, RSH ($\text{R} = \text{CHMe}_2, \text{CH}_2\text{Ph}, 4\text{-C}_6\text{H}_4\text{Me}$) (*ii*), but this gave no reaction as did the treatment of 40 with $\text{Me}_2\text{HCS}(\text{phth})$ (*iii*) and the disulfide $\text{Me}_2\text{HCSSCHMe}_2$ (*iv*). Therefore, the synthesis of $\text{CpW}(\text{CO})_2(\text{PPh}_3)\text{SR}$, 42, reported here (Scheme 2.2) is the most reliable to date. The formation of 42 via the anion $[\text{CpW}(\text{CO})_2(\text{PPh}_3)]^-$, 41, is similar to the

treatment of $[\text{CpW}(\text{CO})_3]^-$ with RS-phth (Equation 2.5) (10) and the chloro anion displacement reaction of $[\text{CpCr}(\text{CO})_3]^-$ and S_2Cl_2 (Equation 2.8) (17). In accord with



previous results (10) with $[\text{CpW}(\text{CO})_3]^-$, no further reaction of **42** and the lithium-phthalimide byproduct occurred to give a metal-phthalimide complex as was noted with the molybdenum analogue, $[\text{CpMo}(\text{CO})_3]^-$ (Equation 2.6).

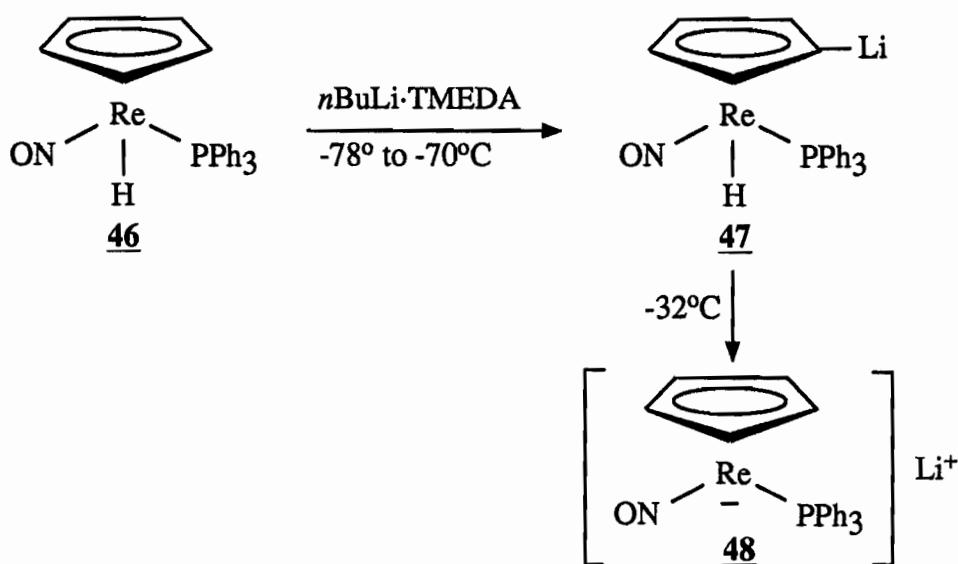
The only disadvantage to Scheme 2.2 for the preparation of thiolate complexes is the time-consuming syntheses of the sulfur transfer reagents. In addition, not all these reagents can be prepared in the same manner since disulfides (needed as starting material) with unusual R groups are not always commercially available. However, this inconvenience may be alleviated by thiolate exchange of **42** with organic thiol, RSH. An NMR scale experiment in CDCl_3 showed that the SR groups were exchanged when the tungsten thiolate **42a** was treated with PhCH_2SH (Scheme 2.3 reaction (vi)) at room temperature to give **42b** and Me_2CHSH in quantitative yield within 3 hours. No reaction occurred with the disulfide $\text{PhCH}_2\text{SSCH}_2\text{Ph}$ (v). Thus, route (vi) outlines the possibility of preparing different tungsten thiolates, needing the synthesis of only one sulfur transfer reagent, RS-phth where R is a small alkyl group leading to a volatile RSH which is easily removed by evaporation.

B. Characterization of $[\text{CpW}(\text{CO})_2(\text{PPh}_3)]^-$

The anion, **41**, is an interesting species that is a potential source of new tungsten complexes in the same way $[\text{CpW}(\text{CO})_3]^-$ (18) and other organometallic anions (7,10) have been utilized. A report briefly mentions **41** as one of many products generated from the reaction of $\text{CpW}(\text{CO})_2(\text{PPh}_3)\text{Cl}$ and Na amalgam (15). In our study, the anion, **41**,

was treated with I_2 , D_2O , and $ClCH_2Ph$, giving the iodide $CpW(CO)_2(PPh_3)I$, **43** (19), the deuteride $CpW(CO)_2(PPh_3)D$, **44** (W-D:W-H 65:35 determined by 1H NMR and mass spectral analyses) (16c), and $CpW(CO)_2(PPh_3)CH_2Ph$, **45**, respectively. The relatively high yield of $CpW(CO)_2(PPh_3)H$ (**40**) isolated from a preparation designed to produce ~100% of the deuterated compound **44** may be accounted for by: 1) traces of H_2O in the THF solvent; 2) H_2O in the D_2O itself, a hygroscopic material; 3) incomplete reaction with $MeLi$ or 4) a combination of these reasons.

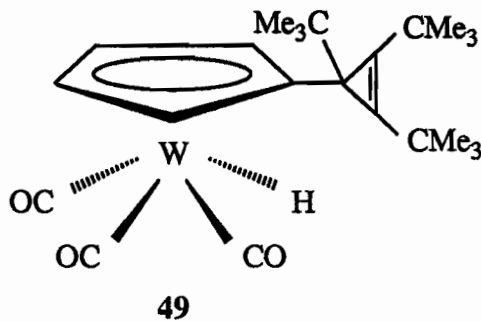
Recently, it was reported that treatment of $CpRe(NO)(PPh_3)H$, **46**, (20-23) with $nBuLi \cdot TMEDA$ caused initial deprotonation at the Cp ring, followed by migration of the



Scheme 2.4

hydride from the metal to the ring (Scheme 2.4). Treatment of $CpRe(NO)(PPh_3)D$ resulted in ring-proton abstraction rather than abstraction of the deuterium coordinated to the metal. The ^{31}P NMR spectrum of **46** treated with $nBuLi \cdot TMEDA$ at $-78^\circ C$ showed three distinct peaks due to **46**, **47**, and **48** as the sample was warmed to $-30^\circ C$. Treating the anion at $-42^\circ C$ with $MeOSO_2CF_3$ gave $(C_5H_4Me)Re(NO)(PPh_3)H$, whereas

treatment of the sample with other electrophiles **E**, gave $\text{CpRe}(\text{NO})(\text{PPh}_3)\text{E}$, indicating that **48** was more stable than **47**. In a closely related system, $\text{CpRe}(\text{NO})(\text{PPh}_3)\text{CHO}$ (22,24), the deprotonation of the Cp ring occurs due to the greater acidity of the Cp hydrogen atom than the formyl hydrogen atom. The tungsten tricarbonyl anion,



$[\text{CpW}(\text{CO})_3]^-$ undergoes substitution at the ring with 1,2,3-tri-*t*-butylpropenium ion to give **49** (25); however, this is the only example known for this system.

Based on these reports, a brief study of the deprotonation of $\text{CpW}(\text{CO})_2(\text{PPh}_3)\text{H}$ (**40**) was carried out. The variable temperature ^{31}P NMR spectra of a sample of **40** in THF-d_8 at -80°C revealed two peaks due to *cis* and *trans*-**40** (43.2 ppm, $J(\text{P-}^{183}\text{W}) = 332$ Hz and 43.0 ppm, $J(\text{P-}^{183}\text{W}) = 364$ Hz, respectively). After treatment with MeLi an additional peak due to $[\text{CpW}(\text{CO})_2(\text{PPh}_3)]^-$ (**41**) (57.9 ppm, $J(\text{P-}^{183}\text{W}) = 590$ Hz) appeared. The ^1H NMR spectrum of **40** in the absence of MeLi at -78°C showed 2 Cp singlets (5.32, 5.05 ppm) due to *cis* and *trans*-**40**. After the addition of MeLi, another Cp singlet at 4.65 ppm was observed. The peaks due to the *cis* and *trans* isomers of **40** were consumed as the reaction continued, until only the peak at 4.65 ppm remained. The ^1H NMR spectrum of $\text{CpW}(\text{CO})_2(\text{PPh}_3)\text{D}$ (**44**) treated with MeLi at -78°C also showed these three Cp singlets exhibiting the same behavior.

The results from the low temperature ^1H NMR study of $\text{CpW}(\text{CO})_2(\text{PPh}_3)\text{H}$ (**40**) (or $\text{CpW}(\text{CO})_2(\text{PPh}_3)\text{D}$, **44**) and MeLi giving 3 Cp resonances may indicate the presence of a tungsten species analogous to **47** that is unstable or is consumed in the reaction to

give **41**. As well, the 35% yield of **40** obtained in the synthesis of **44** might imply some abstraction and migration of hydrogen atoms from the Cp ring to the metal. However, there are other results that conflict with this view. All of the Cp resonances in any of the low temperature spectra are singlets which is inconsistent with what would be expected if the Li^+ was coordinated to the ring as in **47**. Also, the two Cp peaks which were consumed in the reaction were due to the cis and trans isomers of **40**. The relatively high yield of **40** found from the preparation of **44** may be accounted for as mentioned earlier. In the ^1H NMR study of **40** and **44** treated with MeLi, slow gas evolution was observed although neither CH_3D nor CH_4 could be identified in the spectrum. Although 3 resonances were observed in the low temperature ^{31}P NMR spectrum, these could be accounted for by considering that the two isomers of **40** and the anion **41** are present. An additional resonance that might signify the presence of a tungsten species similar to **47** was not observed in contrast to the results from the $\text{CpRe}(\text{NO})(\text{PPh}_3)\text{H}$ system. The formation of the compounds $\text{CpW}(\text{CO})_2(\text{PPh}_3)\text{I}$ (**43**), $\text{CpW}(\text{CO})_2(\text{PPh}_3)\text{D}$ (**44**), and $\text{CpW}(\text{CO})_2(\text{PPh}_3)\text{CH}_2\text{Ph}$ (**45**) is more evidence that substitution takes place at the tungsten center. Although the formation of a tungsten species analogous to **47**, which is highly unstable even at low temperatures, cannot be ruled out, there is no real indication that deprotonation of the Cp ring of **40** is occurring.

General Experimental

I. Apparatus and General Procedures

All reactions were performed in three-necked flasks or Schlenk tubes of the appropriate size and equipped with a nitrogen inlet. Standard inert atmosphere techniques (26) were used in all manipulations. Flasks were charged with solids and then evacuated and filled with nitrogen twice. Solvents were transferred by syringe. Filtrations were performed under nitrogen and filtrates were reduced to dryness using an oil pump. The packing and elution of chromatography columns were performed in air using solvents as purchased. Activated alumina (80-200 mesh) was purchased from Anachemia.

Recrystallizations were done under nitrogen in Schlenk tubes or three-necked flasks using distilled solvents. A layering technique was employed to recrystallize most compounds. This consisted of dissolving the crude product in a minimal amount of solvent, then carefully adding a precipitating solvent such that it did not mix with the lower layer. Mixing then occurred slowly as the flask was left overnight or longer at -16°C . The mother liquors were removed via a disposable pipette, then the crystals were washed with the precipitating solvent and dried overnight under vacuum.

Solution infrared (IR) spectra were recorded through a 0.1 mm pathlength between NaCl plates on a Perkin-Elmer 457 grating infrared spectrophotometer, calibrated using the 1601.4 cm^{-1} band of polystyrene film. Band positions are accurate to $\pm 6\text{ cm}^{-1}$. Spectra of solids as Nujol mulls between NaCl or KCl plates were recorded on an Analect AQS-18 fourier-transform infrared (FT-IR) spectrophotometer, equipped with a

KBr beam splitter ($4400\text{--}450\text{ cm}^{-1}$) and referenced using the red line (632.8 nm) of a He/Ne laser. A triglycine sulfate (TGS) detector was used with a standard resolution of 4 cm^{-1} .

Fourier transform infrared photoacoustic spectroscopy (PAS) was also used to record IR spectra for complexes $\text{CpW}(\text{CO})_2(\text{PPh}_3)\text{S}(\text{SO}_2)\text{R}$ **80a-c**. This method requires no sample preparation. The technique involves an intensity-modulated light beam incident on the sample placed in a closed cell. Light absorption causes a temperature rise within the sample, which propagates to the surface as a thermal wave. Since the cell is closed, the increase in temperature leads to a pressure rise. As the light is modulated, the pressure is also modulated, and can thus be detected by a microphone and lock-in amplifier (27). The FTIR-PAS spectra were recorded on a FT-IR Mattson Cygnus 25 spectrometer, factory modified to add a second speed on the mirror drive of the interferometer to facilitate photoacoustic measurements. The standard TGS (triglycine sulfate) detector was used for transmission spectroscopy. An EG & G Princeton Applied Research Model 6003 photoacoustic cell was employed. The sample cup had a 5 mm diameter and was 1 mm deep. The output from the microphone was fed to an EG & G PAR Model 6005 preamplifier and then to the detector input of the spectrometer. Typically, the preamplifier gain was 2000 and the spectrometer gain was unity. The PAS spectra were obtained by averaging 100 scans of 2048 data points, each corresponding to an 8 cm^{-1} resolution. The interferometer mirror velocity was 0.084 cm/s. A double-sided interferogram and a triangular apodization function were used to generate the spectra. Spectra were all ratioed against a background of carbon black (Norit Type A from Polysciences Inc. Warrington, PA, USA) at the same instrument settings. The photoacoustic signal intensity was corrected by subtracting the signal due to positively rectified noise, measured at about 4000 cm^{-1} where no absorption occurs.

The ultraviolet-visible (UV-Vis) spectra of the complexes $\text{CpW}(\text{CO})_2\text{S}_2\text{CSR}$

(62a-c) were recorded on a Hewlett-Packard 8451 diode array spectrophotometer equipped with a deuterium lamp and a Lauda RM6 thermostat. Band positions are correct within ± 2 nm.

Proton nuclear magnetic resonance (^1H NMR) and phosphorus-31 (^{31}P) NMR spectra were recorded on Varian XL-200 and XL-300 spectrometers and all chemical shifts are in δ ppm units relative to an internal standard, tetramethylsilane (TMS) and an external reference, phosphoric acid, H_3PO_4 , respectively. Referencing to H_3PO_4 was performed at room temperature. Shift values are accurate to ± 0.002 ppm. All NMR spectra were measured at ambient temperature ($22^\circ\text{C} \pm 2$) unless otherwise indicated. Variable temperature controllers calibrated with methanol and ethylene glycol gave temperatures that are considered accurate to $\pm 0.5^\circ\text{C}$. The integrity of the samples were checked at ambient temperature following variable temperature experiments.

Low resolution mass spectra were measured on a Hewlett-Packard 5980A mass spectrometer at the McGill University Biomedical Mass Spectrometry Unit, and on a Dupont 21-492B mass spectrometer in the Otto Maass Chemistry Building. At the Biomedical Unit, high resolution and Fast Atom Bombardment (FAB) mass spectra were measured on a ZAB-HS mass spectrometer. FAB samples in a glycerol matrix were measured with an ionization potential (IP) of 10 eV and those in a nitrobenzyl alcohol matrix (NBA) used IPs of 8 eV. Some samples were treated with heptafluorobutyric acid (HFBA) to aid analysis by inducing protonation and forcing the compounds to the surface of the matrix. Electron Impact (EI) mass spectra used ionization potentials of 10 or 70 eV. Chemical ionization (CI) was achieved with an NH_3 source. The isotopes (natural abundance) of W are 180 (0.1%), 182 (26.3%), 183 (14.3%), 184 (30.7%) and 186 (28.6%) and the mass spectral data are reported with respect to ^{184}W as: ionization method, m/z, assignment, rel. int..

Elemental analyses were carried out by Spang Microanalytical Laboratories in

Eagle Harbor, Michigan. Compounds for melting point determinations were placed in grease-sealed capillary tubes under nitrogen. Melting points were determined with a Thomas Hoover capillary melting point apparatus and are uncorrected.

II. CHEMICALS

Tetrahydrofuran (THF), toluene, and hexanes were refluxed over sodium metal and benzophenone and collected by distillation under nitrogen. Dichloromethane was refluxed over P_2O_5 and distilled just prior to use. Absolute ethanol was purged with nitrogen before using. Deuterated solvents were purchased from Merck, Sharp and Dohme in Montréal, Québec and were used as purchased. Methylithium was purchased from Aldrich as a 1.4M solution in diethyl ether and used as received. The chemicals, $PhCH_2Cl$, MeNCO, Me_2CHNCS , and MeNCS also obtained from Aldrich, were used as received. Dicyclohexylcarbodiimide, $(C_6H_{11}N)_2C$, from Sigma Chemicals was kindly supplied by Dr. J. Chin's laboratory. Carbon disulfide (CS_2) was purchased from A & C Chemicals. Sulfur dioxide (SO_2), 99.98%, hydrogen sulfide (H_2S), 99.5% and carbonyl sulfide (COS), 97.5% were used as purchased from Matheson Gas Products, Whitby, Ont. Carbon dioxide (CO_2) obtained as slabs was used as a crushed solid.

The following sulfur transfer reagents, 2-propyl thiophthalimide ($Me_2HCS-phth$), phenylmethyl thiophthalimide ($PhCH_2S-phth$), phenyl thiophthalimide ($PhS-phth$), 4-methylbenzene thiophthalimide ($4-MeC_6H_4S-phth$), and thiobisphthalimide ($phth-S-phth$) were prepared according to the method of Back (12a). Cyclopentadienyltricarbonylhydridotungsten(II), $CpW(CO)_3H$ (28), cyclopentadienyldicarbonyltriphenylphosphinechlorotungsten(II), $CpW(CO)_2(PPh_3)Cl$ (29) and cyclopentadienyldicarbonyltriphenylphosphinehydridotungsten (II), $CpW(CO)_2(PPh_3)H$ **40** (14), were prepared as reported.

Experimental

A. Cis and trans cyclopentadienyldicarbonyltriphenylphosphine-2-propylthiolato-tungsten(II), $\text{CpW}(\text{CO})_2(\text{PPh}_3)\text{SCHMe}_2$, **42a**

The anion, $[\text{CpW}(\text{CO})_2(\text{PPh}_3)]^-$, (**41**), was generated by treating $\text{CpW}(\text{CO})_2(\text{PPh}_3)\text{H}$, (**40**), (1.15 g, 2.0 mmol) in THF (40 mL) at 0°C with a slight excess of MeLi (1.6 mL, 2.2 mmol) added by syringe. After approximately 10 minutes, the clear orange solution became cloudy as a precipitate formed. Five minutes later, a THF solution (20 mL) of 2-propyl thiophthalimide (0.65 g, 2.9 mmol) was slowly added by cannula to the suspension. The solution became clear orange in colour but soon a precipitate formed. Stirring was continued for 3 hours as the slurry was allowed to warm to room temperature. The suspension was then filtered through Celite through a medium-porosity Schlenk filter, and the filtrate reduced to dryness. The dark orange-brown residue was dissolved in a small volume of CH_2Cl_2 and chromatographed on activated alumina (3 x 50 cm column). Elution with CH_2Cl_2 gave a red-orange band followed by a yellow band both of which were collected and reduced to dryness. The residues from both bands were recrystallized from CH_2Cl_2 /hexanes (1:4), each giving a mixture of red and yellow (cis and trans, respectively) crystals of **42a** (0.60 g, 46%, m.p.=158-160°C). Equilibrium constant determined by ^1H NMR (CDCl_3) for trans-42a : cis-42a is 3.5 ± 0.3 . Anal. Calc'd for $\text{C}_{28}\text{H}_{27}\text{O}_2\text{PSW}$: C, 52.35; H, 4.24; S, 4.99. Found: C, 52.20; H, 4.17; S, 4.91.

IR (toluene), $\nu(\text{CO})$: 1930 (m), 1849 (m) cm^{-1} . IR (Nujol): 2742 (w, br), 1939 (m), 1924 (m), 1857 (s), 1842(s), 1310 (w), 1274 (w), 1148 (w), 1090 (m, sh), 1040 (w), 973 (w), 817 (m, sh), 744 (m, sh), 722 (w), 694 (m, sh) cm^{-1} .

Mass spectrum, EI: 380 ($M^+ - PPh_3$, 7.8); 337 ($M^+ - PPh_3 - CH(CH_3)_2$, 39.4); 309 ($M^+ - PPh_3 - CH(CH_3)_2 - CO$, 24.3); 281 ($M^+ - PPh_3 - CH(CH_3)_2 - 2CO$, 34.0); unidentified peaks at 320 (8.4), 294 (3.0).

B. Cis and trans cyclopentadienyldicarbonyltriphenylphosphinephenylmethylthiolatotungsten(II), $CpW(CO)_2(PPh_3)SCH_2Ph$, **42b**

As for **42b**, the anion **41**, was prepared by addition of MeLi (2.0 mL, 2.8 mmol) to a THF solution (40 mL) of **40** (1.35 g, 2.4 mmol). Phenylmethyl thiophthalimide (0.71 g, 2.7 mmol) in THF (15 mL) was added by cannula. Chromatography (2.5 x 10 cm, CH_2Cl_2) gave an orange band that was collected and reduced to dryness. The residue was dissolved in CH_2Cl_2 (10 mL) and ethanol (20 mL) was added. The solvents were well mixed as the flask was swirled and placed under a slight vacuum. Evaporation was stopped at the first sign of recrystallization and the flask was left at room temperature for 1 hour to give **42b** as an orange powder (1.14 g, 69%, m.p.=100-102°C). Equilibrium constant determined by 1H NMR ($CDCl_3$) for trans-42b : cis-42b is 2.6 ± 0.2 . Anal. Calc'd for $C_{32}H_{27}O_2PSW$: C, 55.67; H, 3.94; S, 4.64. Found: C, 54.09; H, 4.16; S, 4.02.

IR (toluene), $\nu(CO)$: 1939 (w), 1859 (m) cm^{-1} . IR (Nujol): 2726 (w), 2673 (w), 1934 (m, sh), 1847 (m, sh), 1310 (w), 1156 (w), 1089 (m), 1026 (w), 817 (w), 743 (w), 694 (w) cm^{-1} .

Mass spectrum, FAB in glycerol: 691 ($M^+ + H$, 0.4); 510 ($M^+ - 2CO - SCH_2Ph - H$, 1.0); 429 ($M^+ + H - PPh_3$, 1.2); 279 ($OPPh_3^+ + H$, 100.0); unidentified peaks at 245 (8.5), 215 (10.8).

C. Cis and trans cyclopentadienyldicarbonyltriphenylphosphine-4-methylbenzene
thiolatotungsten(II), $\text{CpW}(\text{CO})_2(\text{PPh}_3)\text{S}-4\text{-C}_6\text{H}_4\text{Me}$, **42c**

As in A, **41** was prepared by addition of MeLi (2.0 mL, 2.8 mmol) to a THF (50 mL) solution of **40** (1.4 g, 2.5 mmol) and treated with 4-methylbenzene thiophthalimide (0.76 g, 2.8 mmol) in THF (25 mL). After chromatography, recrystallization from $\text{CH}_2\text{Cl}_2/\text{ethanol}$ gave **42c** as a fluffy orange powder (1.16 g, 71%, m.p.=151-153°C). Equilibrium constant determined by ^1H NMR (CDCl_3) for trans-42c : cis-42c is 2.8 ± 0.2 . Anal. Calc'd for $\text{C}_{32}\text{H}_{27}\text{O}_2\text{PSW}$: C, 55.67; H, 3.84; S, 4.64. Found: C, 55.57; H, 3.84; S, 4.69.

IR (toluene), $\nu(\text{CO})$: 1947 (w), 1858 (m) cm^{-1} . IR (Nujol): 2726 (w), 2673 (w), 2356 (w), 2345 (w), 1946 (m), 1933 (m), 1868 (m), 1846 (m), 1310 (w), 118 (w), 1158 (w), 1104 (w), 1089 (w, sh), 1013 (w), 1000 (w), 823 (w), 805 (w), 743 (w), 693 (w) cm^{-1} .

Mass spectrum, EI: 800 ($2\text{M}^+-2\text{CO}^-$, 1.1); 772 ($2\text{M}^+-2\text{PPh}_3^-3\text{CO}^-$, 23.5); 744 ($2\text{M}^+-2\text{PPh}_3^-4\text{CO}^-$, 49.9); 652 ($2\text{M}^+-2\text{PPh}_3^-4\text{CO}^-4\text{-C}_6\text{H}_4\text{Me-H}^+$, 100.0); 562 ($2\text{M}^+-2\text{PPh}_3^-4\text{CO}^-2(4\text{-C}_6\text{H}_4\text{Me})^-$, 38.4); 124 ($\text{SCH}_2\text{Ph}^++\text{H}^-$, 12.5); 91 (CH_2Ph^- , 79.0); unidentified peaks at 534 (16.3), 325 (15.7), 156 (15.3).

D. Cis and trans cyclopentadienyldicarbonyltriphenylphosphinephenylthiolato-
tungsten(II), $\text{CpW}(\text{CO})_2(\text{PPh}_3)\text{SPh}$, **42d**

As for A, **41**, prepared by addition of MeLi (1.5 mL, 2.1 mmol) to a THF (40 mL) solution of **40** (1.0 g, 1.8 mmol) was treated with phenyl thiophthalimide (0.49 g, 1.9 mmol) in THF (10 mL). After chromatography, recrystallization ($\text{CH}_2\text{Cl}_2/\text{ethanol}$ as for **42c**) gave orange microcrystals of **42d** (0.79 g, 65%, m.p.=168-170°C). Anal. Calc'd for

$C_{31}H_{25}O_2PSW$: C, 55.05; H, 3.72; S, 4.74. Found: C, 54.87; H, 3.71; S, 4.78.

IR (toluene), $\nu(CO)$: 1946 (w), 1869 (m) cm^{-1} . IR (Nujol): 2720 (w), 2671 (w), 1940 (s), 1929 (s), 1858 (s), 1844 (s), 1733 (w), 1183 (w), 1157 (w), 1118 (w), 1088 (w), 1026 (w), 1011 (w), 820 (w), 753 (w), 738 (m), 692 (m) cm^{-1} .

Mass spectrum, EI: 772 ($2M^+-2PPh_3\cdot-2CO\cdot$, 0.35); 744 ($2M^+-2PPh_3\cdot-3CO\cdot$, 0.82); 715 ($2M^+-2PPh_3\cdot-4CO\cdot-H\cdot$, 1.7); 638 ($2M^+-2PPh_3\cdot-4CO\cdot-Ph\cdot-H\cdot$, 3.1); 562 ($2M^+-2PPh_3\cdot-4CO\cdot-2Ph\cdot$, 1.1); 358 ($M^+-PPh_3\cdot-2CO\cdot$, 4.0); 281 ($M^+-PPh_3\cdot-2CO\cdot-Ph\cdot$, 0.8); 262 (PPh_3^+ , 100.0); 183 (W^+ , 66.3); 108 ($SPh^+-H\cdot$, 31.3); unidentified peaks at 609 (0.3), 587(0.2), 535 (0.8), 510 (0.3), 481 (0.2).

E. Trans cyclopentadienyldicarbonyltriphenylphosphine-N-phthalimido
thiolatotungsten(II), $CpW(CO)_2(PPh_3)Sphth$, **42e**

Again, as in A, $[CpW(CO)_2(PPh_3)]^-$ prepared by addition of MeLi (1.7 ml, 2.4 mmol) to a THF (40 mL) solution of **40** (1.2 g, 2.1 mmol) was treated with a suspension of phthalimide thiophthalimide (0.71 g, 2.2 mmol) in THF (20 mL) and stirred for 4 hours as the solution was allowed to warm slowly to room temperature. Chromatography gave a dark yellow band which was collected first, closely followed by a large, lighter yellow band collected in two portions which were combined. Both bands were reduced to dryness and the residues recrystallized from CH_2Cl_2 /ethanol to give a fluffy yellow solid, **42e** (total yield: 0.62 g, 40%, m.p.(dec.)=111-112°C.). Anal. Calc'd for $C_{33}H_{24}NO_4PSW$: C, 53.17; H, 3.25; S, 4.30; N, 1.88. Found: C, 52.94; H, 3.31; S, 4.22; N, 1.95.

IR (toluene), $\nu(CO)$: 1950 (m), 1857 (s), 1715 (m), 1692 (shoulder, w) cm^{-1} . IR (Nujol): 1949 (s), 1859 (s), 1715 (s), 1695 (m), 1435 (m), 1342 (s), 1278 (m), 1186 (w), 1162 (s), 1090 (m), 1062 (m), 1000 (w), 864 (w), 825 (w), 748 (w), 715 (m), 694 (m)

cm⁻¹.

Mass spectrum, FAB in glycerol with HFBA: 571 (M⁺-CO-NC(O)C(O)C₆H₄; 39.0); 567 (M⁺-SNC(O)C(O)C₆H₄; 25.2); 543 (M⁺-2CO-NC(O)C(O)C₆H₄; 20.6); 541 (M⁺-CO-SNC(O)C(O)C₆H₄-2H; 21.0); 511 (M⁺-2CO-SNC(O)C(O)C₆H₄; 19.4); 429 (M⁺-2CO-PPh₃+2H; 28.7); 295 (SPPPh₃⁺+H; 50.0); 279 (OPPh₃⁺+H; 100.0); 263 (PPh₃⁺+H; 73.9); 184 (W⁺; 10.0); 130 (Cp₂⁺; 23.5); unidentified peaks at 509 (24.5), 463 (5.2), 399 (10.0), 357 (13.2), 335 (17.7), 217 (9.0), 201 (20.3), 155 (11.9).

F. Other Attempted Preparations of CpW(CO)₂(PPh₃)SR

1. CpW(CO)₂(PPh₃)H, **40**, and Me₂HCSH

In an NMR tube, a small amount of **40** was dissolved in CDCl₃ and Me₂CHSH was added. ¹H NMR spectra were recorded at ambient temperature after 5 minutes, 1, 3.5, 26 and 72 hours but no signals due to **42a** were observed. The peaks due to the starting materials were unchanged. Similar results were obtained for R=CH₂Ph and 4-C₆H₄Me.

2. CpW(CO)₂(PPh₃)H, **40**, and 2-propyl thiophthalimide

To an NMR tube containing a solution of **40** in CDCl₃, a small amount of 2-propyl thiophthalimide was added and the tube shaken. A ¹H NMR spectrum taken after 1.5 hours showed peaks due to the starting materials only.

3. CpW(CO)₂(PPh₃)H, **40**, and Me₂HCSSCHMe₂

To an NMR tube containing a solution of **40** in CDCl₃, a small amount of Me₂CHSSCHMe₂ was added and the tube shaken. After 10 minutes, 30 minutes, 2.5 hours and 6 hours the ¹H NMR spectra were recorded but the peaks due to the starting materials were unchanged.

4. $\text{CpW}(\text{CO})_2(\text{PPh}_3)\text{Cl}$ and LiSCHMe_2

A solution of LiSCHMe_2 was prepared in situ by addition of HSCHMe_2 (0.096 g, 1.3 mmol) to MeLi (0.9 mL, 1.3 mmol) in THF (50 mL) at -78°C . The solution was allowed to warm to room temperature and the reaction completed by warming the flask to $\sim 30^\circ\text{C}$ with stirring for 20 minutes. The complex, $\text{CpW}(\text{CO})_2(\text{PPh}_3)\text{Cl}$, (0.37 g, 0.62 mmol) was added to the above solution as a solid and the resulting solution refluxed for 2 hours. After cooling to room temperature, the solution was reduced to dryness. The ^1H NMR spectrum in CDCl_3 of the residue revealed Cp peaks due to 42a (50%) and $\text{CpW}(\text{CO})_2(\text{PPh}_3)\text{Cl}$ were present in about equal intensities. The residue was dissolved in a minimal amount of CH_2Cl_2 and chromatographed on activated alumina (1.5 x 50 cm). Elution with CH_2Cl_2 gave an orange-yellow band that was collected and reduced to dryness. Recrystallization from CH_2Cl_2 /hexanes gave orange crystals (0.066 g) identified by NMR as $\text{CpW}(\text{CO})_2(\text{PPh}_3)\text{Cl}$. A second crop (0.15 g) was identified as a 50:50 mixture of the thiolate (42a) and the starting chloride.

5. $\text{CpW}(\text{CO})_2(\text{PPh}_3)\text{SCHMe}_2$, 42a, and $\text{PhCH}_2\text{SSCH}_2\text{Ph}$

An NMR sample of 42a, was prepared in CDCl_3 and a small amount of $\text{PhCH}_2\text{SSCH}_2\text{Ph}$ was added. The solution was monitored by NMR with spectra being recorded after 1, 2.5, 6.5 and 24 hours. After one day no reaction between the two starting materials had taken place. Peaks due to a small amount (10%) of the dimer $[\text{CpW}(\text{CO})_2\text{SCHMe}_2]_2$ were observed.

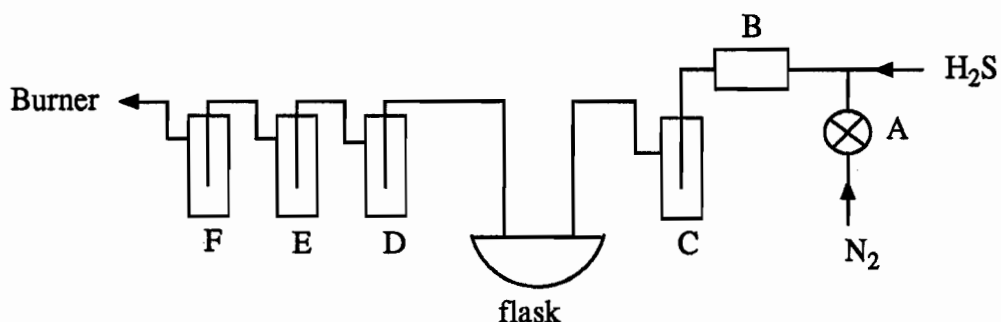
6. $\text{CpW}(\text{CO})_2(\text{PPh}_3)\text{SCHMe}_2$, 42a, and PhCH_2SH

To an NMR sample of 42a in CDCl_3 , an excess of PhCH_2SH was added and the spectrum recorded after 10 minutes. Comparison of the integral region of the Cp peaks

showed greater than 50% of **42a** had been consumed and peaks due to **42b** were present, as well as those of Me_2HCSH . After 30 minutes, 75% of the starting thiolate had disappeared and within three hours the reaction was complete, showing **42b** as the major organometallic species present.

G. Attempted Preparation of $\text{CpW}(\text{CO})_2(\text{PPh}_3)\text{SH}$, **42f**,
from $\text{CpW}(\text{CO})_2(\text{PPh}_3)\text{Cl}$ and NaSH .

Caution: The preparation of NaSH involves the use of H_2S which is very toxic and smelly. Extreme care must be exercised. The reactions must be conducted in an efficient fume hood and every effort must be made to ensure containment of the gas. The use of an H_2S manifold such as the one shown below is strongly recommended.



The gas was dried by means of a calcium chloride column (B) and passed through a Nujol bubbler (C) before entering the reaction vessel. Unreacted gas was passed through three washing towers containing, successively, 5M NaOH (D), saturated aqueous lead acetate (E), and 5M NaOH (F). Any gas not neutralized in these steps was burned. Prior to and after the use of H_2S , the system was flushed for approximately 10 minutes with a strong stream of nitrogen via stopcock (A).

The reagent NaSH was prepared in situ by reacting sodium metal (0.3g, 12.1

mmol) in absolute EtOH (25 mL), and treating with H₂S for 30 minutes. The NaSH solution was then reduced to dryness and a red-brown THF (60 mL) solution of CpW(CO)₂(PPh₃)Cl (1.90g, 3.15 mmol) was added and the reaction allowed to stir overnight. After filtration through Celite, the brown filtrate was reduced to dryness. The NMR and IR spectra of the residue were identical to the starting chloride.

H. Reactions with the anion, [CpW(CO)₂(PPh₃)]⁻, 41

1. With I₂ to give CpW(CO)₂(PPh₃)I, 43 (19)

To a THF (40 mL) solution of 40 (0.52g, 0.92 mmol) at 0°C, MeLi (0.85 mL, 1.19 mmol) was added and the suspension allowed to stir for 15 minutes. Iodine (0.25g, 1.0 mmol) dissolved in toluene (10 mL) was added by cannula and stirring was continued for 5 hours. The reaction solution was reduced to dryness and the red-brown residue extracted with a minimal amount of CH₂Cl₂, leaving a white solid which was soluble in water (LiI). The CH₂Cl₂ extract was chromatographed (activated alumina, 2.5 x 40 cm). Elution with CH₂Cl₂ gave a single red-brown band which was collected and reduced to dryness. The residue was recrystallized from CH₂Cl₂/hexanes (1:1) to give purple-red 43 (0.32 g, 51%, m.p.=190-193°C, lit. m.p.=193°C (21c)). The ¹H NMR spectrum of this product was the same as that reported (19).

2. With D₂O to give CpW(CO)₂(PPh₃)D, 44

To a THF (50 mL) solution of 40 (1.00 g, 1.8 mmol) at 0°C, MeLi (1.5 mL, 2.1 mmol) was added and the yellow solution became a clear orange. After 15 minutes, D₂O (3.0 mL, 165 mmol) was added and the stirred solution allowed to warm to room temperature. Stirring continued for 6 hours during which the reaction solution returned to a clear yellow colour. The solvent was removed in vacuo and the residue extracted with a

1:1 solution of THF/ether (30 mL). This extract was filtered through activated alumina and washed with THF (3 x 10 mL). The filtrate was concentrated to 20 mL and hexanes (~15 mL) was added. After reducing the volume to 15 mL, the solution was filtered to isolate a yellow powder. The mother liquor was reduced to dryness and the residue recrystallized from CH₂Cl₂/hexanes to give yellow-green crystals of **44** (total yield 0.55 g, 55%, m.p.=208-210°C).

Mass spectrum, EI: 566 (3.48), 567 (7.65), 568 (8.25), 569 (7.38), 570 (5.90), 571 (6.08), 572 (1.53) isotope pattern corresponded well with M⁺: 35%/65%, W-H/W-D.

3. With PhCH₂Cl to give CpW(CO)₂(PPh₃)CH₂Ph, **45**

In THF (40 mL), **40** (1.00 g, 1.76 mmol) was treated with MeLi (1.5 mL, 2.1 mmol) to give an orange solution that became cloudy within 15 minutes. To this suspension of **41**, a THF (25 mL) solution of PhCH₂Cl (0.28g, 2.21 mmol) was added by cannula. After 30 minutes, a suspension still remained so a second aliquot of PhCH₂Cl (total 0.50g, 3.9 mmol) was added. Within the next half hour the solution became clear orange in colour and stirring was continued for another 3.5 hours. The solvent was removed in vacuo and the residue extracted with a minimal amount of CH₂Cl₂, leaving a white, watersoluble film (LiCl). The concentrated extract was chromatographed on alumina (3 x 50 cm). Elution with CH₂Cl₂ gave one yellow band which was collected and reduced to dryness. The residue was recrystallized from CH₂Cl₂/hexanes to yield yellow crystals of **45** (0.47 g, 42%; m.p.=175-179°C). Anal. Calc'd for C₃₂H₂₇O₂PW: C, 58.38; H, 4.13; P, 4.70. Found: C, 58.32; H, 4.07; P, 4.62.

IR (toluene) ν(CO): 1929 (m), 1845 (s) cm⁻¹. IR (Nujol): 1928 (s), 1921 (s), 1847 (s), 1837 (s), 1598 (w), 1312 (w), 1186 (w), 1090 (w), 1095 (w), 999 (w), 822 (m), 756 (m), 744 (m), 697 (m), 592 (w), 541 (m), 523 (s), 499 (s) cm⁻¹.

Mass spectrum, CI: 610 (2M⁺-2PPh₃-2CH₂Ph, 0.3); 582

($2M^+ - 2PPh_3 - 2CH_2Ph - CO$, 0.9); 554 ($2M^+ - 2PPh_3 - 2CH_2Ph - 2CO$, 0.04); 526 ($2M^+ - 2PPh_3 - 2CH_2Ph - 3CO$, 0.1); 498 ($2M^+ - 2PPh_3 - 2CH_2Ph - 4CO$, 1.2); 432 ($2M^+ - 2PPh_3 - 2CH_2Ph - 4CO - Cp - H$, 0.3); 396 ($M^+ - PPh_3$, 0.9); 340 ($M^+ - PPh_3 - 2CO$, 7.3); 262 (PPh_3^+ , 100.0); 182 (W^+ , 80); unidentified peaks at 566 (0.8); 511 (0.5); 468 (0.1); 416 (0.06).

References

1. a) Adams, R.; Collins, D.M.; Cotton, F.A. *Inorg. Chem.* **1974**, *13*, 1086.
b) Birdwhistell, R.; Hackett, P.; Manning, A.R. *J. Organomet. Chem.* **1978**, *157*, 239.
2. Weinmann, D.J.; Abrahamson, H.B. *Inorg. Chem.* **1987**, *26*, 2133.
3. Treichel, P.M.; Morris, J.H.; Stone, F.G.A. *J. Chem. Soc. (A)* **1963**, 720.
4. Havlin, R.; Knox, G.R. *Z. Naturforschg.* **1966**, *21b*, 1108.
5. Watkins, D.D.; George, T.A. *J. Organomet. Chem.* **1975**, *102*, 71.
6. Hartgerink, J. M.Sc. Thesis, McGill University, 1981.
7. Treichel, P.M.; Nakagaki, P.C. *Organometallics*, **1986**, *5*, 711.
8. Nosco, D.L.; Elder, R.C.; Deutsch, E. *Inorg. Chem.* **1980**, *19*, 2545.
9. Shaver, A.; Hartgerink, J.; Lai, R.D.; Bird, P.; Ansari, N. *Organometallics*, **1983**, *2*, 938.
10. Treichel, P.M.; Nakagaki, P.C.; Haller, K.J. *J. Organomet. Chem.* **1987**, *327*, 327.
11. Lau, P.T.S. *Eastman Org. Chem. Bull.* **1975**, *46*, 1.
12. a) Harpp, D.N.; Ash, D.K.; Back, T.G.; Gleason, J.G.; Orwig, B.A.; van Horn, W.F.; Snyder, J.P. *Tetrahedron Lett.* **1970**, 3551.
b) Boustany, K.S.; Sullivan, A.B. *Tetrahedron Lett.* **1970**, 3547.
c) Harpp, D.N.; Ash, D.K. *Int. J. Sulfur Chem., Part A* **1971**, *1*, 211.
d) Behforouz M.; Kerwood, J.E. *J. Org. Chem.* **1969**, *34*, 51.
e) Abe, Y.; Nakabayashi, T.; Tsurugi, J. *Bull. Chem. Soc. Jpn.* **1973**, *46*, 1898.
13. Shaver, A.; Hartgerink, J. *Can. J. Chem.* **1987**, *65*, 1190.

14. a) Bainbridge, A.; Craig, P.J.; Green, M. *J. Chem. Soc. (A)*, **1968**, 2715.
b) Kalck, P.; Prince, R.; Poilblanc, R.; Rousel, J. *J. Organomet. Chem.* **1970**, *24*, 445.
15. Goldman, A.S.; Tyler, D.R. *J. Am. Chem. Soc.* **1986**, *108*, 89.
16. a) Manning, A.R. *J. Chem. Soc. (A)* **1967**, 1984.
b) Craig, P.J.; Green, M. *J. Chem. Soc. (A)* **1968**, 1978.
c) Faller, J.W.; Anderson, A.S. *J. Am. Chem. Soc.* **1970**, *92*, 5852.
d) Beach, D.L.; Datillo, M.; Barnett, K.W. *J. Organomet. Chem.* **1977**, *140*, 47.
17. El-Hinnawi, M.A.; El-Quaseer, A.K. *J. Organomet. Chem.* **1985**, *296*, 393.
18. Davis, R.; Kane-Maguire, L.A.P. in "Comprehensive Organometallic Chemistry"; Wilkinson, G., Ed.; Pergamon Press: Oxford, 1987; Vol 3, p 1333.
19. a) Alway, D.G.; Barnett, K.W. *J. Organomet. Chem.* **1975**, *99*, C52.
b) Alway, D.G.; Barnett, K.W. *Inorg. Chem.* **1980**, *19*, 1533.
c) Beach, D.L.; Barnett, K.W. *J. Organomet. Chem.* **1975**, *97*, C27.
20. Crocco, G.L.; Gladysz, J.A. *J. Chem. Soc. Chem. Commun.* **1985**, 283.
21. Merrifield, J.H.; Gladysz, J.A. *Organometallics*, **1983**, *2*, 782.
22. Milleti, M.C.; Fenske, R.F. *Organometallics*, **1989**, *8*, 420.
23. Crocco, G.L.; Gladysz, J.A. *J. Am. Chem. Soc.* **1988**, *110*, 6110.
24. a) Heah, P.C.; Gladysz, J.A. *J. Am. Chem. Soc.* **1984**, *106*, 7636.
b) Heah, P.C.; Gladysz, J.A. *J. Mol. Catal.* **1985**, *31*, 207.
c) Heah, P.C.; Patton, A.T.; Gladysz, J.A. *J. Am. Chem. Soc.* **1986**, *108*, 1185.
25. Green, M.; Hughes, R.P. *J. Chem. Soc. Chem. Commun.* **1975**, 862.
26. Shriver, D.L. "The Manipulations of Air-Sensitive Compounds"; McGraw-Hill: New York, 1969; p 141.
27. a) Rosencwaig, A.; Gersho, A. *Science*, **1975**, *190*, 556.
b) Rosencwaig, A. "Photoacoustics and Photoacoustic Spectroscopy", Wiley:

New York, 1980.

28. King, R.B. in "Organometallic Syntheses"; Academic Press: New York, 1965;

Vol. 1, p 156.

29. Fischer, E.O.; Moser, E. *J. Organomet. Chem.* **1966**, *5*, 63.

CHAPTER 3

The Preparation of $[\text{CpW}(\text{CO})_2\text{SCHMe}_2]_2$ and $[\text{CpW}(\text{CO})\text{SCHMe}_2]_2$

Introduction:

The preparation of dimeric compounds of the type $[\text{CpM}(\text{CO})_x\text{SR}]_2$ ($x = 1$ (A), 2 (B); $\text{Cp} = \eta^5\text{-C}_5\text{H}_5$; $\text{R} = \text{alkyl, aryl}$) containing bridging thiolato ligands has been investigated (1-14) for various transition metals. There are several isomers possible for these dimers; the M_2S_2 ring can either be non-planar (type A dimers) or planar (type B dimers) (15). The presence of the Cp rings introduces the opportunity for cis or trans isomerism about the M-M vector and axial/equatorial isomerism is possible for the R groups on the bridging sulfur atoms. Figure 3.1 depicts the conformational isomers for type A dimers with a non-planar M_2S_2 core, bearing two Cp rings and two R groups (12,16). The sharing of an edge of the basal planes of the two pyramidal fragments gives rise to the so-called "butterfly" geometry (16-20). The ability of the M_2S_2 ring to invert generates nine different isomers. Examination of molecular models for VII, VIII and IX suggests that the very close proximity of the Cp rings make them unlikely candidates (12) and they will not be considered further. The above structures are reduced to five possibilities when a planar M_2S_2 core, found in type B dimers, is present as shown in Figure 3.2. In this case, the axial/equatorial isomerism for the R groups is labelled using anti/syn nomenclature.

Although many complexes with μ_2 -bridging thiolato ligands have been prepared (15), relatively few structural analyses of dimers of the types A and B have been reported (2-5). In the complex $[\text{CpRhSPh}]_2$ (20), the Cp rings are mutually cis while the phenyl groups are in axial-equatorial positions as in I. The structure of $[\text{CpFe}(\text{CO})\text{SPh}]_2$

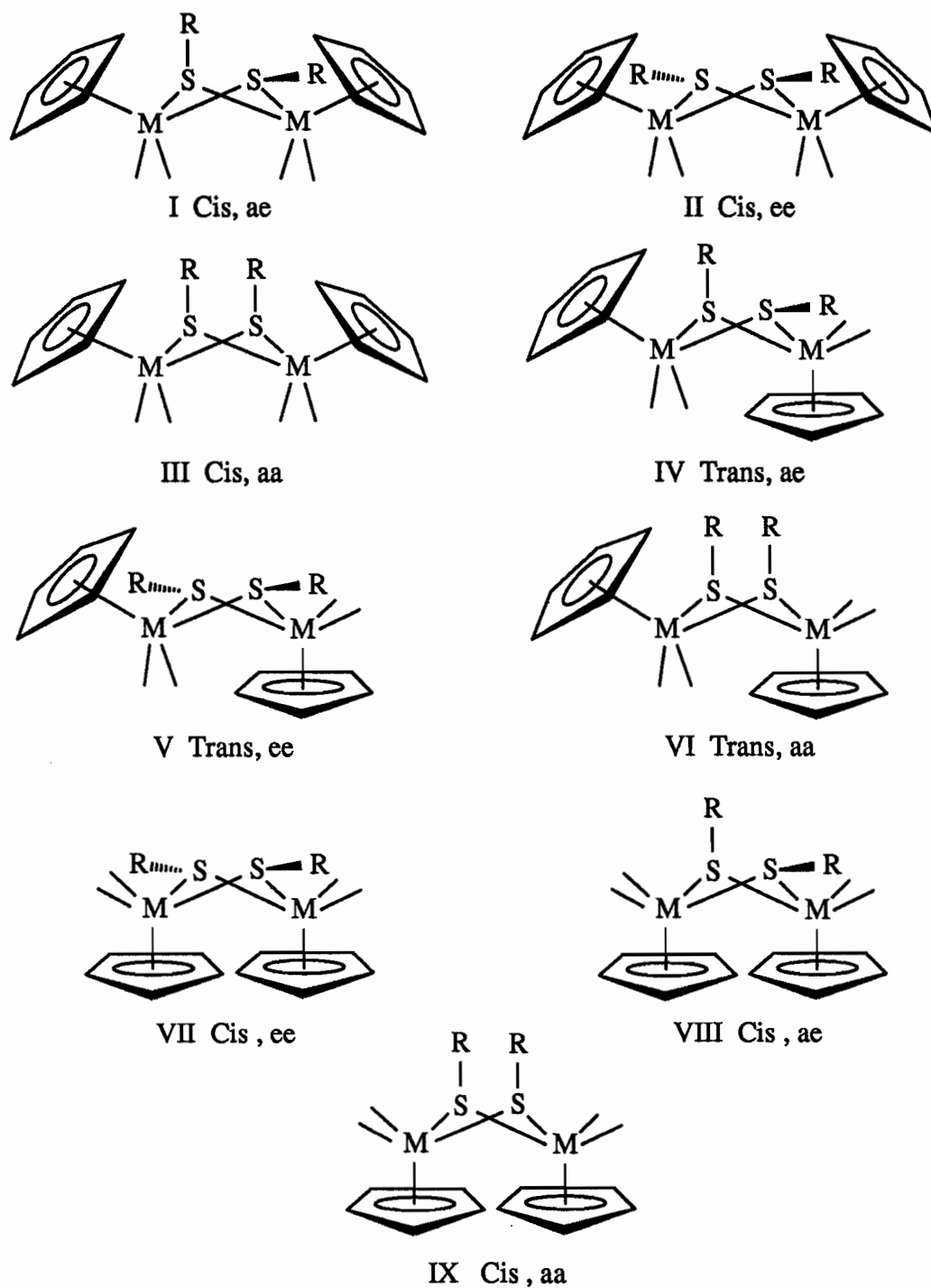


Figure 3.1 Conformational isomers for type A dimers: non-planar M_2S_2 core, two Cp rings, and two R groups on S atoms; a = axial, e = equatorial. Structure types VII, VIII and IX are deemed unlikely due to steric hindrances.

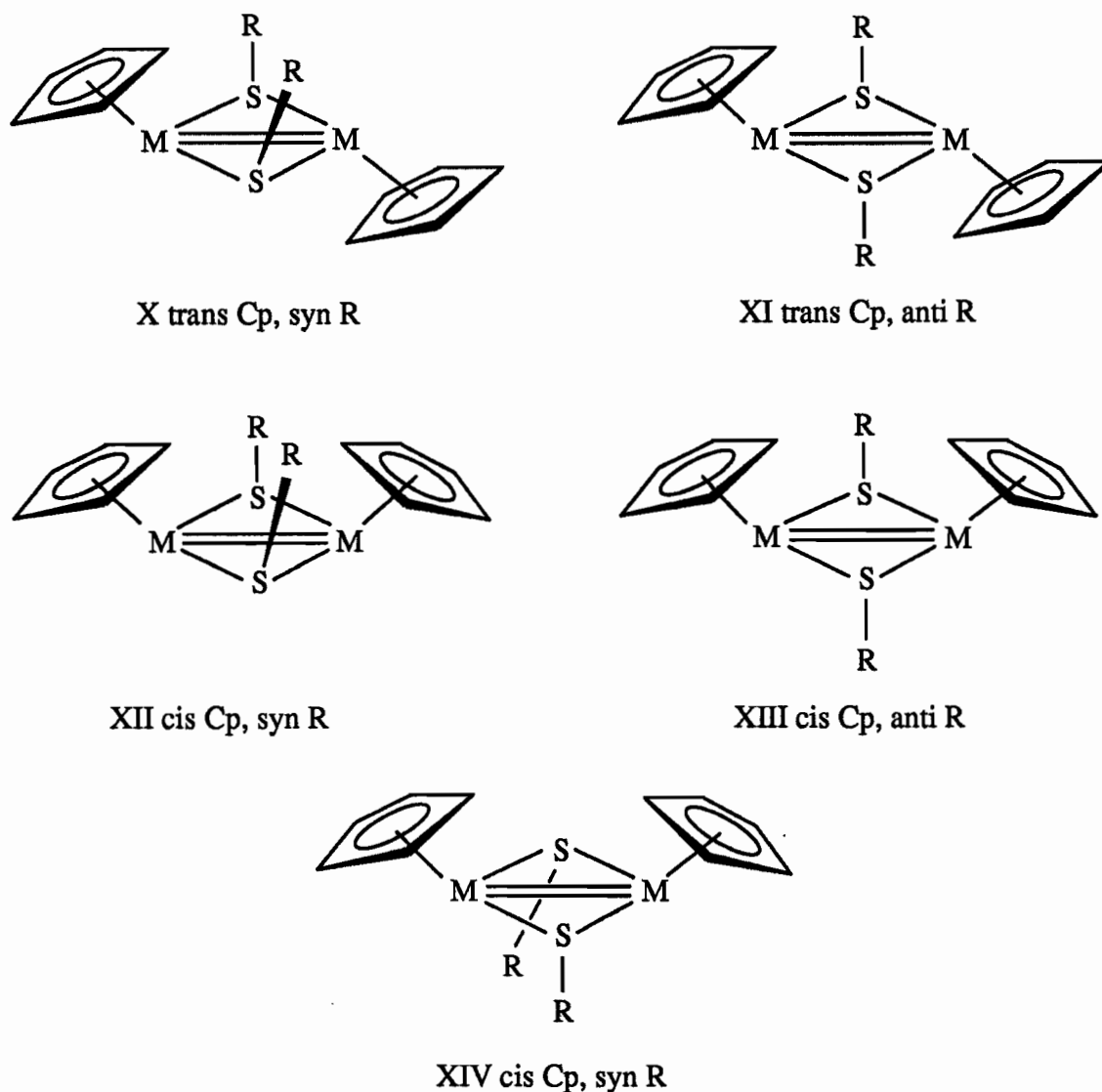


Figure 3.2 Five geometrical isomers for type B dimers: planar M_2S_2 core with two Cp rings and two R groups on bridging S atoms.

(5,9,21) has a non-planar Fe_2S_2 ring, the Cp ligands in mutually cis positions and an equatorial-equatorial arrangement of the phenyl groups as in II. The cation, $[CpFe(CO)SMe]_2^+$ (22) has a structure similar to XIV with a planar iron-sulfur core, cis Cp ligands and syn Me groups. The molybdenum dimer, $[CpMo(CO)_2SPh]_2$ (2-4), aligns its Cp rings in relative trans positions and the phenyl units in an axial-equatorial arrangement as in IV, but in the dication, $[Cp_2Mo_2(CO)_3(MeCN)(SPh)_2]^{2+}$ (23) and

$[\text{CpMo}(\text{CO})_2\text{SCMe}_3]_2^{2+}$ (3), the Cp rings are mutually cis and the R groups are equatorial-equatorial as in II. The *t*-butyl groups in $[\text{CpMo}(\text{CO})\text{SCMe}_3]_2$ (2) occupy a syn conformation while the Cp rings are mutually trans, as in X.

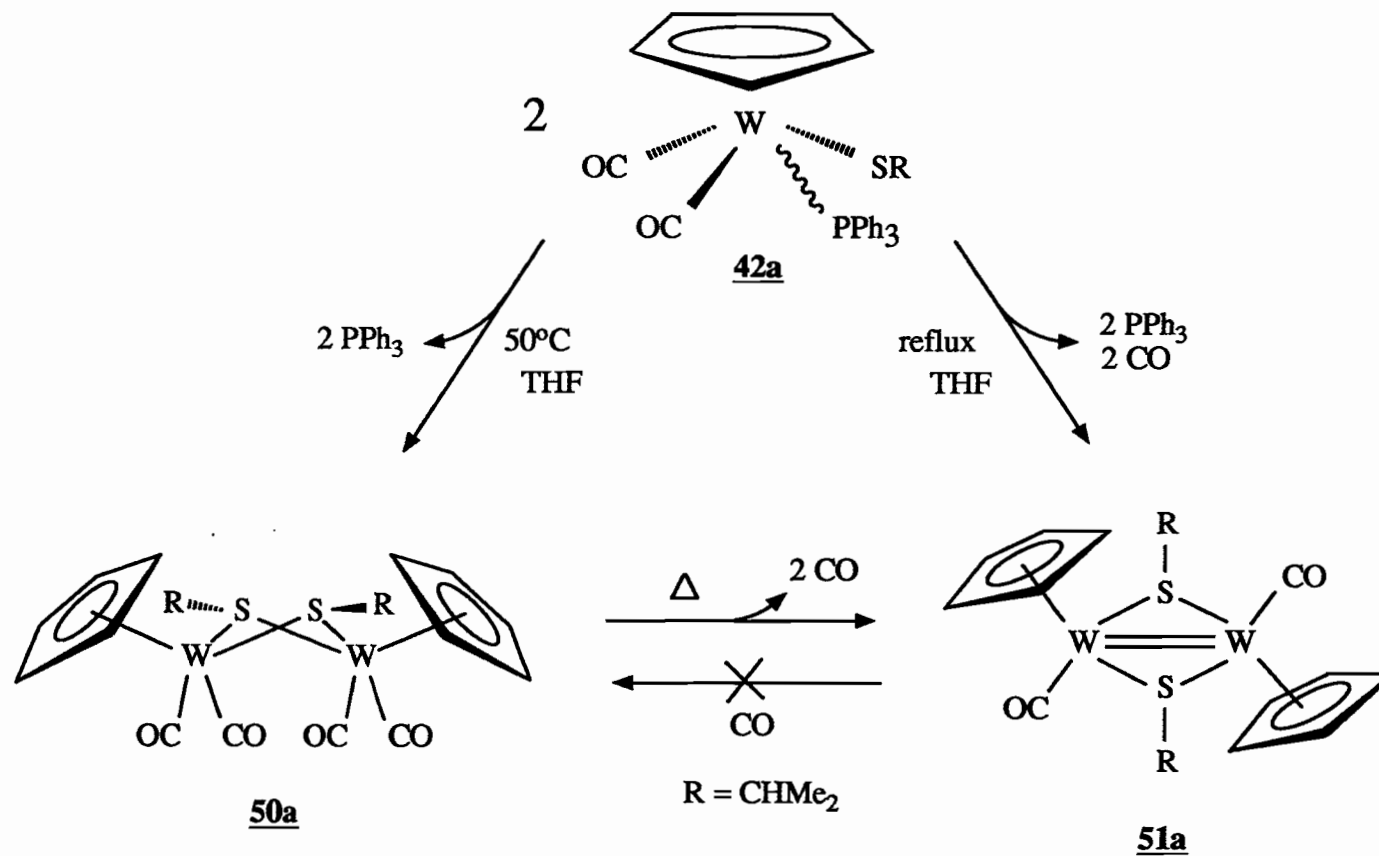
Attempts to prepare tungsten analogues of such dimers were first reported by Stone *et al* (13) via the reaction of $\text{CpM}(\text{CO})_3\text{H}$ ($\text{M} = \text{Mo}, \text{W}$) with dimethyl sulfide. Their formulation as $[\text{CpM}(\text{CO})_2\text{SMe}]_2$ was disputed by Havlin and Knox (24) who suggested that the products are the mononuclear compounds, $\text{CpM}(\text{CO})_3\text{SR}$, but gave no supporting evidence. Watkins and George (6) also reported the preparation of $[\text{CpW}(\text{CO})_2\text{SR}]_2$ ($\text{R} = \text{Me}, 4\text{-C}_6\text{H}_4\text{Me}$) by refluxing $\text{CpW}(\text{CO})_3\text{SR}$ in benzene. These dimers were identified by elemental analysis, ^1H NMR and infrared spectroscopy but no structures were determined. Recently, Abrahamson and Weinmann (1) reported their study of the tungsten complexes $[\text{CpW}(\text{CO})_x\text{SR}]_2$ ($x = 1, 2; \text{R} = \text{Ph}, 4\text{-C}_6\text{H}_4\text{Me}$) prepared by the photochemical or thermal treatment of $\text{CpW}(\text{CO})_3\text{SR}$ in toluene or benzene. A mixture of products was obtained that was difficult to separate. This report coincided with our observation that the triphenylphosphine complex, cis/trans $\text{CpW}(\text{CO})_2(\text{PPh}_3)\text{SCHMe}_2$ (42a) (1,25), gave, in a stepwise manner, $[\text{CpW}(\text{CO})_2\text{SCHMe}_2]_2$ (50a) from warm THF and $[\text{CpW}(\text{CO})\text{SCHMe}_2]_2$ (51a) from refluxing THF. While the molybdenum dimers have been thoroughly characterized, it has been suggested that the tungsten compounds are inherently less stable (1). Hence, the isolation and characterization of these stable tungsten analogues are of interest. The x-ray crystal structures analyses (26) of 50a and 51a are the first for any tungsten members of this class of dimer compounds and they show interesting differences from the molybdenum analogues.

Results and Discussion:

Air stable black-brown crystals of $[\text{CpW}(\text{CO})_2\text{SCHMe}_2]_2$ (**50a**) were obtained by heating a THF solution of **42a** at 50°C for 6 hours and recrystallizing the residue from $\text{CH}_2\text{Cl}_2/\text{hexanes}$. A sample of cis/trans-42a was monitored by ^1H NMR in C_6D_6 at 50°C and the cis isomer was consumed first to produce the dimer (Scheme 3.1). The latter had almost completely disappeared before peaks due to trans-42a began to decrease in intensity until both were consumed. The addition of free PPh_3 to the NMR sample slowed the dimerization process. A similar phenomenon was also observed in an insertion reaction of **42a** with CS_2 (Chapter 4) (25); thus, it is likely that the loss of PPh_3 from cis-42a is an important first step in the formation of the dimer **50a**.

The ^1H NMR and IR data of **50a** and **51a** are presented in Table 3.1. The NMR spectrum of **50a** revealed one environment for the Cp protons while the isopropyl methyl protons appeared as a doublet and the methyne protons as a septet. This is consistent with structures II and III (Fig. 3.1) having cis Cp ligands. In toluene, the IR spectrum gave carbonyl stretching bands at 1945 and 1853 cm^{-1} , accordant with the tetracarbonyl dimeric formulation.

An ORTEP diagram of **50a** is shown in Figure 3.3. Table 3.2 lists the bond lengths and angles and is found at the end of this section. The full crystallographic data, atomic coordinates and thermal parameters (Tables A.1-A.3) are given in Appendix A. The two Cp rings lie in respective cis positions and the isopropyl groups exist in an equatorial-equatorial geometry (II). A crystallographically imposed mirror plane containing the Cp-carbon atoms, C15 and C25, and the two tungsten atoms is also present. The non-planar butterfly conformation of the W_2S_2 ring is obvious from Figure



Scheme 3.1 The preparation of [CpW(CO)₂SCHMe₂]₂ (**50a**) and [CpW(CO)SCHMe₂]₂ (**51a**). Heating **50a** gives **51a** with the loss of 2 molecules of CO. However, the treating **51a** with CO does not give **50a**.

Table 3.1 ^1H NMR^a and IR^b data for $[\text{CpW}(\text{CO})_2\text{SCHMe}_2]_2$ (**50a**) and $[\text{CpW}(\text{CO})\text{SCHMe}_2]_2$ (**51a**).

		$[\text{CpW}(\text{CO})_2\text{SCHMe}_2]_2$	$[\text{CpW}(\text{CO})\text{SCHMe}_2]_2$
		50a	51a
	Cp	5.55	5.49
NMR δ (ppm)	<u>CH</u>	3.13 ^c	2.14 ^c
	<u>CH</u> ₃	1.13 ^d	1.49, 1.31 ^e
IR ν (CO) (cm ⁻¹)		1945, 1853	1840

^a In CDCl₃. ^b In toluene. ^c Septet, $J(\text{H-H}) = 6.6$ Hz.

^d Doublet, $J(\text{H-H}) = 6.6$ Hz. ^e Doublet of doublets, $J(\text{H-H}) = 6.6$ Hz.

3.3, with a calculated separation of 1.63 Å from the S-S vector to the W-W vector. A long W-W distance of 3.835(4) Å clearly indicates no metal-metal interaction. The W-S bond lengths are inequivalent (2.528(6), 2.509(6) Å) but the difference is not considered statistically significant. The W-S-W angle (99.17(22)°) and the S-W-S angles (69.54(21)°, 70.13(21)°) are comparable with the average values for $[\text{CpMo}(\text{CO})_2\text{SPh}]_2$ (101.0°, 71.7° and 71.5° respectively) (2-4). However, the structures for these two compounds differ since **50a** corresponds to II with equatorial-equatorial R groups while the molybdenum dimer resembles IV having axial-equatorial R substituents. Interestingly, the relative arrangement of the Cp and R groups in $[\text{CpW}(\text{CO})_2\text{SCHMe}_2]_2$ (**50a**) are the same as that in the dications, $[\text{CpMo}(\text{CO})_2\text{SCMe}_3]_2^{2+}$ (3) and $[\text{Cp}_2\text{Mo}_2(\text{CO})_3(\text{MeCN})(\text{SPh})_2]^{2+}$ (23). The S-Mo-S angle in both species are 70° (avg), similar to **50a** and $[\text{CpMo}(\text{CO})_2\text{SPh}]_2$ but the Mo-S-Mo angle in the dications decreases to 75° (avg) to accommodate the Mo-Mo single bond (3.00 Å avg) present in these dimers.

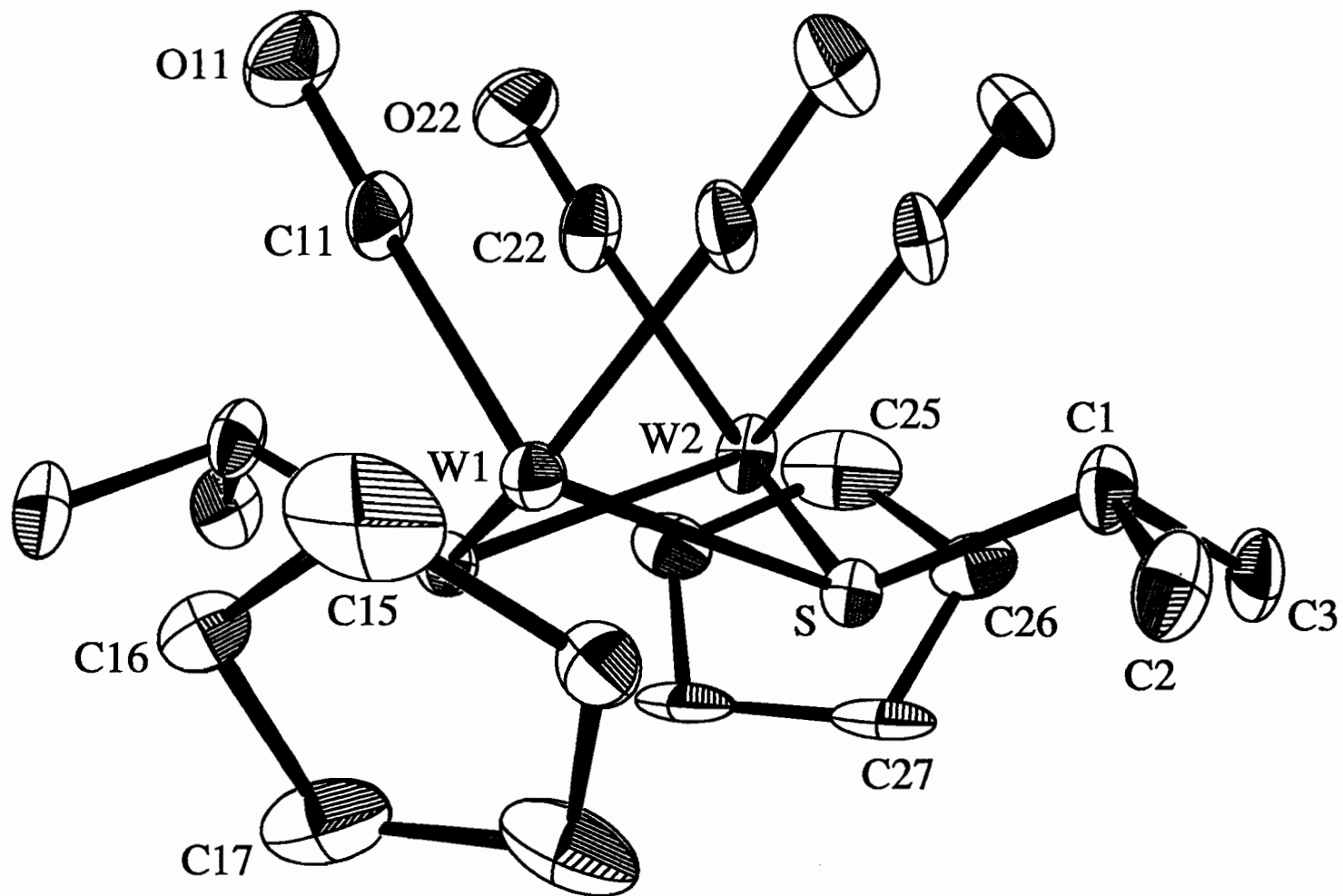


Figure 3.3 ORTEP view of [CpW(CO)₂SCHMe₂]₂ (**50a**).

The air-sensitive black-green crystals of $[\text{CpW}(\text{CO})\text{SCH}(\text{Me})_2]_2$ (**51a**) were formed by refluxing a THF solution of **42a** for 7 hours and recrystallizing the residue from $\text{CH}_2\text{Cl}_2/\text{hexanes}$. This dimer was also observed by NMR as a product of heating a sample of **51a** in toluene- d_8 (Scheme 3.1). The NMR spectrum (Table 3.1) of the methyl region showed two doublets indicating inequivalent methyl groups and thus, mutual trans positions for the Cp rings. A singlet resonance for the ring protons was observed, consistent with structure type XI. In toluene, one $\nu(\text{CO})$ band at 1840 cm^{-1} was observed in the IR spectrum. An ORTEP diagram of **51a** is shown in Figure 3.4. Table 3.3 gives bond lengths and angles, respectively, at the end of this section. Full crystallographic data, final atomic coordinates and thermal parameters are listed in Tables A.4-A.6, respectively in Appendix A. The molecule possesses a crystallographically imposed inversion centre, hence, all the ligands are in mutually trans positions and the isopropyl groups are anti. Loss of the two carbonyl groups, upon going from **50a** to **51a**, transforms the W_2S_2 rhombus into a planar ring, bringing the metal atoms to within $2.602(5)\text{ \AA}$ of each other, which is 1.23 \AA shorter than in **50a**. Therefore, a W-W double bond is implied, similar to the double bond ($2.616(2)\text{ \AA}$) in the molybdenum dimer $[\text{CpMo}(\text{CO})\text{SCMe}_3]_2$ (2). The close proximity of the tungsten atoms is also evidenced by dramatic changes in the bond angles of the W_2S_2 core. The W-S-W angle decreases from $99.17(22)^\circ$ in **50a** to $65.30(12)^\circ$ in **51a**, and the S-W-S bond angles increase from 69.54° , 70.13° to 114.7° in going from **50a** to **51a**, respectively. The M_2S_2 ring parameters of **51a** are comparable to those in $[\text{CpMo}(\text{CO})\text{SCMe}_3]_2$ (65.5° and 114.4° avg.) and in $[\text{W}_2(\text{S}_2)(\text{S}_2\text{CNEt}_2)_4]$ (27) ($65.5(1)^\circ$ and $114.5(1)^\circ$), a W(IV) complex containing a planar W_2S_2 core. Again, the molybdenum dimer analogous to **51a** has a different structure with syn R groups as in X, rather than the anti R groups in the tungsten analogue, **51a**, as in XI. In both dimers **50a** and **51a**, the Cp ligands are tilted, that is they are unsymmetrically bonded to the tungsten atoms with some of the carbon atoms in the Cp

ring closer to the metal atoms than others. This is also observed in the structures of the dications $[\text{CpMo}(\text{CO})_2\text{SCMe}_3]_2^{2+}$ (3) and $[\text{CpMo}(\text{CO})_2\text{SPh}]_2$ (5).

The dicarbonyl dimer **51a** shows no tendency to undergo carbonylation to give **50a** even after treating an NMR sample with 1 atmosphere of CO for more than 2 hours. Knox *et al* (2) reported that the Mo analogue, $[\text{CpMo}(\text{CO})\text{SCMe}_3]_2$, also did not add CO to give the corresponding tetracarbonyl dimer.

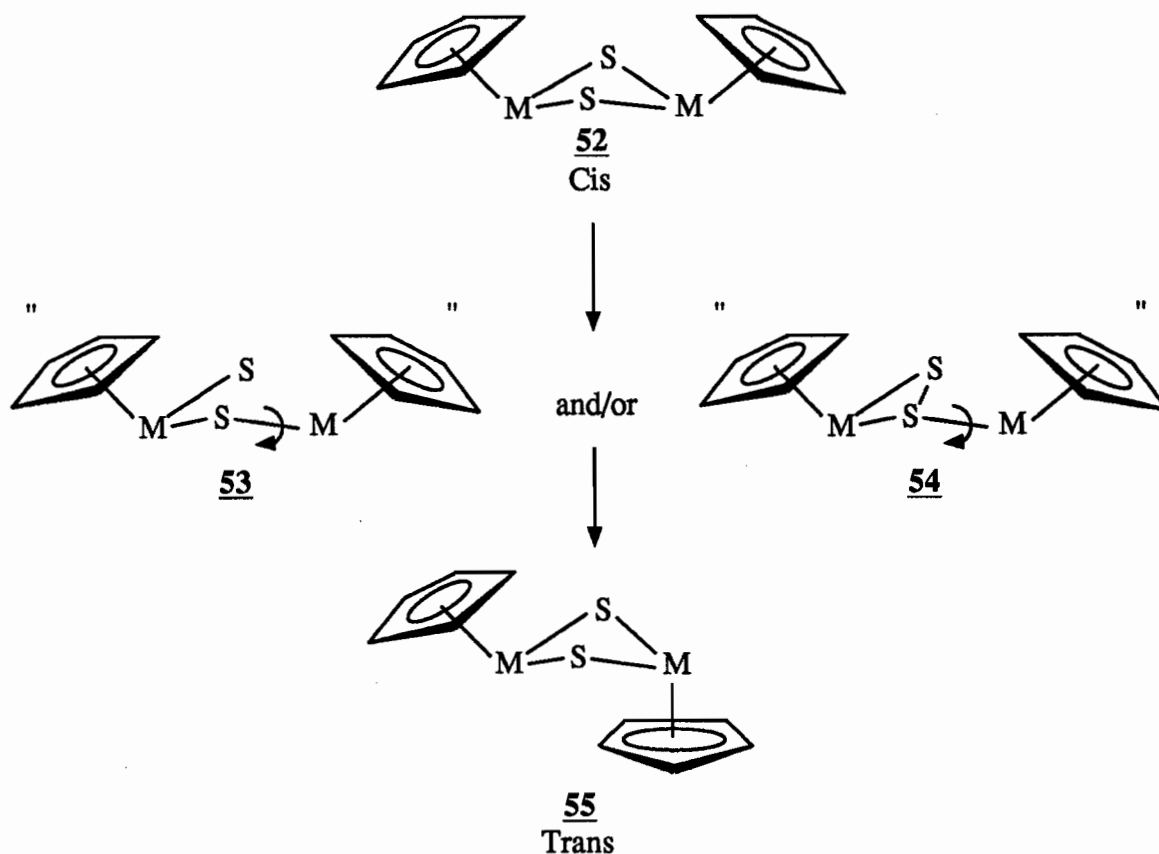
Recently, it has been suggested that steric, not electronic, factors may determine the structure of a particular dimer (28). Molecular orbital calculations were performed for the dications, $[\text{CpMo}(\text{CO})_2\text{SCMe}_3]_2^{2+}$ (3) and $[\text{Cp}_2\text{Mo}_2(\text{CO})_3(\text{MeCN})(\text{SPh})_2]^{2+}$ (23), which both have structures corresponding to II with a Mo-Mo single bond. Comparisons of calculations of the axial-equatorial (I) and equatorial-equatorial (II) geometries for the R groups of the bridging sulfur atoms revealed a very small energy difference (0.06 eV); hence, the experimentally observed conformation (type II) for the two dications is likely due to steric requirements. The calculations for a trans isomer as in IV, V, or VI suggested while considerable steric repulsion exists between the bridging sulfur atoms and carbonyl groups on Mo, no strong electronic factor disfavors the trans structures. The alternative cis conformations VII, VIII or IX were calculated to be highly disfavoured because of severe steric interactions between the Cp rings. This is consistent with a previous report (12) and from examination of molecular models as performed here.

Based on the calculations for the dication complexes, it was postulated (28) that with respect to electronic requirements, cis and trans isomers were equally probable for the neutral dimer, $[\text{CpMo}(\text{CO})_2\text{SPh}]_2$ (2-4) and that only steric factors could disfavor one or two conformations. The cis conformations (VII, VIII or IX) had already been ruled out, but the trans structure IV has been observed for $[\text{CpMo}(\text{CO})_2\text{SPh}]_2$ and a cis

conformation (II) was identified for $[\text{CpW}(\text{CO})_2\text{SCHMe}_2]_2$ (**50a**). Although the appropriate molecular orbital calculations have not been performed, it seems reasonable to suggest that the structures observed for $[\text{CpMo}(\text{CO})\text{SCMe}_3]_2$ (**3**) (type X) and $[\text{CpW}(\text{CO})\text{SCHMe}_2]_2$ (**51a**) (type XI), are also be determined by steric rather than electronic requirements. Nevertheless, even if steric factors are established as the forces which determine the structural conformation of these dimers (type A and B), it may not be possible to reliably predict which structural type (cis versus trans, axial versus equatorial, syn versus anti) would be favoured for these complexes.

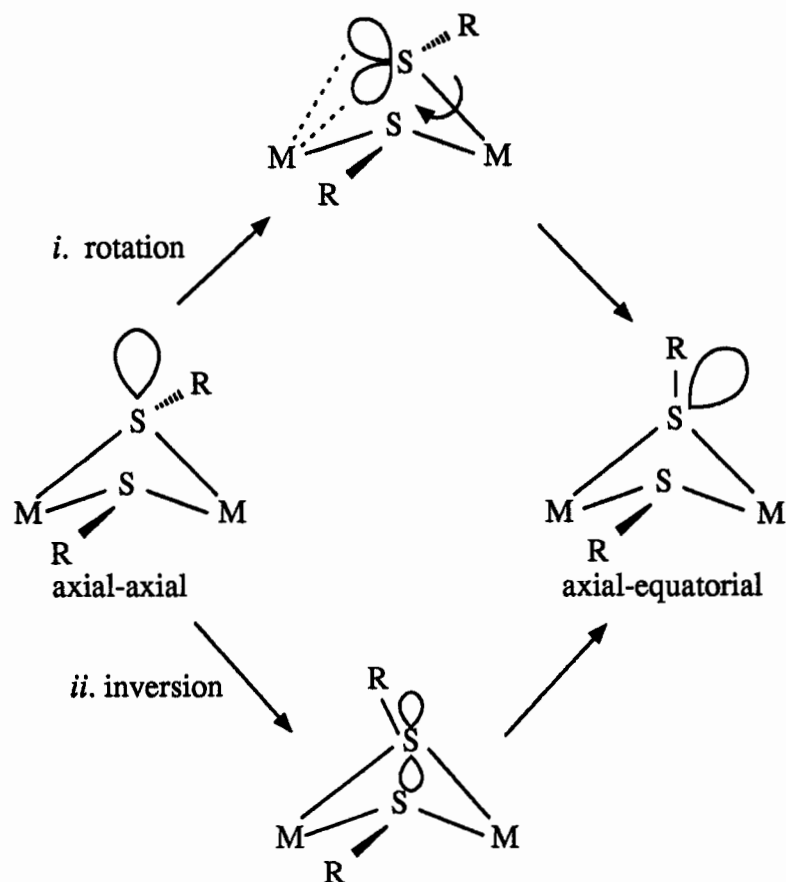
Despite the number of potential isomers for both dimers **50a** and **51a**, it is interesting that only one major isomer is formed. No evidence for additional isomers for **50a** or **51a** was detected in their NMR or IR spectra. The preparations of the molybdenum dimers (2-4,23) also gave only one isomer. For both $[\text{CpFe}(\text{CO})(\text{SPh})]_2$ (5,9,21) and $[\text{CpRu}(\text{CO})\text{SR}]_2$ (R = Me, Ph, CH_2Ph) (12) more than one isomer was observed. The isomers in the iron system resemble structures II (identified by x-ray crystallography (5)) and possibly IV. In the ruthenium system, for both R = Me, Ph, one cis and one trans isomer are detected, while for R = CH_2Ph , one cis and two trans isomers were observed by ^1H NMR spectroscopy. Both the Fe and Ru dimers (R = Ph) underwent cis/trans isomerization when heated. The mechanism of isomerization is thought to involve the breaking of one M-S bond (**52**) followed by rotation about the remaining M-S bond (**53-54**) and subsequent reformation of the broken bond (**55**) (Scheme 3.2) (12,20,28).

Pyramidal inversion at the bridging sulfur atom(s) giving axial-equatorial isomerization of the R substituent on the bridging S atom has been well-studied (28-39) for other metal systems. Two mechanistic pathways have been proposed (12,29-39) and are shown in Scheme 3.3. One mechanism (i) features an intramolecular displacement of



Scheme 3.2 Mechanism of isomerization of cis-[CpM(μ -S)]₂ to trans-[CpM(μ -S)]₂ (12,20,28).

one sulfur lone pair from the metal by another via rotation about a M-S bond. The other pathway (ii) depicts inversion at sulfur via a planar transition state. No evidence has been found to favour one mechanism over the other and the choice between the two is one of personal preference (33). Inversion energies (ΔG^\ddagger) in the range 40-80 kJ/mol have been calculated for a variety of transition metal bridging thiolate dimers (39). Sulfur inversion has been detected for [CpMo(CO)₂SR]₂ (R = Me, Ph) (3). Variable temperature ¹H NMR spectroscopy of these dimers showed broadening and eventually splitting of the Cp proton resonances when cooled to -96°C. A variable temperature NMR study of **50a** in toluene-d₈ showed no changes down to -100°C, thus it is probable that the barrier to



Scheme 3.3 Pyramidal inversion at sulfur in complexes containing $M_2(\mu-SR)_2$ ring. Pathways (i) and (ii) are considered equally likely (12,29-39).

sulfur inversion is very small for **50a** and **51a**.

The dimerization reaction of $CpW(CO)_2(PPh_3)SCH_2Ph$ (**42b**) gave a brown-black solid, isolated from a toluene solution of **42b** refluxed for 1.5 hours. According to the 1H NMR spectrum of the resultant solid, the Cp ring protons (5.20 ppm) are equivalent giving a singlet and the CH_2 protons of the benzyl groups are inequivalent, appearing as an AB quartet (4.15, 3.17 ppm). However, the ratio of the integrations of the Ph (7.33 ppm), Cp and the CH_2 peaks are 6.8:3.2:2, respectively, which does not correspond well to that expected 5:5:2. The IR spectrum of the product gave a weak $\nu(CO)$ band at 1973

cm^{-1} and a strong band at 1834 cm^{-1} . The appearance of the weak 1973 cm^{-1} band suggested the presence of a tetracarbonyl (type A) dimer but the strong band at 1834 cm^{-1} indicated the major species in solution was a dicarbonyl (type B) dimer. Tetracarbonyl dimers, $[\text{CpM}(\text{CO})_2\text{SR}]_2$, exhibit $\nu(\text{CO})$ bands between $2000\text{-}1800 \text{ cm}^{-1}$, while dicarbonyl compounds, $[\text{CpM}(\text{CO})\text{SR}]_2$, show bands in the $1900\text{-}1800 \text{ cm}^{-1}$ region (1,2). Dimer **50a** gave two peaks of equal intensity in the region $2000\text{-}1800 \text{ cm}^{-1}$ and one peak in the range $1900\text{-}1800 \text{ cm}^{-1}$ was observed for **51a**. Hence, it is likely that a mixture of type A and B dimers are present in the solid isolated from the dimerization of **42b**. The mass spectrum gave a peak corresponding to $[\text{Cp}_2\text{W}_2(\text{CO})_2(\text{SCH}_2\text{Ph})_3]^+$, a species with three μ_2 -SR bridges and its related fragments. However, the elemental analysis does not compare well with this formulation, nor does it agree with $[\text{CpW}(\text{CO})_2\text{SCH}_2\text{Ph}]_2$ or $[\text{CpW}(\text{CO})\text{SCH}_2\text{Ph}]_2$. It is difficult then to identify either A or B type dimers from this reaction.

The dimerization reaction of $\text{CpW}(\text{CO})_2(\text{PPh}_3)\text{S-4-C}_6\text{H}_4\text{Me}$ (**42c**) gave a grey-brown solid that was isolated from a toluene solution of **42c** heated to 110°C for 3 hours. The products in the *p*-tolyl system were also difficult to identify. The ^1H NMR and IR data for the resultant solid are given in Table 3.4. The NMR spectrum in C_6D_6 showed two peaks for the *p*-tolyl protons, three different Cp singlets of approximately equal intensity, and one peak for the methyl protons. The ratio of the integrations of the *p*-tolyl, Cp and methyl protons, was 4.5:4:3, respectively, compared to the expected 4:5:3. The NMR spectrum in CDCl_3 gave three Cp singlets and one peak for the methyl protons. The ratio of integration of these Cp resonances and the methyl protons (3.9:3) does not correspond to that expected (5:3). The IR spectrum (toluene) showed 3 peaks in the $1900\text{-}1800 \text{ cm}^{-1}$ region. These NMR and IR data are compared to those of previous reports in Table 3.4. Comparison of the NMR data shows that the chemical shifts of the

Table 3.4 Comparison of ^1H NMR and IR data of $[\text{CpW}(\text{CO})_x\text{S-4-C}_6\text{H}_4\text{Me}]_2$ ($x = 1, 2$)

		$[\text{CpW}(\text{CO})_2\text{S-4-C}_6\text{H}_4\text{Me}]_2$ ($x = 2$)		$[\text{CpW}(\text{CO})\text{S-4-C}_6\text{H}_4\text{Me}]_2$ ($x = 1$)	$[\text{CpW}(\text{CO})_x\text{S-4-C}_6\text{H}_4\text{Me}]_2$ ($x = \text{unknown}$)	
^1H NMR δ (ppm)	Cp	5.40 ^a	5.44 ^a	5.30 ^a	5.67 ^a 5.45 5.33	5.29 ^b 5.04 4.98
	CH ₃	2.23	2.30	2.16	2.29	2.07
IR $\nu(\text{CO})$ cm^{-1}		1948, 1851 ^c	1893, 1848 ^d	1892, 1849 ^e	1893, 1847, 1820 ^c	
Ref.		1	6	1	this work	

^a CDCl_3 ^b C_6D_6 ^c toluene ^d CCl_4 ^e benzene

Cp resonances (5.45, 5.33 ppm) of the unknown product in CDCl_3 agrees with the data from both $[\text{CpW}(\text{CO})_2\text{S-4-C}_6\text{H}_4\text{Me}]_2$ (5.40 (1), 5.44 (6) ppm) and $[\text{CpW}(\text{CO})\text{S-4-C}_6\text{H}_4\text{Me}]_2$ (5.30 ppm (1)). The chemical shift of the methyl protons (2.29 ppm) corresponds well with that of the former (2.30 ppm (6)). The IR data (toluene) of the unknown (1893, 1847, 1820 cm^{-1}) does not agree favourably with the data of $[\text{CpW}(\text{CO})_2\text{S-4-C}_6\text{H}_4\text{Me}]_2$ (1948, 1851 cm^{-1} (1)) in the same solvent. However, the data reported for this complex in benzene (1893, 1848 cm^{-1} (6)) and for $[\text{CpW}(\text{CO})_2\text{S-4-C}_6\text{H}_4\text{Me}]_2$ in CCl_4 (1892, 1849 cm^{-1} (1)) does correspond with the IR data of the unknown. These comparisons suggest that the unknown product is a mixture of tetracarbonyl (type A) and dicarbonyl (type B) dimers. Specific details of the structures of the dimers cannot, however, be determined from these data. The mass spectral data of the unknown showed a peak corresponding to $[\text{Cp}_2\text{W}_2(\text{CO})_2(\text{S-4-C}_6\text{H}_4\text{Me})_3]^+$ but this evidence is unreliable since peaks due to dimeric species were also observed in the mass spectrum of the starting complex, **42c**, indicating a facile tendency to form clusters in this system. The elemental analysis found does not agree with $[\text{Cp}_2\text{W}_2(\text{CO})_2(\text{S-4-C}_6\text{H}_4\text{Me})_3]^+$ nor does it correspond to either $[\text{CpW}(\text{CO})_2(\text{S-4-C}_6\text{H}_4\text{Me})]_2$ or $[\text{CpW}(\text{CO})(\text{S-4-C}_6\text{H}_4\text{Me})]_2$.

It appears from our results and those of others (1), that the tungsten dimers for R = aryl are more difficult to prepare than their molybdenum counterparts (2-4) although it is not immediately obvious why this should be so. However, complexes **50a** and **51a** where R = CHMe_2 are stable compounds, easily distinguishable by their NMR and IR spectra and elemental analyses. The method reported here worked well for R = CHMe_2 which suggests that the intrinsic instability proposed for such tungsten dimers may only apply to the aryl derivatives.

Table 3.2 Bond Lengths (Å) and Angles (deg) for [CpW(CO)₂SCHMe₂]₂ (**50a**).

W1-W2	3.835(4)	S-C1	1.83(2)
W1-S	2.528(6)	C11-O11	1.09(3)
W1-C11	2.03 (3)	C22-O22	1.16(3)
W1-C15	2.27 (4)	C1-C2	1.56(3)
W1-C16	2.37 (2)	C1-C3	1.55(3)
W1-C17	2.41 (2)	C15-C16	1.47(3)
W2-S	2.509(6)	C16-C17	1.43(3)
W2-C22	1.93 (2)	C17-C17'	1.58(6)
W2-C25	2.26 (3)	C25-C26	1.49(4)
W2-C26	2.35 (2)	C26-C27	1.44(4)
W2-C27	2.43 (2)	C27-C27'	1.55(6)
S-W-S'	69.5(2)	W1-C11-O11	175.7(20)
S-W1-C11	82.1(7)	W2-C22-O22	175.8(20)
S-W1-C11'	124.6(7)	S-C1-C2	105.9(16)
C11-W1-C11'	76.4(10)	S-C1-C3	107.0(16)
S-W2-S	70.1(2)	C2-C1-C3	109.1(19)
S-W2-C22	82.5(7)	C16-C15-C16'	115.0(3)
S-W2-C22'	123.3(7)	C15-C16-C17	104.5(25)
C22-W-C22'	72.6(10)	C16-C17-C17'	108.2(21)
W1-S-W2	99.2(2)	C26-C25-C26'	109.0(3)
W1-S-C1	113.2(8)	C25-C26-C27	107.9(24)
W2-S-C1	112.8(8)	C26-C27-C27'	107.6(21)

Table 3.3 Bond Lengths (Å) and Angles (deg) for [CpW(CO)SCHMe₂]₂ (**51a**).

W-W	2.602(5)	S-C7	1.86(1)
W-S	2.412(4)	C1-O1	1.12(1)
W-S'	2.411(3)	C2-C3	1.31(2)
W-C1	1.95 (1)	C2-C6	1.47(3)
W-C2	2.29 (1)	C3-C4	1.35(3)
W-C3	2.30 (1)	C4-C5	1.20(3)
W-C4	2.31 (1)	C5-C6	1.45(3)
W-C5	2.31 (1)	C7-C8	1.53(2)
W-C6	2.30 (2)	C7-C9	1.49(2)
W-W-S	57.3(1)	C3-C2-C6	106.2(2)
W-W-S'	57.4(9)	C2-C3-C4	108.4(2)
S-W-S	114.7(1)	C3-C4-C5	115.2(2)
S-W-C1	84.5(3)	C4-C5-C6	107.6(2)
W-S-W	65.3(1)	C2-C6-C5	102.5(2)
W-S-C7	112.0(4)	S-C7-C8	104.8(8)
W-S-C8	116.0(4)	S-C7-C9	111.2(8)
W-S-C9	129.9(4)	C8-C7-C9	113.3(1)
W-S'-C7'	112.9(4)		
W-S'-C8'	146.1(4)		
W-S'-C9'	96.7(3)		

Experimental:

A. Bis(cyclopentadienyl)tetracarbonylbis(μ -2-propylthiolato)ditungsten(II),
[CpW(CO)₂SCHMe₂]₂, **50a**

In a 100 mL three-necked round bottom flask equipped with a condenser, *cis/trans*-CpW(CO)₂(PPh₃)SCHMe₂ (**42a**), (2.17 g, 3.38 mmol) was dissolved in THF (75 mL) and the stirred solution was heated to 40°C (oil bath) for 6 hours. The brown solution was cooled to room temperature and the solvent removed by vacuum. The brown residue was dissolved in a minimal amount of CH₂Cl₂ and chromatographed on an alumina column (5 x 45 cm, 1:1 CH₂Cl₂/hexanes eluant). A brown-red band eluted first and was collected. An orange-yellow band due to a small amount of unreacted **42a** followed but was not isolated. A brown residue remained at the top of the column. The brown-red band was reduced to dryness and recrystallized (1:4 CH₂Cl₂/hexanes) to give brown/black crystals (0.15 g, 11.3%, m.p. >250°C). Anal. Calc'd for C₂₀H₂₄O₄S₂W₂: C, 31.59; H, 3.18; S, 8.43. Found: C, 31.58; H, 3.29; S, 8.31.

IR (Nujol): 1934 (s), 1905 (w), 1848 (s), 1818 (w), 1232 (w), 1147 (w), 1060 (w), 1042 (w), 1006 (w), 859 (w), 844 (w), 831 (shoulder, w), 820 (m), 723 (w) cm⁻¹.

Mass spectrum, EI: 704 (M⁺-2CO, 0.5); 661 (M⁺-2CO-CHMe₂, 8.5); 594 (M⁺-2CO-CHMe₂-Cp-2H, 100.0); 534 (M⁺-3CO-SCHMe₂-Cp-2H, 18.0); 529 (M⁺-2CO-2S-CHMe₂-Cp-2H, 26.2).

B. Bis(cyclopentadienyl)dicarbonylbis(μ -2-propylthiolato)ditungsten(II),
 $[\text{CpW}(\text{CO})\text{SCHMe}_2]_2$, **51a**

In a 100 mL three-necked round bottom flask equipped with a condenser, cis/trans-42a, (1.59 g, 2.47 mmol) was dissolved in THF (45 mL) and the stirred solution refluxed for 7 hours. During this time, the colour of the solution changed from orange to brown to black-green. The solution was cooled to room temperature and the solvent removed by vacuum. The residue was dissolved in a minimal amount of CH_2Cl_2 and chromatographed on alumina (5 x 50 cm). Elution with CH_2Cl_2 /hexanes (1:2) gave a dark-green band followed by a brown band and an orange band. A brown residue remained at the top of the column. The brown and orange bands were identified by ^1H NMR spectroscopy to be 50a and 42a, respectively. The dark-green band was reduced to dryness and recrystallized from CH_2Cl_2 /hexanes (1:4) to give air-sensitive dark black-green crystals of 51a (0.13 g, 14.6%, m.p. > 200°C). Anal. Calc'd for $\text{C}_{18}\text{H}_{24}\text{O}_2\text{S}_2\text{W}_2$: C, 30.70; H, 3.44; S, 9.11. Found: C, 30.49; H, 3.55; S, 9.09.

IR (Nujol): 1835 (s), 1832 (s), 1800 (shoulder, m), 1049 (w), 1031 (w), 1006 (w), 804 (m), 723 (m) cm^{-1} .

Mass spectrum, EI: 705 ($\text{M}^+ + \text{H}^+$, 2.8); 661 ($\text{M}^+ - \text{CHMe}_2$, 8.8); 633 ($\text{M}^+ - \text{CHMe}_2 - \text{CO}$, 2.1); 592 ($\text{M}^+ - \text{CHMe}_2 - \text{Cp} - 4\text{H}$, 5.7); 590 ($\text{M}^+ - 2\text{CHMe}_2 - \text{CO}$, 5.7); 562 ($\text{M}^+ - \text{CHMe}_2 - 2\text{CO}$, 25.1); 534 ($\text{M}^+ - \text{SCHMe}_2 - \text{Cp} - \text{CO} - 2\text{H}$, 6.7); 43 (CHMe_2^+ , 100).

C. Attempted dimerization of $\text{CpW}(\text{CO})_2(\text{PPh}_3)\text{SCH}_2\text{Ph}$, 42b

The complex 42b (0.99 g, 1.4 mmol) was dissolved in toluene (100 mL) and was refluxed for 1.5 hrs. The brown solution was reduced to dryness and the residue extracted

with hexanes (2 x 40 mL) to remove PPh₃. After extraction, the remaining residue was dissolved in a minimal amount of CH₂Cl₂ and chromatographed on alumina (3 x 40 cm). Elution with CH₂Cl₂/hexanes (1:1) gave a pale yellow band followed by a brown-green band. A black band was eluted with CH₂Cl₂. All were reduced to dryness. The first fraction contained some XPPH₃ (X = O, S?) and last fraction showed only residual CH₂Cl₂ by ¹H NMR. The brown-green band was recrystallized from CH₂Cl₂/hexanes to give a brown solid (0.17 g, m.p. = 160-165°C dec.). Anal. Calc'd for C₂₈H₂₄O₄S₂W₂ ([CpW(CO)₂SCH₂Ph]₂): C, 39.27; H, 2.82; S, 7.49. Calc'd for C₂₆H₂₄O₂S₂W₂ ([CpW(CO)SCH₂Ph]₂): C, 39.02; H, 3.02; S, 8.01. Calc'd for C₃₃H₃₁O₂S₃W₂ (Cp₂W₂(CO)₂(SCH₂Ph)₃): C, 42.92; H, 3.38; S, 10.41. Found. C: 33.98; H, 2.62; S, 7.66.

¹H NMR (CDCl₃): 7.33 (mult, 6.8H, CH₂C₆H₅); 5.20 (sing, 3.2H, Cp); 4.15, 3.17 (AB qt, Δv=196 Hz, J(H-H)=12 Hz, 2H, CH₂C₆H₅).

IR (CH₂Cl₂) ν(CO): 1973 (w), 1834 (s) cm⁻¹. IR (Nujol): 1965 (m), 1831 (s), 1821 (s), 1782 (w), 1654 (sh, m), 1540 (sh, w), 810 (m), 764 (w), 723 (w), 697 (m) cm⁻¹.

Mass spectrum, FAB in NBA: 923 ([Cp₂W₂(CO)₂(SCH₂Ph)₃]⁺, 11.8); 832 ([Cp₂W₂(CO)₂S(SCH₂Ph)₂]⁺, 0.8); 817 ([Cp₂W₂(CO)(SCH₂Ph)₂(SCH₂)⁺-H⁺, 1.4); 713 ([Cp₂W₂(SCH₂)₂(SCH₂Ph)]⁺, 2.6); 701 ([Cp₂W₂OS₂(SCH₂Ph)]⁺, 2.1); 699 ([Cp₂W₂S(SCH₂)(SCH₂Ph)]⁺, 2.0); 685 ([Cp₂W₂S₂(SCH₂Ph)]⁺, 11.8); 651 ([Cp₂W₂(CO)₂S₃]⁺+H⁺, 1.2); 619 ([Cp₂W₂(CO)₂S₂]⁺+H⁺, 1.8); 610 ([Cp₂W₂OS₃]⁺, 4.3); 594 ([Cp₂W₂S₃]⁺, 34.4); 578 ([Cp₂W₂OS₂]⁺, 5.6); 562 ([Cp₂W₂S₂]⁺, 4.2); 530 ([Cp₂W₂S]⁺, 1.9); unidentified peaks at 711 (2.7), 545 (2.0).

D. Attempted dimerization of CpW(CO)₂(PPh₃)S-4-C₆H₄Me, **42c**

In a 100 mL three-necked round bottom flask, cis/trans-42c, (0.59 g, 0.85 mmol) was dissolved in toluene (40 mL) and the solution was refluxed for 3 hrs. The brown

solution was allowed to cool then reduced to dryness. The residue was dissolved in a minimal amount of CH_2Cl_2 and chromatographed on alumina (2 x 40 cm). Elution with hexanes (~100 mL) removed any PPh_3 . A grey-brown band then eluted with 1:1 toluene/ CH_2Cl_2 . This band was reduced to dryness and recrystallized from CH_2Cl_2 /ethanol to afford a grey-brown solid (0.14 g, m.p. >250°C). Anal. Calc'd for $\text{C}_{28}\text{H}_{24}\text{O}_4\text{S}_2\text{W}_2$ ($[\text{CpW}(\text{CO})_2\text{S}-4-\text{C}_6\text{H}_4\text{Me}]_2$): C, 39.27; H, 2.82; S, 7.49. Calc'd for $\text{C}_{26}\text{H}_{24}\text{O}_2\text{S}_2\text{W}_2$ ($[\text{CpW}(\text{CO})\text{S}-4-\text{C}_6\text{H}_4\text{Me}]_2$): C, 39.02; H, 3.02; S, 8.01. Calc'd for $\text{C}_{33}\text{H}_{31}\text{O}_2\text{S}_3\text{W}_2$ ($\text{Cp}_2\text{W}_2(\text{CO})_2(\text{S}-4-\text{C}_6\text{H}_4\text{Me})_3$): C, 42.92; H, 3.38; S, 10.41. Found. C: 32.10, H: 2.82, S: 7.80.

^1H NMR (CDCl_3): 7.20 (mult, 20H, $4-\text{C}_6\text{H}_4\text{CH}_3$); 5.67 (sing, 6H, Cp); 5.45 (sing, 6.9H, Cp); 5.33 (sing, 5H, Cp); 2.29 (br sing, 13.7H, $4-\text{C}_6\text{H}_4\text{CH}_3$). In (C_6D_6): 7.43, 7.00 (AB qt, $\Delta\nu=85.4$ Hz, $J(\text{H}-\text{H})=8$ Hz, 9.4H, $4-\text{C}_6\text{H}_4\text{CH}_3$); 7.33, 7.00 (AB qt, $\Delta\nu=64.3$ Hz, $J(\text{H}-\text{H})=6.5$ Hz, 9H, $4-\text{C}_6\text{H}_4\text{CH}_3$); 5.29 (sing, 5.7H, Cp); 5.04 (sing, 5.9H, Cp); 4.98 (sing, 5H, Cp); 2.07 (sing, 12.4H, $4-\text{C}_6\text{H}_4\text{CH}_3$).

IR (toluene), $\nu(\text{CO})$: 1893 (s), 1847 (s), 1820 (shoulder, m) cm^{-1} . IR (Nujol): 1896 (s), 1836 (s), 1823 (s), 1177 (w), 1103 (w), 1062 (w), 1016 (w), 838 (w), 805 (m), 721 (m) cm^{-1} .

Mass spectrum, FAB in NBA: 923 ($[\text{Cp}_2\text{W}_2(\text{CO})_2(\text{S}-4-\text{C}_6\text{H}_4\text{Me})_3]^+$, 1.7); 817 ($[\text{Cp}_2\text{W}_2(\text{CO})_2\text{S}_3(4-\text{C}_6\text{H}_4\text{Me})(\text{C}_6\text{H}_4)]^+$, 12.0); 789 ($[\text{Cp}_2\text{W}_2(\text{CO})\text{S}_3(4-\text{C}_6\text{H}_4\text{Me})(\text{C}_6\text{H}_4)]^+$, 3.0); 776 ($[\text{Cp}_2\text{W}_2\text{S}_3(4-\text{C}_6\text{H}_4\text{Me})(\text{C}_6\text{H}_4)]^+$, 3.5); 744 ($[\text{CpW}(\text{S}-4-\text{C}_6\text{H}_4\text{Me})_2]^+$, 3.3); 685 (5.0), $[\text{Cp}_2\text{W}_2\text{S}_3(4-\text{C}_6\text{H}_4\text{Me})]^+$; 669 ($[\text{Cp}_2\text{W}_2\text{S}_3(\text{C}_6\text{H}_4)]^+-\text{H}$, 13.5); 651 ($[\text{Cp}_2\text{W}_2(\text{CO})_2\text{S}_3]^++\text{H}$, 4.5); 637 ($[\text{Cp}_2\text{W}_2\text{S}_2(\text{C}_6\text{H}_4)]^+-\text{H}$, 4); 614 ($[\text{W}(\text{S}-4-\text{C}_6\text{H}_4\text{Me})_2]^+$, 2); unidentified peaks at 596 (5), 578 (4), 560 (5).

References

1. Weinmann, D.J.; Abrahamson, H.B. *Inorg. Chem.* **1987**, *26*, 2133.
2. Benson, I.B.; Killops, S.D.; Knox, S.A.R.; Welch, A.J. *J. Chem. Soc. Chem. Commun.* **1980**, 1137.
3. Courtot-Coupez, J.; Guéguen, M.; Guerchais, J.E.; Pétilion, F.Y.; Talarmin, J. *J. Organomet. Chem.* **1986**, *312*, 81.
4. Adams, R.; Chodosh, D.F.; Faraci, E. *Cryst. Struct. Comm.* **1978**, *7*, 145.
5. Ferguson, G.; Hannaway, C.; Islam, K.M.S. *J. Chem. Soc. Chem. Commun.* **1968**, 1165.
6. Watkins, D.D.; George, T.A. *J. Organomet. Chem.* **1975**, *102*, 71.
7. Grobe, J.; Haubold, R. *Z. Anorg. Allg. Chem.* **1985**, *522*, 159.
8. Jaitner, P.; Wohlgenannt, W. *Inorg. Chim. Acta* **1985**, *101*, L43.
9. Knox, G.R.; Bruce, R.; Ahmad, M. *J. Organomet. Chem.* **1966**, *6*, 1.
10. Knox, G.R.; Robertson, C.G.; Dekker, M. *J. Organomet. Chem.* **1969**, *18*, 161.
11. Knox, G.R.; Pryde, A. *J. Organomet. Chem.* **1974**, *74*, 105.
12. Knox, S.A.R.; Killops, S.D. *J. Chem. Soc. Dalton Trans.* **1978**, 1260.
13. Treichel, P.M.; Morris, J.H.; Stone, F.G.A. *J. Chem. Soc.* **1963**, 720.
14. King, R.B.; Treichel, P.M.; Stone, F.G.A. *J. Amer. Chem. Soc.* **1961**, *83*, 3600.
15. Blower, P.J.; Dilworth, J.R. *Coord. Chem. Rev.* **1987**, *76*, 121.
16. Shaver, A.; Fitzpatrick, P.J.; Steliou, K.; Butler, I.S. *J. Am. Chem. Soc.* **1979**, *101*, 1313.
17. Dahl, L.F.; Wei, C.H. *Inorg. Chem.* **1963**, *2*, 328.
18. Henslee, W.; Davis, R.E. *Cryst. Struct. Commun.* **1972**, *1*, 403.

19. Prout, K.; Critchley, S.R.; Rees, G.V. *Acta Crystallogr. Sect. B* **1974**, *30*, 2305.
20. Connelly, N.G.; Johnson, G.A.; Kelly, B.A.; Woodward, P. *J. Chem. Soc. Chem. Commun.* **1977**, 436.
21. Haines, R.J.; DeBeer, J.A.; Greatex, R. *J. Organomet. Chem.* **1975**, *85*, 89.
22. Connelly, N.G.; Dahl, L.F. *J. Am. Chem. Soc.* **1970**, *92*, 7472.
23. El Khalifa, M.; Guéguen, M.; Mercier, R.; Pétilion, F.Y.; Saillard, J.-Y.; Talarmin, J. *Organometallics*, **1989**, *8*, 140.
24. Havlin, R.; Knox, G.R. *Z. Naturforsch.* **1966**, *21b*, 1108.
25. Shaver, A.; Soo Lum, B.; Bird, P.; Arnold, K. *Inorg. Chem.* **1989**, *28*, 1900.
26. X-ray crystal structure analyses determined in the laboratory of Dr. Peter Bird, Department of Chemistry, Concordia University, Montréal, Québec, Canada.
27. Bino, A.; Cotton, F.A.; Dori, Z.; Sekutowski, J.C. *Inorg. Chem.* **1978**, *17*, 2946.
28. El Khalifa, M.; Pétilion, F.Y.; Saillard, J.-Y.; Talarmin, J. *Inorg. Chem.* **1989**, *28*, 3849.
29. Abel, E.W.; Bush, R.P.; Hopton, F.J. Jenkins, C.R. *J. Chem. Soc. Chem. Commun.* **1966**, 58.
30. Ahmad, M.; Bruce, R.; Knox, G. *Z. Naturforsch.* **1966**, *21b*, 289.
31. Cross, R.J.; Dalglish, I.G.; Smith, G.J.; Wardle, R. *J. Chem. Soc. Dalton Trans.* **1972**, 992.
32. Cross, R.J.; Green, T.H.; Keat, R. *J. Chem. Soc. Chem. Commun.* **1974**, 207.
33. Abel, E.; Farrow, G.W.; Orrell, K.G. *J. Chem. Soc. Dalton Trans.* **1977**, 42.
34. Abel, E.; Shamsuddin Ahmed, A.K.; Farrow, G.W.; Orrell, K.G.; Sik, V. *J. Chem. Soc. Dalton Trans.* **1977**, 47.
35. Natile, G.; Maresca, L.; Bor, G. *Inorg. Chim. Acta* **1977**, *23*, 37.
36. Benson, I.B.; Knox, S.A.R.; Naish, P.J.; Welch, A.J. *J. Chem. Soc. Chem. Commun.* **1978**, 878.

37. Kuhn, N.; Schumann, H.; Zauder, E. *J. Organomet. Chem.* **1987**, 327, 17
38. Turley, P.C.; Haake, P. *J. Amer. Chem. Soc.* **1967**, 89, 4617.
39. Abel, E.W.; Bhargava, S.K.; Orrell, K.G. *Prog. Inorg. Chem.* **1984**, 32, 1.

CHAPTER 4

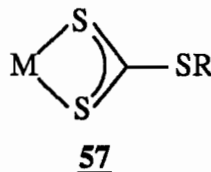
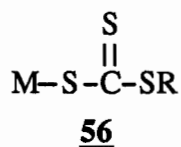
The Preparation of the Thioxanthate Complexes, $\text{CpW}(\text{CO})_2\text{S}_2\text{CSR}$

(R = CHMe_2 , CH_2Ph , 4- $\text{C}_6\text{H}_4\text{Me}$)

Introduction

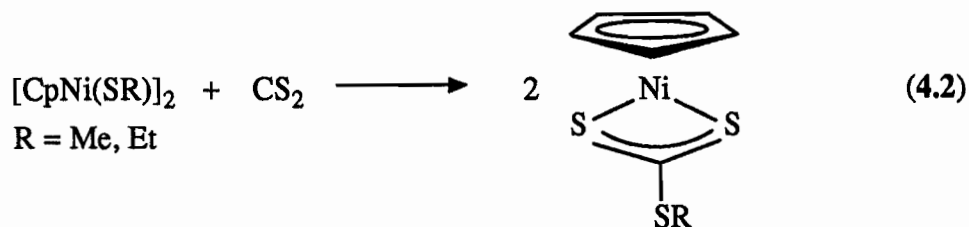
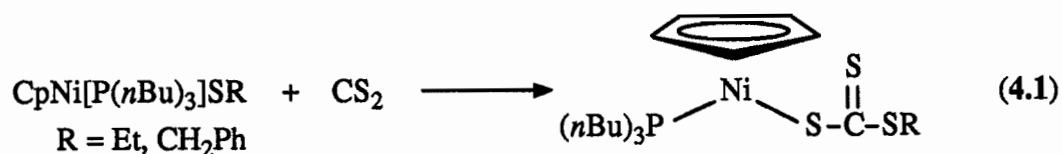
The studies of organometallic complexes with CS_2 stems from the interest in CO_2 activation. Carbon dioxide is a potential feedstock of C_1 for organic molecules (1) and a possible substrate in the storage of solar energy (2). Its ever-increasing levels in the atmosphere has made its presence an environmental concern (3). These factors have prompted many studies investigating the reaction of CO_2 (4-29) and CO_2 -like molecules, CS_2 (24,30-57), COS (48-50,58-66), RNCS (64,67-72), RNCO (12,22,64,67-73), RNCNR (12,64,72,74) with organometallic complexes.

Reactions of CS_2 and thiolate compounds are known to give complexes in which the thioxanthate ligand, $[\text{S}_2\text{CSR}]^-$, is formed (33-36,38,39). This ligand can bind to the metal either in a monodentate fashion through one sulfur atom as shown in 56 or as a bidentate ligand through two sulfur atoms as in 57.

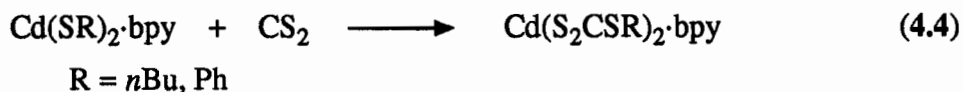
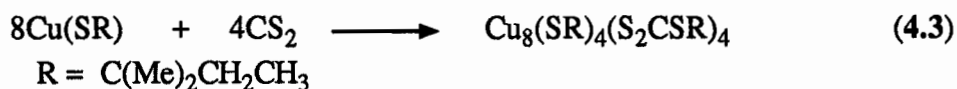


Thioxanthate complexes with either of these linkages are produced via insertion of CS_2 into a M-SR bond. For instance, $\text{CpNi}[\text{P}(n\text{Bu})_3](\text{S}_2\text{CSR})$ with a type 56 linkage, was formed from a reaction between $\text{CpNi}[\text{P}(n\text{Bu})_3](\text{SR})$ (R = Et, CH_2Ph) and CS_2 (Equation 4.1) (34). The dimer, $[\text{CpNiSR}]_2$ (R = Me, Et) and CS_2 reacted to give $[\text{CpNiS}_2\text{CSR}]$,

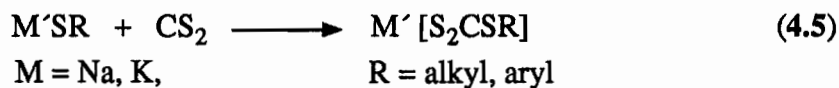
containing a type 57 ligand (Equation 4.2) (33). Other examples include the thiolates,



Cu(SC₅H₁₁) and Cd(SR)₂·bpy (bpy = bipyridine; R = *n*Bu, Ph) which both react with CS₂ to give Cu₈(SC₅H₁₁)₄(S₂CSC₅H₁₁)₄ (Equation 4.3) (38) and Cd(S₂CSR)₂·bpy (Equation 4.4) (39), respectively. Alkali salts of the thioxanthato anion, M'[S₂CSR] (M'

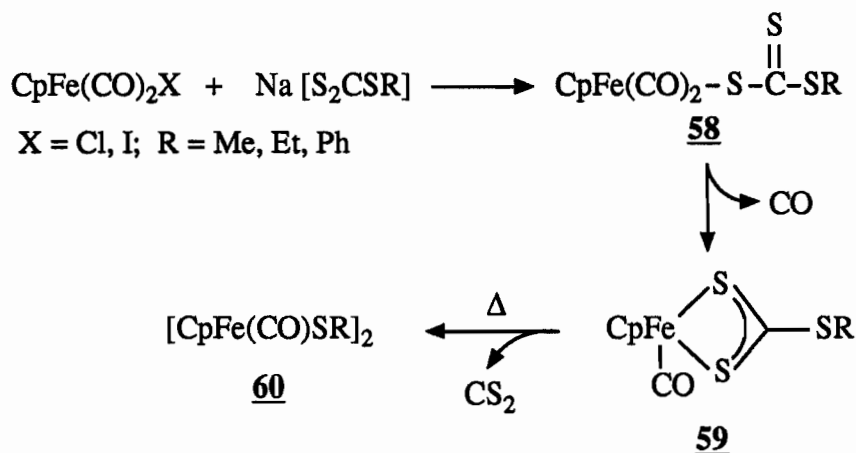


= Na, K) are also prepared from the reaction of CS₂ and M'SR, exemplified by Equation 4.5 (30).



The most common route to thioxanthate complexes is the reaction of these thioxanthate salts with an organometallic halide, MX (X = Cl, I). Numerous complexes have been produced by this method and have been reviewed (30-32). An example of this synthetic mode is shown in Scheme 4.1 (75). The complex CpFe(CO)₂X reacted with

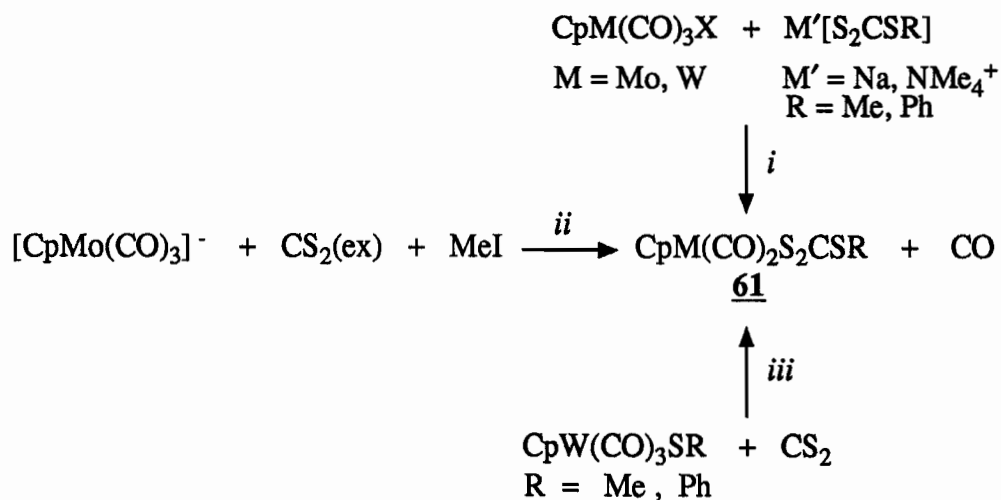
$\text{Na}[\text{S}_2\text{CSR}]$ to produce a complex with a monodentate $[\text{S}_2\text{CSR}]^-$ coordination, **58**. Complex **58** in turn, slowly decomposed to **59** in solution at ambient temperature.



Scheme 4.1

Interestingly, when heated, **59** eliminated CS_2 to give the dimer, $[\text{CpFe}(\text{CO})\text{SR}]_2$ (**60**).

The complexes $\text{CpM}(\text{CO})_2\text{S}_2\text{CSR}$ ($\text{M} = \text{Mo, W}$; $\text{R} = \text{Me, Et, Ph}$) (**61**) have been prepared by both routes discussed above and are outlined in Scheme 4.2. Both the Mo



Scheme 4.2

and W analogues of **61** have been prepared by the reaction (i) of $\text{CpM}(\text{CO})_3\text{Cl}$ with $\text{M}'(\text{S}_2\text{CSR})$ ($\text{M}' = \text{Na}, \text{NMe}_4^+$) (**76**). The complex $\text{CpMo}(\text{CO})_2\text{S}_2\text{CSMe}$ has also been produced in low yield by the treatment of $[\text{CpMo}(\text{CO})_3]^-$ with excess CS_2 , followed by addition of MeI as in reaction (ii) (**77**). As reaction (iii) shows, $\text{CpW}(\text{CO})_3\text{SR}$ and CS_2 was reported to form $\text{CpW}(\text{CO})_2\text{S}_2\text{CSR}$ (**36**).

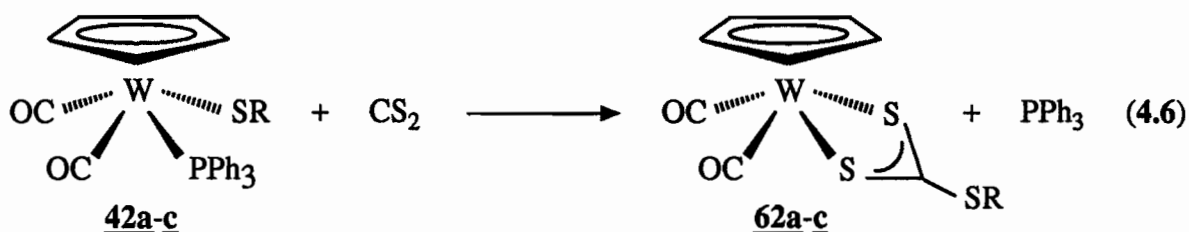
In our preparation of the tungsten thiolate complexes, $\text{CpW}(\text{CO})_2(\text{PPh}_3)\text{SR}$ (**42a-c**), a colour change was observed upon the dissolution of these complexes in CS_2 . This colour change was an indication that chemical reaction had occurred and thus, the characterization of the resulting product was pursued. Based on this reactivity with CS_2 , reactions of **42a-c** with CO_2 , COS and the heterocumulenes MeNCO , RNCS ($\text{R} = \text{Me}, \text{CHMe}_2$), and $\text{RN}=\text{C}=\text{NR}$ ($\text{R} = \text{C}_6\text{H}_{11}$) were also investigated.

Results and Discussion

A. The Reaction of $\text{CpW}(\text{CO})_2(\text{PPh}_3)\text{SR}$ with CS_2 :

Preparation and Characterization of $\text{CpW}(\text{CO})_2\text{S}_2\text{CSR}$

The orange-yellow tungsten thiolate complexes $\text{CpW}(\text{CO})_2(\text{PPh}_3)\text{SR}$ ($\text{R} = \text{CHMe}_2$, CH_2Ph , $4\text{-C}_6\text{H}_4\text{Me}$) (**42a-c**) gave red solutions when dissolved in CS_2 (Equation 4.6).



The thioxanthate products **62a-c** were isolated in 45-67% yield. Although quantitative yields were observed by NMR, appreciable solubility of the products lowered the yields. The thioxanthate complexes **62b** and **62c** are highly crystalline and interestingly, transmit red light while reflecting green light with a high luster. The λ_{max} and ϵ_0 values for **62a-c** were measured to be ~ 503 nm and $\sim 8.0 \times 10^3$ L·moles $^{-1}$ ·cm $^{-1}$, respectively, in CH_2Cl_2 . The isosbestic point for the reaction shown in Equation 4.6 appeared at ~ 390 nm. These values and the NMR and solution IR data of **62a-c** are presented in Table 4.1. For $\text{CpW}(\text{CO})_2\text{S}_2\text{CSCHMe}_2$, **62a**, the methyl protons are equivalent and appear as one doublet in the NMR spectrum, consistent with the thioxanthate structure. As well, the methylene protons in $\text{CpW}(\text{CO})_2\text{S}_2\text{CSCH}_2\text{Ph}$, **62b**, appear as a singlet, consistent with the equivalent nature of these protons. The carbonyl symmetric and asymmetric stretching frequencies of **62a-c** appear in the ranges $1950\text{-}60$ cm $^{-1}$ and $1875\text{-}85$ cm $^{-1}$,

Table 4.1 ^1H NMR^a, IR and UV-Vis Data for $\text{CpW}(\text{CO})_2(\text{PPh}_3)\text{SH}$ (**42f**)^b and $\text{CpW}(\text{CO})_2\text{S}_2\text{CSR}$ (**62a-c**)

	$\text{CpW}(\text{CO})_2(\text{PPh}_3)\text{SH}$		$\text{CpW}(\text{CO})_2\text{S}_2\text{CSR}$		
	cis	trans	R = CHMe ₂	R = CH ₂ Ph	R = 4-C ₆ H ₄ Me
	42f		62a	62b	62c
C_5H_5	5.45	5.06 ^c	5.64	5.64	5.59
SH	-2.35 ^d				
CHMe_2			4.02 ^e		
CH_2Ph				4.42	
CH_3			1.44 ^f		2.40
C_6H_x				7.33 ^g	7.43, 7.28 ^h
$\nu(\text{CO}) \text{ cm}^{-1}$	1955, 1855 ⁱ		1954, 1877 ^j	1957, 1881 ^j	1955, 1878 ^j
$\lambda_{\text{max}} \text{ (nm)}^k$			502	503	504
$\epsilon_0 \times 10^3 \text{ (}\pm 0.2\text{)}^k$			8.3	8.6	7.8
Isobestic Point (nm) ^k 42 + CS ₂ → 62			403	388	382

^a In CDCl₃ solution; reported in ppm. ^bPPh₃ phenyl resonances appeared at 7.4 ppm.

^cDoublet, $J(\text{P-H}) = 2 \text{ Hz}$. ^dDoublet, $J(\text{P-H}) = 19 \text{ Hz}$. ^eSeptet, $J(\text{H-H}) = 6.9 \text{ Hz}$.

^fDoublet, $J(\text{H-H}) = 6.9 \text{ Hz}$. ^gmultiplet, $x = 5$. ^hAB quartet, $\Delta\nu = 29 \text{ Hz}$, $J(\text{H-H}) = 8 \text{ Hz}$, $x = 4$.

ⁱIn toluene solution. ^jIn CS₂ solution. ^kIn CH₂Cl₂ solution.

respectively.

An x-ray crystal structure analysis (78) for $\text{CpW}(\text{CO})_2\text{S}_2\text{CSCH}_2\text{Ph}$, **62b**, confirmed the thioxanthate structure as determined by the NMR, IR, mass spectral and analytical data. An ORTEP diagram is shown in Figure 4.1. The crystallographic data, atomic coordinates and anisotropic thermal parameters are listed in Tables A.7-A.9, respectively, in Appendix A. The bond lengths and angles are presented in Tables 4.2 and 4.3, respectively, at the end of this section. The S1-C8-S2 bond angle, $111.6(3)^\circ$ is comparable to those in similar compounds (43,79). The S1-C8 ($1.693(5)\text{\AA}$) and S2-C8 ($1.687(6)\text{\AA}$) bond lengths are equal within experimental error and also compare well with the distances found elsewhere (43,79).

A ^1H NMR study of the reaction of $\text{CpW}(\text{CO})_2(\text{PPh}_2)\text{SCHMe}_2$ (**42a**) and CS_2 revealed that the signals due to the cis isomer rapidly decreased in intensity followed by a gradual decrease in the intensity of those of the trans isomer, while peaks due to $\text{CpW}(\text{CO})_2\text{S}_2\text{CSCHMe}_2$ appeared. This behaviour suggested that the sterically more crowded cis isomer reacted faster than the trans compound. The reaction of **42a**, where R is an electron-donating group, CHMe_2 , was much faster than that of **42c** where R is an electron-withdrawing group, $4\text{-C}_6\text{H}_4\text{Me}$. After 8 hours in CDCl_3 , in the presence of a 270-fold excess of CS_2 , the reaction was 95%, 25%, and 1% complete for **42a-c**, respectively. In neat CS_2 , the reactions proceeded much faster. Figure 4.2 plots the rate of the reaction of **42a** with CS_2 according to the first order rate equation, Equation 4.7.

$$\begin{aligned} \text{A} &= \text{CpW}(\text{CO})_2(\text{PPh}_3)\text{SR} & -\ln[\text{A}]_t + \ln[\text{A}]_0 &= kt & (4.7) \\ k &= \text{rate constant} \\ t &= \text{time} \end{aligned}$$

The data for Figure 4.2 is found in Table B.1 in Appendix B. The rate of production of $\text{CpW}(\text{CO})_2\text{S}_2\text{CSCH}_2\text{Me}_2$ declines as the amount of CS_2 present decreases from 209 equivalents (A) to 43 equivalents (C). While the rate of the reaction is plotted according

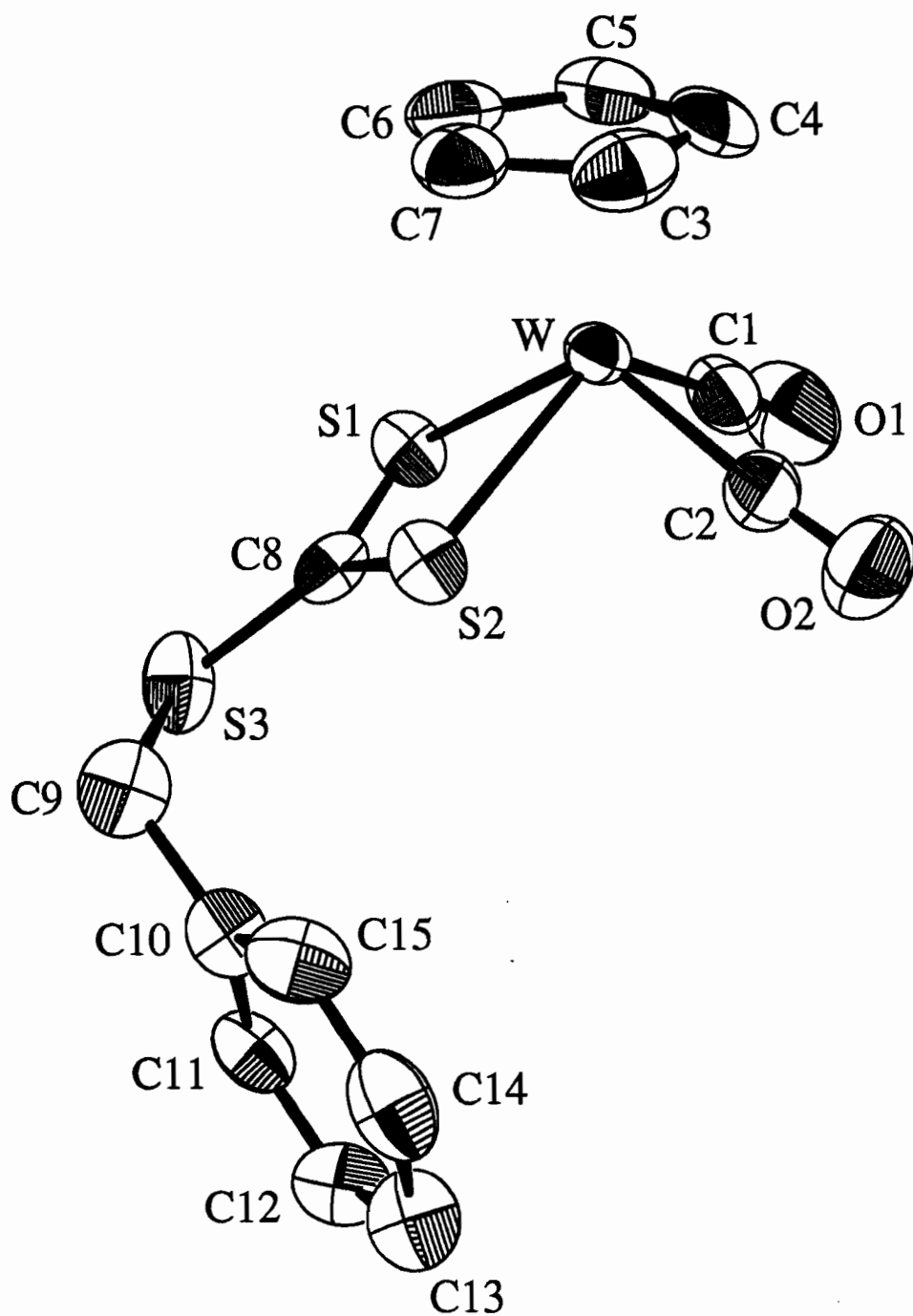


Figure 4.1 ORTEP view of CpW(CO)₂S₂CSCH₂Ph (**62b**).

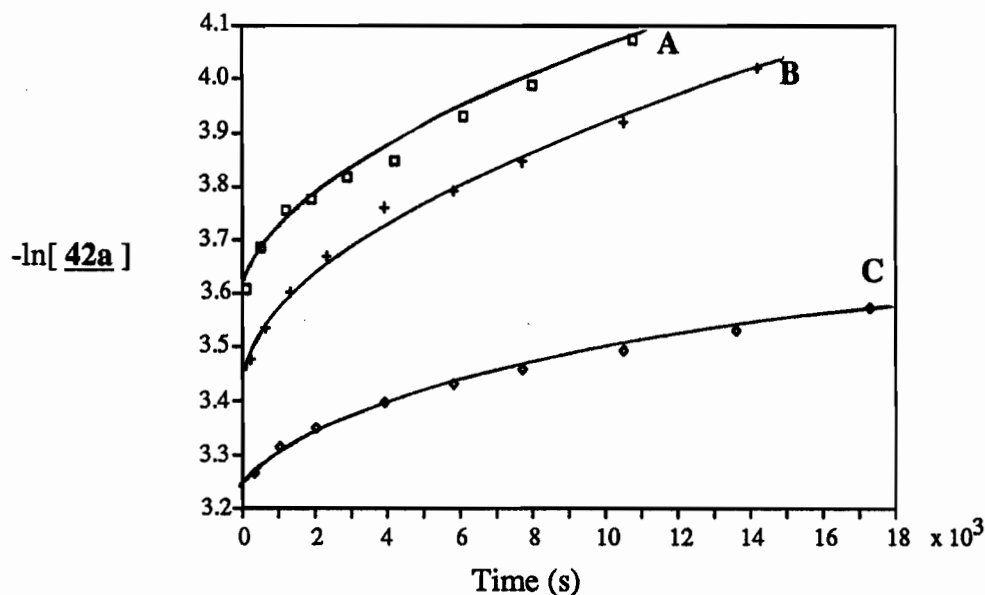


Figure 4.2 The effect of CS₂ concentration on the reaction of CpW(CO)₂(PPh₃)SCHMe₂ (**42a**) with CS₂. First order plots of **42a** with increasing CS₂ concentration: A) 209 equivalents of CS₂; B) 130 equivalents of CS₂; C) 43 equivalents of CS₂. (See Appendix B for [**42a**].)

to the first order rate law, the curves indicate that the reaction is not first order. An initial curve changes to a more or less straight line as the reaction proceeds. This non-linearity indicates that the CS₂ insertion reaction (Equation 4.6) is not first order even at the highest CS₂ concentrations employed.

The addition of excess PPh₃ appears to slow the formation of CpW(CO)₂S₂CSCHMe₂. Curves A-C in Figure 4.3 show the first order plots of the reaction of **42a** with CS₂ in the presence of 0, 3.5 and 7.0 equivalents of excess PPh₃, respectively. The data for Figure 4.3 is listed in Table B.2 in Appendix B. As the amount of excess PPh₃ increases, the rate decreases; 7 equivalents decreased the rate dramatically. While line C appears linear it is curved at the beginning of the reaction. The equilibrium between *cis* and *trans*-CpW(CO)₂(PPh₃)SCHMe₂ (equilibrium constant for *trans*-**42a** : *cis*-**42a** is 3.5 ± 0.3) may affect the rate of the reaction and may be the cause of the steep initial slope observed in Figures 4.2 and 4.3. Scheme 4.3 depicts the

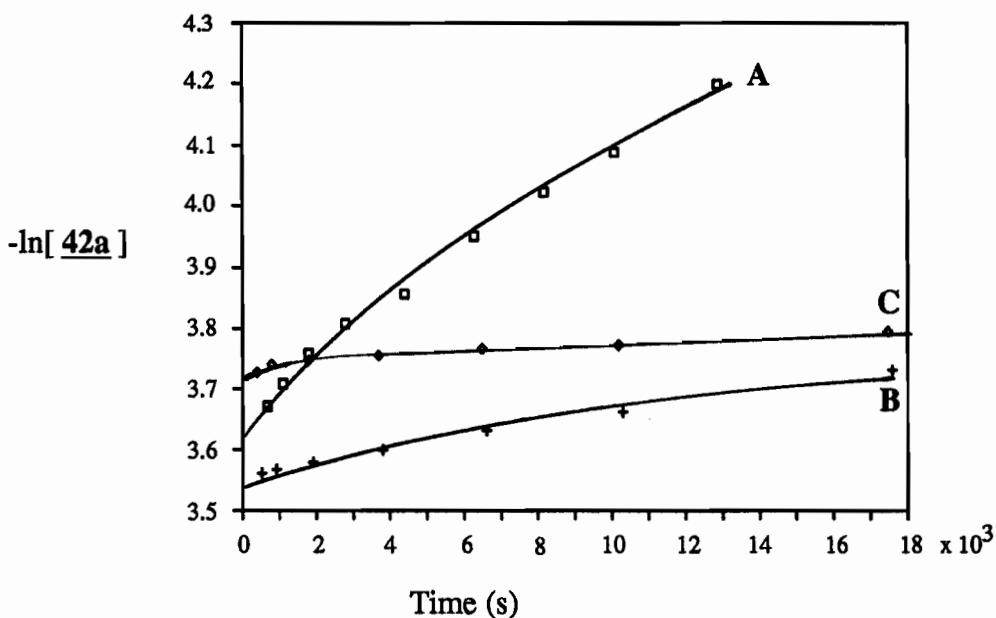
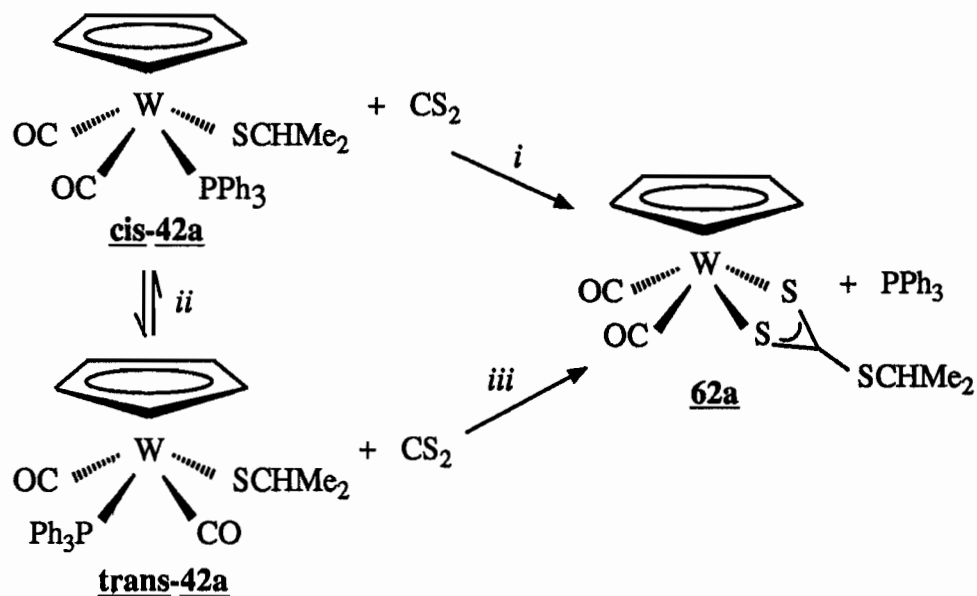


Figure 4.3 The effect of excess PPh_3 on the reaction of $\text{CpW}(\text{CO})_2(\text{PPh}_3)\text{SCHMe}_2$ (**42a**) with CS_2 . First order plots of **42a** with excess PPh_3 : A) 0 equivalents of PPh_3 B) 3.5 equivalents of PPh_3 C) 7.0 equivalents of PPh_3 . (See Appendix B for [**42a**].)

$\text{trans} \rightleftharpoons \text{cis}$ isomerization of **42a** with the addition of CS_2 to give $\text{CpW}(\text{CO})_2\text{S}_2\text{CSR}$ (**62**). As the NMR study indicated, the *cis* isomer reacted with CS_2 faster than the *trans* isomer; thus, as *cis-42a* is consumed, the rate of the reaction would be reflected by a certain rate constant, the steep initial slope, (i). Clearly, $\text{trans} \rightleftharpoons \text{cis}$ isomerization (ii) is slower than the CS_2 insertion reaction. Subsequently, *trans-42a* must isomerize to *cis-42a* to complete the reaction (ii \rightarrow i) and/or *trans-42a* itself, reacts with CS_2 at a slower rate (iii), resulting in the linear portion of curves A-C in Figures 4.2 and 4.3.

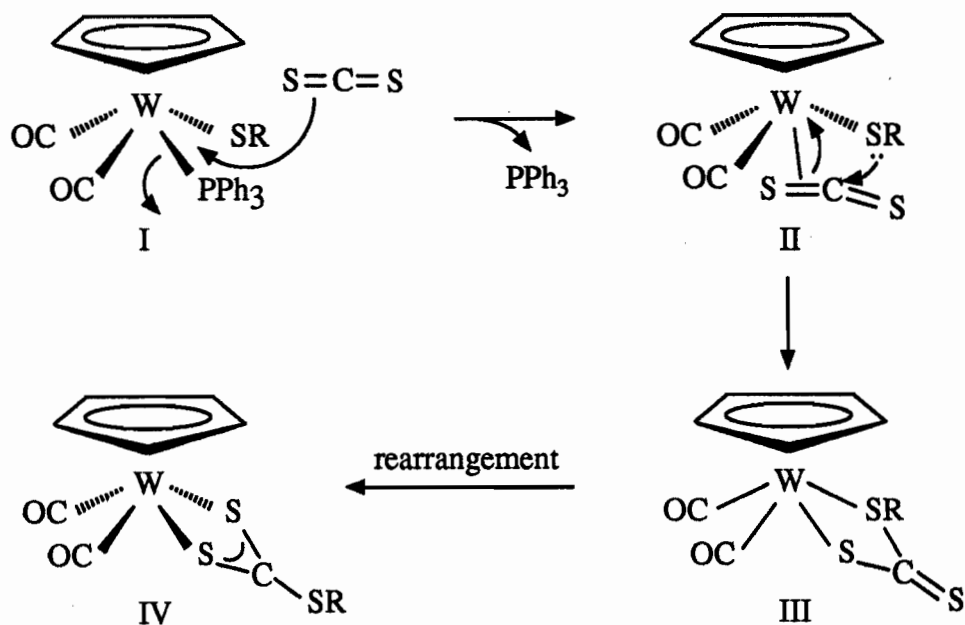
Purging an NMR sample of **42a** with CO after the addition of CS_2 also slowed the reaction markedly. Moreover, signals due to $\text{CpW}(\text{CO})_3\text{SCHMe}_2$ appeared in the NMR spectrum. The reaction of $\text{CpW}(\text{CO})_3\text{SCHMe}_2$ and CS_2 is comparatively very slow, only 70% conversion to $\text{CpW}(\text{CO})_2\text{S}_2\text{CSCHMe}_2$ (**62a**) was observed after 4 days. The preparation of $\text{CpW}(\text{CO})_2\text{S}_2\text{CSR}$ (R = Me, Ph) from $\text{CpW}(\text{CO})_3\text{SR}$ and CS_2 has been reported. However, this publication, which appeared more than 20 years ago, did not



Scheme 4.3 Reaction of *cis/trans*- $\text{CpW}(\text{CO})_2(\text{PPh}_3)\text{SCHMe}_2$ (**42a**) with CS_2 to give $\text{CpW}(\text{CO})_2\text{S}_2\text{CSCHMe}_2$ (**62a**).

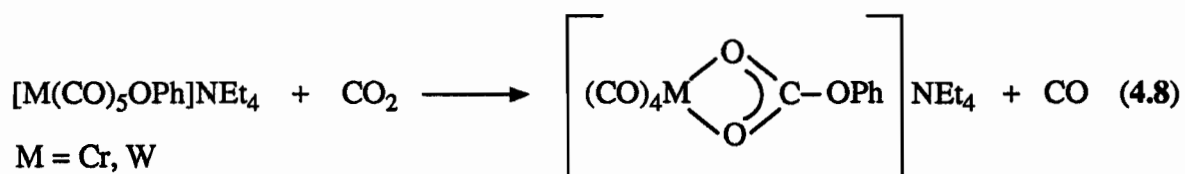
mention the lengthy reaction time for the production of the thioxanthate, moreover, it contained no characterization evidence such as NMR, IR, mass spectral data or elemental analysis (36).

Scheme 4.4 incorporates the following observations of the rate of thioxanthate formation: 1) faster for the *cis* isomer than the *trans* isomer, 2) inhibited by excess PPh_3 or CO , 3) decreased as the R group becomes increasingly electron-withdrawing ($\text{CHMe}_2 < \text{CH}_2\text{Ph} < 4\text{-C}_6\text{H}_4\text{Me}$), and 4) reacted faster for $\text{CpW}(\text{CO})_2(\text{PPh}_3)\text{SR}$ than for $\text{CpW}(\text{CO})_3\text{SR}$. These observations suggest that electrophilic attack by *precoordinated* CS_2 on the coordinated sulfur atom is the major pathway to the thioxanthate product. Attack by free CS_2 can not be ruled out but is inconsistent with the inhibition of the reaction by free PPh_3 or CO . In a related system, Darenbourg et al (80,81) found that CO_2 inserted into the W-OR bond of $\text{W}(\text{CO})_5\text{OR}$ anions (Equation 4.8). Attack of *free* CO_2 was proposed to be the likely route to the products, since the reaction was not



Scheme 4.4 Proposed pathway for the formation of CpW(CO)₂S₂CSR (**62**) from the insertion of CS₂ into CpW(CO)₂(PPh₃)SR (**42**).

inhibited by free CO. In our study, the appearance of CpW(CO)₃SCHMe₂, after purging



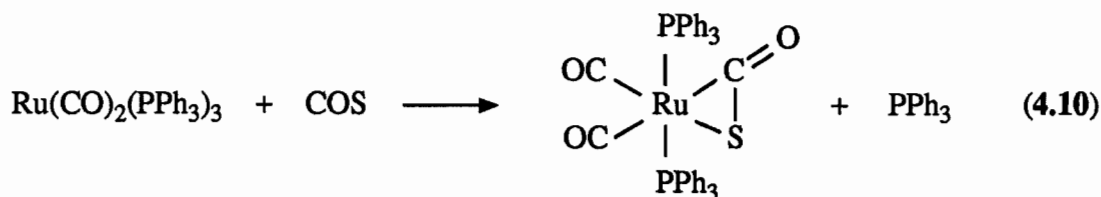
an NMR sample containing **42a** and CS₂, with CO indicates that PPh₃ dissociated easily, giving a coordinatively unsaturated species, CpW(CO)₂SR. Thiolate ligands are known to stabilize 16 electron coordinatively unsaturated organometallic species by π-dπ donation to the empty metal d orbitals from the sulfur 3p lone pair orbitals (82-84) as discussed in Chapter 1. The species, CpW(CO)₂SR, could coordinate a molecule of CS₂ as shown and followed by electrophilic attack on the sulfur atom of the thiolate ligand to give III, rearrangement of which gives the thioxanthate product, IV.

B. The Reaction of $\text{CpW}(\text{CO})_2(\text{PPh}_3)\text{SCHMe}_2$, **42a**, with COS

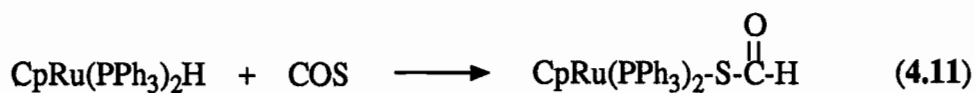
In reactions with COS, organometallic complexes usually give carbonylation products, arising from C-S bond cleavage (58,60,62,64), or η^2 -COS coordination complexes (60,61,63,85-87). Insertion compounds with linkages such as **56** or **57** (50,81) are rare. Carbon-sulfur bond cleavage occurred when $\text{Rh}(\text{H})(\text{PPh}_3)_4$ reacted with COS to give $\text{Rh}(\text{SH})(\text{CO})(\text{PPh}_3)_2$ (Equation 4.9) (62). Products with an η^2 -COS linkage have



also been observed and $\text{Ru}(\text{CO})_2(\text{PPh}_3)_2(\eta^2\text{-COS})$, was identified from the reaction of $\text{Ru}(\text{CO})_2(\text{PPh}_3)_3$ and COS (Equation 4.10) (60). In the reaction of $\text{CpRu}(\text{PPh}_3)_2\text{H}$ and



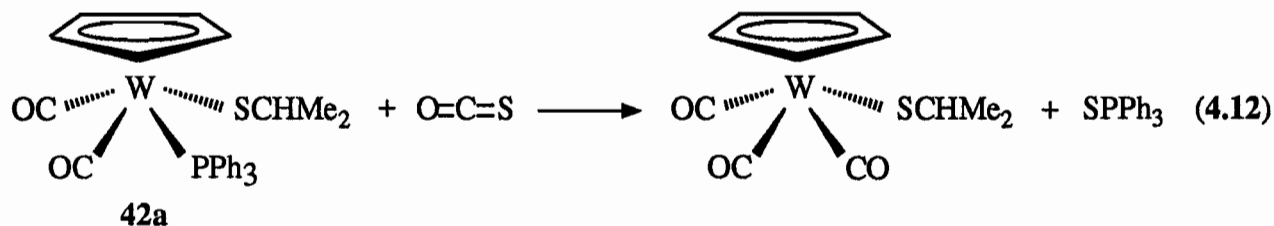
COS, an η^1 -COS complex, $\text{CpRu}(\text{PPh}_3)_2\text{SC}(\text{O})\text{H}$, was produced (Equation 4.11) (50).



No reaction has been reported between COS and metal thiolate complexes (81).

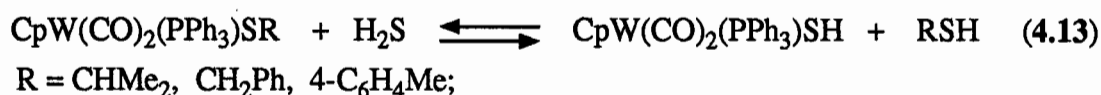
Based on the reactivity of $\text{CpW}(\text{CO})_2(\text{PPh}_3)\text{SR}$ (**42a-c**) with CS_2 and the above examples of COS reactivity, the reaction of (**42a-c**) with COS was attempted. Treatment of an NMR sample of $\text{CpW}(\text{CO})_2(\text{PPh}_3)\text{SCHMe}_2$ (**42a**) with gaseous COS for four hours showed that the major species in solution was the starting complex, **42a**. The presence of the dimer, $[\text{CpW}(\text{CO})_2\text{SCHMe}_2]_2$ (**50a**), and an unassigned singlet Cp peak (5.44 ppm)

and doublet in the methyl region (0.98 ppm) of moderate intensity were also detected. Peaks due to $\text{CpW}(\text{CO})_3\text{SCHMe}_2$ and SPPH_3 were also observed and were likely formed from C-S bond cleavage of COS (Equation 4.12), similar to Equation 4.9.

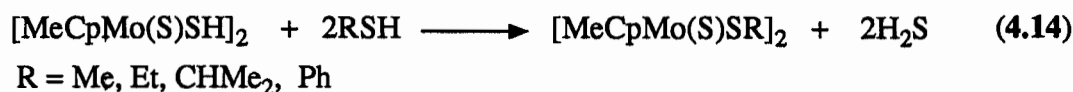


In a preparative scale reaction, treatment of the thiolate complex, **42a**, with liquid COS at room temperature after 3 days gave the unexpected product, $\text{CpW}(\text{CO})_2(\text{PPh}_3)\text{SH}$, **42f**, as orange microcrystals, characterized by NMR, IR, mass spectroscopy and elemental analysis. The *cis*-**42f**:*trans*-**42f** ratio was 9:1, as observed by NMR. In the NMR spectrum, a doublet upfield of TMS at -2.35 ppm ($J(\text{P-H}) = 19$ Hz) was assigned to the thiol proton of *cis*-**42f**. Further, upon treatment of the NMR sample with CO for 30 minutes, peaks due to $\text{CpW}(\text{CO})_3\text{SH}$ (**88**) appeared, consistent with the displacement of PPh_3 from **42f**.

Recalling Chapter 2, the preparation of **42f** was first attempted by treatment of $\text{CpW}(\text{CO})_2(\text{PPh}_3)\text{Cl}$ and NaSH but the reaction gave only starting materials. Thus, the production of **42f** from the reaction of **42a** and liquid COS was both interesting and puzzling. However, specification data from Matheson Gas Products revealed that the commercial COS used contained 0.5% H_2S . This percentage would give approximately 10 equivalents of H_2S to 1 equivalent of **42a** in 15 mL of liquid COS used. Hence, a thiolate exchange reaction (Equation 4.13) was the likely route to $\text{CpW}(\text{CO})_2(\text{PPh}_3)\text{SH}$.



The byproduct, Me_2HCSH , was also observed in the NMR spectrum of the residue of the liquid COS reaction. A reaction between **42a** and H_2S gave **42f** in 84% yield. NMR samples of **42b** and **42c** treated with H_2S also showed the production of **42f** and the appropriate organic thiol, PhCH_2SH and $4\text{-C}_6\text{H}_4\text{MeSH}$, respectively. However, these reactions appeared to be reversible. If the thiol byproduct, RSH , is not removed then some of the original thiolate, $\text{CpW}(\text{CO})_2(\text{PPh}_3)\text{SR}$ is reformed. Thiolate exchange reactions have been observed for Me_3MSR ($\text{M} = \text{Si}, \text{Ge}, \text{Sn}, \text{Pb}$) complexes (87) and more recently, $[(\text{MeCp})\text{Mo}(\text{S})\text{SH}]_2$ was shown to react with RSH ($\text{R} = \text{Me}, \text{Et}, \text{CHMe}_2, \text{Ph}$) to give $[(\text{MeCp})\text{Mo}(\text{S})\text{SR}]_2$ (Equation 4.14) (90). The thiolate exchange reactions



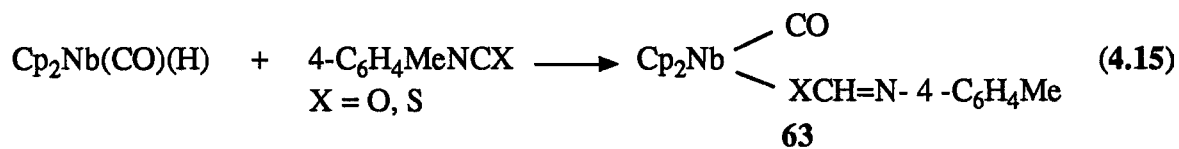
between $\text{CpW}(\text{CO})_2(\text{PPh}_3)\text{SR}$ and $\text{R}'\text{SH}$ are discussed in Chapter 2 (Scheme 2.3).

C. The Treatment of $\text{CpW}(\text{CO})_2(\text{PPh}_3)\text{SCHMe}_2$, **42a**, with CO_2

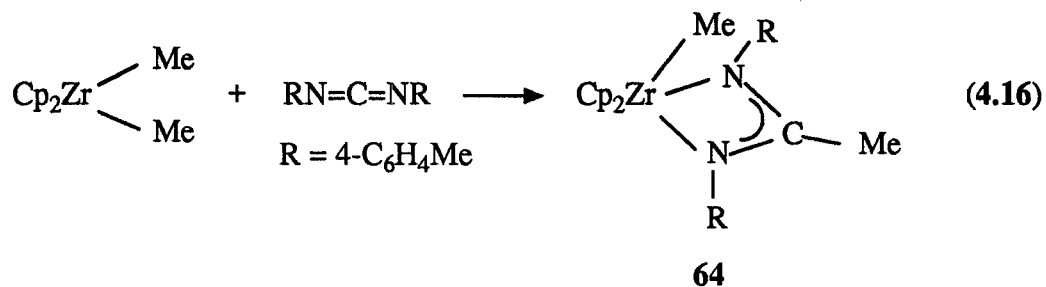
Treatment of the tungsten thiolate complex, **42a**, with gaseous CO_2 gave the dimer, $[\text{CpW}(\text{CO})_2\text{SCHMe}_2]_2$ (**50a**), which was also prepared from the reaction of **42a** in the absence of CO_2 under the same conditions. The lack of reactivity of CO_2 with this tungsten thiolate complex is similar to results previously reported for $[\text{M}(\text{CO})_5\text{SR}]^-$ ($\text{M} = \text{Cr}, \text{W}; \text{R} = \text{H}, \text{Ph}$) (65). However, CO_2 does react with the alkoxides, $[\text{M}(\text{CO})_5\text{OPh}]^-$ ($\text{M} = \text{Cr}, \text{W}$) to give $[\text{M}(\text{CO})_4\text{O}_2\text{COPh}]^-$ as shown earlier in Equation 4.8 (27-29,80,81).

D. The Treatment of $\text{CpW}(\text{CO})_2(\text{PPh}_3)\text{SCHMe}_2$, **42a**, with MeNCO , RNCS ($\text{R} = \text{Me}, \text{CHMe}_2$) and RNCNR ($\text{R} = \text{C}_6\text{H}_{11}$)

The heterocumulenes, RNCS (64,67-72), RNCO (12,22,64,67-74), RNCNR (12,64,72,74) have been reported to react with organometallic complexes to give insertion products. Both $4\text{-C}_6\text{H}_4\text{MeNCS}$ and $4\text{-C}_6\text{H}_4\text{MeNCO}$ reacted with $\text{Cp}_2\text{Nb}(\text{CO})(\text{H})$ to give $\text{Cp}_2\text{Nb}(\text{CO})(\text{XCH}=\text{N}-4\text{-C}_6\text{H}_4\text{Me})$ ($\text{X} = \text{O}, \text{S}$) **63** (Equation 4.15) (70,72). The carbodiimide, $\text{RN}=\text{C}=\text{NR}$ ($\text{R} = 4\text{-C}_6\text{H}_4\text{Me}$) and Cp_2ZrMe_2 reacted to give



complex **64** (Equation 4.16) (74). However, reactions of mercaptide complexes with



these heterocumulenes have not been reported.

In our work, the complex, $\text{CpW}(\text{CO})_2(\text{PPh}_3)\text{SCHMe}_2$ (**42a**), showed little or no reactivity with the heterocumulenes, MeNCO , RNCS ($\text{R} = \text{Me}, \text{CHMe}_2$) and RNCNR ($\text{R} = \text{C}_6\text{H}_{11}$). Treatments of **42a** with MeNCO , MeNCS and RNCNR ($\text{R} = \text{C}_6\text{H}_{11}$) were monitored by NMR for 1 day. Typically, ~80% of the Cp resonances observed were due to **42a**. Most of **42a** did not undergo any reaction other than some dimerization since peaks due to $[\text{CpW}(\text{CO})_2\text{SCHMe}_2]_2$ (**50a**) were observed. In the case of **42a** and MeNCO , the spectrum showed an unassigned doublet at 2.77 ppm but no corresponding

Cp or methyne peaks attributable to a new complex was detected. The spectrum of **42a** with MeNCS showed two new Cp resonances at 5.67 and 5.66 ppm but these comprised less than 20% of the total Cp resonances. For **42a** and $H_{11}C_6NCNC_6H_{11}$, the spectrum exhibited peaks due only to the starting materials and **50a**. Initially, the treatment of **42a** in neat Me_2HCNCS appeared to give a reaction since a colour change from orange-yellow to orange-red was observed after the solution had been stirred for 3 weeks. Column chromatography of the solution residue yielded a red-orange band. A yellow band followed and was identified as **42a** by NMR. In the spectrum of the red-orange band several new Cp resonances at 5.67, 5.66, and 5.64 ppm were detected, however, these and the Cp peak due to **50a** comprised <30% of the total Cp resonances present; the two Cp peaks at 5.49 and 5.04 ppm accounting for the remaining 70% were due to unreacted *cis/trans*-**42a**. The treatments of **42a** and the heterocumulenes above were all performed at room temperature since, as shown by the presence of the dimer $[CpW(CO)_2SCHMe_2]_2$ in all the NMR spectra of the resulting residues, **42a** exhibits a facile tendency to dimerize which is accelerated when heated (Chapter 3).

The reaction of the thiolate compounds, **42a-c**, with CS_2 to give the thioxanthate complexes, **62a-c**, shows that the W-SR bond is reactive toward this electrophile and is in accord with other reports of thiolate complexes with CS_2 (30,33-36,38,39). The lack of reactivity of $CpW(CO)_2(PPh_3)SCHMe_2$ with COS and CO_2 is consistent with previous reports of the general reactivity pattern for CS_2 , COS, and CO_2 with organometallic complexes (58). Carbon dioxide and carbonyl sulfide show limited reactivity toward organometallic complexes, while carbon disulfide is prolific in its general reactivity towards this class of compounds.

The heterocumulenes, RNCNCO, RNCS and RNCNR showed little or no reactivity with $CpW(CO)_2(PPh_3)SCHMe_2$. A full comparative study of the reactivity of these

heterocumulenes is lacking in the literature but there are many reports of these electrophiles reacting with metal-carbon bonds (12,22,64,67-74). No reports of reactions with metal thiolate compounds are known. In our study, it is possible that the nucleophilic nature of the thiolate sulfur atom in $\text{CpW}(\text{CO})_2(\text{PPh}_3)\text{SCHMe}_2$ was insufficient to initiate a reaction. Changing the electronic environment of the complex by using a more basic ligand such as Me_5Cp might result in greater nucleophilicity and prompt reactions with these heterocumulenes as well as with CO_2 and COS .

Table 4.2 Bond Distances (Å) for CpW(CO)₂S₂CSCH₂Ph (**62b**)

W-S1	2.489(3)	C1-O1	1.160(7)
W-S2	2.481(2)	C2-O2	1.169(8)
W-C1	1.968(6)	C3-C4	1.42 (1)
W-C2	1.967(7)	C3-C7	1.38 (1)
W-C3	2.377(6)	C4-C5	1.42 (1)
W-C4	2.289(6)	C5-C6	1.42 (1)
W-C5	2.267(6)	C6-C7	1.40 (1)
W-C6	2.312(6)	C9-C10	1.495(9)
W-C7	2.400(7)	C10-C11	1.417(8)
S1-C8	1.693(5)	C10-C15	1.392(9)
S2-C8	1.687(6)	C11-C12	1.363(9)
S3-C8	1.735(5)	C12-C13	1.36 (1)
S3-C9	1.833(6)	C13-C14	1.41 (1)
		C14-C15	1.40 (1)

Table 4.3 Bond Angles (deg) for CpW(CO)₂S₂CSCH₂Ph (**62b**)

S1-W-S2	68.5(6)	W-S1-C8	89.8(2)
S1-W-C1	80.0(2)	W-S2-C8	90.2(2)
S1-W-C2	122.8(2)	C8-S3-C9	102.3(3)
S1-W-C4	140.6(2)	W-C1-O1	177.0(6)
S1-W-C5	140.2(2)	W-C2-O2	175.9(5)
S1-W-C6	104.1(2)	C4-C3-C7	108.9(6)
S2-W-C1	122.7(2)	C3-C4-C5	107.4(6)
S2-W-C2	80.2(2)	C4-C5-C6	107.1(6)
S2-W-C4	101.2(2)	C5-C6-C7	108.3(6)
S2-W-C5	137.4(2)	C3-C7-C6	108.3(6)
S2-W-C6	141.3(2)	S1-C8-S2	111.6(3)
C1-W-C2	78.7(3)	S1-C8-S3	121.1(3)
C1-W-C4	131.5(3)	S2-C8-S3	127.3(3)
C1-W-C5	97.1(3)	S2-C9-C10	115.1(4)
C1-W-C6	91.3(3)	C9-C10-C11	122.7(5)
C2-W-C4	90.5(3)	C9-C10-C15	120.7(5)
C2-W-C5	94.9(3)	C11-C10-C15	116.6(5)
C2-W-C6	128.7(3)	C10-C11-C12	122.1(5)
C4-W-C5	36.3(3)	C11-C12-C13	121.5(6)
C4-W-C6	59.5(3)	C12-C13-C14	118.6(7)
C5-W-C6	36.1(3)	C13-C14-C15	120.3(6)
		C10-C15-C14	120.9(6)

Experimental

A. Cyclopentadienyldicarbonyl-2-propylthioxanthanatotungsten(II),



Carbon disulfide, (20 mL) was added to a solid sample of **42a** (0.15 g, 2.33 mmol). The solution became dark blood red almost immediately and stirring was continued for 9 hours. The solvent-reagent was removed by evaporation under vacuum (oil pump) and the residue dissolved in CH_2Cl_2 (4 mL). Chromatography on activated alumina (3 x 40 cm) and elution with CH_2Cl_2 gave a single red band which was collected. Removal of the solvent and recrystallization of the residue from hexanes gave **62a** as a dark red powder (0.062 g, 58%, m.p.=127-128°C) that was dried overnight in vacuo. Anal. Calc'd for $\text{C}_{11}\text{H}_{12}\text{O}_2\text{S}_3\text{W}$: C, 28.96; H, 2.65; S, 21.08. Found: C, 29.52; H, 2.68; S, 20.64.

IR (Nujol): 2728 (w), 2361 (w), 2339 (w), 1934 (s), 1874 (s), 1420 (w), 1063 (w, sh), 990 (m, sh), 972 (m, sh), 831 (w, sh) cm^{-1} .

Mass spectrum: 456 (M^+ , 15.8); 400 (M^+-2CO^+ , 30.6); 357 ($\text{M}^+-2\text{CO}-\text{CHMe}_2$, 100.0); 337 ($\text{M}^+-\text{CS}_2-\text{CHMe}_2$, 9.9); 325 ($\text{M}^+-2\text{CO}-\text{S}-\text{CHMe}_2$, 6.7); 309 ($\text{M}^+-\text{CS}_2-\text{CO}-\text{CHMe}_2$, 17.9); 281 ($\text{M}^+-\text{CS}_2-2\text{CO}-\text{CHMe}_2$, 57.6).

B. Cyclopentadienyldicarbonylphenylmethylthioxanthanatotungsten(II),



As for A, CS_2 (20 mL) was added to a solid sample of **42b** (0.11 g, 1.65 mmol) and the reaction solution was stirred for 2 days. The solution was concentrated to 8 mL and

chromatographed on an alumina column (4 x 48 cm). Elution with CH_2Cl_2 gave a red band which was collected and reduced to dryness. Recrystallization of the residue from CH_2Cl_2 /hexanes (1:4) yielded **62b** as long red needles with a greenish luster (0.056 g, 67%, m.p.=137-138°C). Anal. Calc'd for $\text{C}_{15}\text{H}_{12}\text{O}_2\text{S}_3\text{W}$: C, 35.73; H, 2.40; S, 19.07. Found : C, 36.41; H, 2.36; S, 19.52.

IR (Nujol): 2359 (w), 2337 (w), 1936 (s), 1852 (s), 1157 (w), 1120 (w), 1073 (w), 1029 (w), 1005 (w, sh), 975 (m, sh), 872 (m, sh), 761 (w, sh), 704 (m, sh) cm^{-1} .

Mass spectrum, CI: 505 ($\text{M}^+\text{-H}$, 100); 477 ($\text{M}^+\text{-H-CO}$, 47.1); 449 ($\text{M}^+\text{-H-2CO}$, 5.3); 337 ($\text{M}^+\text{-H-CS}_2\text{-CH}_2\text{Ph}$, 6.6). High resolution mass spectrum, (EI): M^+ , 502.95600 based on ^{182}W .

C. Cyclopentadienyldicarbonyl-4-methylbenzenethioxanthanatotungsten(II),

$\text{CpW}(\text{CO})_2\text{S}_2\text{CS-4-C}_6\text{H}_4\text{Me}$, **62c**

Similar to B, **42c** (0.14 g, 2.2 mmol) was dissolved in neat CS_2 (10 mL) and the reaction solution stirred for 2 days. The solvent was removed under vacuum and the residue dissolved in CH_2Cl_2 (4 mL). Chromatography on activated alumina (1.5 x 50 cm) and elution with CH_2Cl_2 gave a red band followed by an orange band, identified as the starting material, **42c**. The solvent was removed in vacuo from the red band and the residue was recrystallized from CH_2Cl_2 /hexanes (1:5) giving **62c** as red crystals with a greenish luster (0.05 g, 45%, m.p.=172-173°C). Anal. Calc'd for $\text{C}_{15}\text{H}_{12}\text{O}_2\text{S}_3\text{W}$: C, 35.73; H, 2.40; S, 19.07. Found: C, 35.76; H, 2.51; S, 18.93.

IR (Nujol): 1957 (s), 1942 (s), 1929 (s), 1865 (s), 1856 (s), 1843 (s), 1263 (w), 1088 (w), 1011 (w), 962 (m), 828 (w), 809 (m), 755 (w) 698 (w) cm^{-1} .

Mass spectrum, EI: 503 ($\text{M}^+\text{-H}$, 7.7); 447 ($\text{M}^+\text{-H-2CO}$, 31.5); 401 ($\text{M}^+\text{-2CO-S-Me}$, 4.3); 369 ($\text{M}^+\text{-H-2CO-S-Me}$, 9.2); 281 ($\text{M}^+\text{-2CO-CS}_2\text{-4-C}_6\text{H}_4\text{Me}$,

7.4).

D. Attempted Reaction of $\text{CpW}(\text{CO})_2(\text{PPh}_3)\text{SCHMe}_2$, **42a**, and CO_2

In a three-necked 100 mL round bottom flask equipped with a condenser, **42a** (0.25 g, 0.39 mmol) was dissolved in THF (18 mL). A three-necked 2 L round bottom flask, equipped with a stopcock adaptor that was always left slightly open to avoid a pressure build-up, was charged with solid CO_2 . Carbon dioxide was bubbled through the stirred solution for 9 hours. A small aliquot of the red-orange solution was taken and reduced to dryness. A ^1H NMR spectrum of the residue in CDCl_3 showed only peaks due to the starting material, **42a**. The reaction was repeated at 50°C for 12 hours with a slow stream of CO_2 bubbled through the solution. The black-brown solution was reduced to dryness and chromatographed on activated alumina (2 x 50 cm). Elution with CH_2Cl_2 gave a dark brown band followed by a yellow-orange band which were both were collected. ^1H NMR spectroscopy revealed that the yellow-orange band was due to unreacted **42a**. The brown fraction was recrystallized from CH_2Cl_2 /hexanes to give black crystals. The NMR, IR and mass spectra and analytical data of this product was consistent with those of the dimer $[\text{CpW}(\text{CO})_2\text{SCHMe}_2]_2$, **50a**.

E. Attempted Reaction of $\text{CpW}(\text{CO})_2(\text{PPh}_3)\text{SCHMe}_2$, **42a**, and COS

1. NMR study of $\text{CpW}(\text{CO})_2(\text{PPh}_3)\text{SCHMe}_2$ and $\text{COS}(g)$

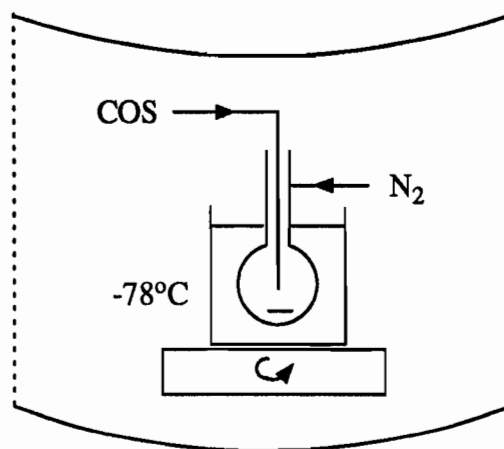
An NMR sample of **42a** in CDCl_3 was treated with a slow stream of $\text{COS}(g)$ for four hours with replenishment of CDCl_3 as needed. After this time, the spectrum showed the major species in solution was the starting material, **42a**. However, peaks due to the

dimer $[\text{CpW}(\text{CO})_2\text{SCHMe}_2]_2$, **50a**, and $\text{CpW}(\text{CO})_3\text{SCHMe}_2$ were also observed. An unassigned singlet Cp peak at 5.44 ppm and a doublet in the methyl region at 0.98 ppm ($J(\text{H-H}) = 6.4 \text{ Hz}$) were also present.

2. Reaction of $\text{CpW}(\text{CO})_2(\text{PPh}_3)\text{SCHMe}_2$, **42a**, and $\text{COS}(l)$

Preparation of $\text{CpW}(\text{CO})_2(\text{PPh}_3)\text{SH}$, **42f**

CAUTION: Liquid COS boils at -50°C and in a closed system generates high pressure. The reaction should be performed in a fumehood using a blast shield and face mask in a high pressure reaction vessel free from stress areas or cracks. The fumehood shutter should be closed when not attending the reaction.



Blast shield

A 100 mL Carius tube (a transparent, thick-walled, pear-shaped flask equipped with a teflon-seal screw valve and outlet) was charged with **42a** (0.14 g, 0.22 mmol) and and twice evacuated and filled with N_2 . The reaction vessel was cooled to -78°C using a dry-ice/acetone bath. The flask was opened under a strong flow of N_2 via the outlet and the teflon screw valve was removed. Carbonyl sulfide gas was condensed into the vessel via a 12" needle. After condensation of liquid COS (~15 mL, 12.4 g, 207 mmol), the

vessel was closed by replacing the teflon valve and the blast shield was placed in front of the reactor. The cooling bath was removed and the stirred orange suspension allowed to warm to room temperature. The fumehood shutter was closed.

Stirring continued for 2 days. The flask was again cooled to -78°C and opened carefully to a strong flow of N₂ via the N₂ outlet. The vessel was opened completely and the system allowed to slowly warm to room temperature. As the flask warmed, the excess COS evaporated, leaving an orange residue; the blast shield was removed. This orange solid was extracted with a minimal amount of CH₂Cl₂ and chromatographed on activated alumina (3 x 50 cm). Elution with 3:1 CH₂Cl₂/hexanes gave one orange band which was collected. Removal of the solvent by evaporation under vacuum and recrystallization of the residue from CH₂Cl₂/hexanes gave CpW(CO)₂(PPh₃)SH, **42f**, as orange microcrystals (0.054 g, 41%, m.p. = 159-160°C). Anal. Calc'd for C₂₅H₂₁O₂PSW: C, 50.02; H, 3.50; S, 5.34. Found: C, 49.73; H, 3.66; S, 5.71.

IR (toluene) $\nu(\text{CO})$: 1955 (w), 1855 (w) cm⁻¹. IR (Nujol): 1921 (s), 1831 (s), 1183 (w), 1090 (m), 851 (w), 831 (w), 823 (m), 748 (m), 723 (w), 689 (m) cm⁻¹.

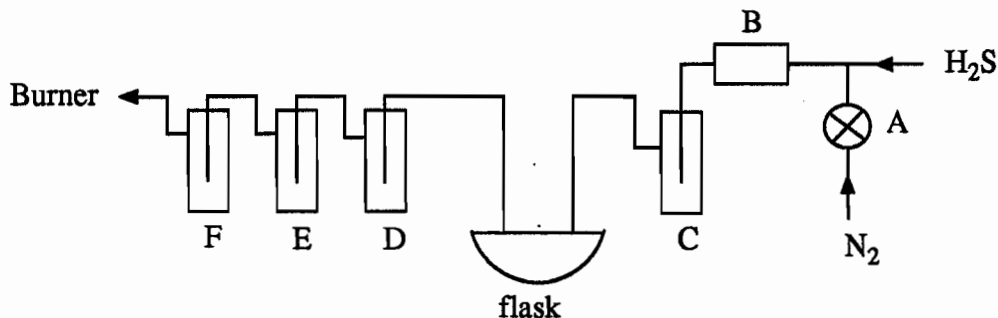
Mass spectrum, CI: 681 (Cp₂W₂(CO)₃S₃⁺, 0.04); 648 (Cp₂W₂(CO)₃S₂⁺, 0.04); 570 (M⁺-CO-2H, 1.9); 567 (M⁺-SH, 2.0); 539 (M⁺-CO-SH, 0.2); 262 (PPh₃⁺, 100); 183 (W⁺, 30). Unidentified peaks at 724 (0.16), 610 (0.08), 509 (1.3), 490 (0.87), 445 (6.6), 370 (2.9).

F. Preparation of CpW(CO)₂(PPh₃)SH, **42f**

Reaction of CpW(CO)₂(PPh₃)SCHMe₂, **42a**, and H₂S

Caution: The preparation of CpW(CO)₂(PPh₃)SH (**42f**) involves the use of H₂S which is very toxic and smelly. Extreme care must be exercised. The reactions must be conducted in an efficient fume hood and every effort must be made to ensure

containment of the gas. The use of an H₂S manifold such as the one shown below is strongly recommended.



The gas was dried by means of a calcium chloride column (B) and passed through a Nujol bubbler (C) before entering the reaction vessel. Unreacted gas was passed through three washing towers containing, successively, 5M NaOH (D), saturated aqueous lead acetate (E), and 5M NaOH (F). Any gas not neutralized in these steps was burned. Prior to and after the use of H₂S, the system was flushed for approximately 10 minutes with a strong stream of nitrogen via stopcock (A).

A 100 mL three-necked round bottom flask was charged with a sample of **42a** (1.2g, 1.8 mmol), partially dissolved in a 1:1 mixture of CH₂Cl₂/ether (50 mL) and then H₂S was bubbled through the solution for 30 minutes. The solvent, partially evaporated by a stream of H₂S, was reduced to dryness under vacuum. The residue was chromatographed on alumina (3 x 40 cm). Elution with CH₂Cl₂ gave a red band followed by an orange band. Both fractions were collected and the solvent removed under vacuum. The first fraction, which contained a mixture of the red and orange compounds was rechromatographed on alumina (1.5 x 30 cm) using a 2:1 solvent mixture of CH₂Cl₂/hexanes. Separation of the two bands was achieved and the orange fraction was combined with the fraction from the first chromatographic column and recrystallized from CH₂Cl₂/hexanes to give orange microcrystals (0.83 g, 84%) of **42f** whose identity

was confirmed by ^1H NMR. The red band gave a red-grey solid (0.038 g, m.p. = 199-203°C) which was identified by ^1H NMR, IR, mass spectral and analytical data to be $\text{CpW}(\text{CO})_2(\text{PPh}_3)\text{H}$, **40**. The mother liquors of the red band were reduced to dryness and the NMR spectrum of the residue (~0.03 g) showed peaks corresponding to $\text{CpW}(\text{CO})_2\text{S}_2\text{CSCHMe}_2$, **62a**.

G. Treatment of $\text{CpW}(\text{CO})_2(\text{PPh}_3)\text{SCHMe}_2$, **42a**, and MeNCO

An NMR sample of **42a** in CDCl_3 was treated with a drop of MeNCO and spectra were recorded after 5 minutes and 3, 5, and 23 hours. After 1 day, 90% of the Cp resonances were due to **42a**. Peaks due to the dimer, $[\text{CpW}(\text{CO})_2\text{SCHMe}_2]_2$ (**50a**), were also observed. An unassigned doublet at 2.77 ppm ($J(\text{H-H}) = 4.8$ Hz) was detected after 3 hours and steadily increased in intensity. However, no corresponding Cp or methyne peaks relating to a new complex were observed and the reaction abandoned.

H. Reaction of $\text{CpW}(\text{CO})_2(\text{PPh}_3)\text{SCHMe}_2$, **42a** and Me_2CHNCS

To a stirred solution of **42a** (0.17 g, 0.26 mmol) in CH_2Cl_2 (5 mL), Me_2CHNCS (0.51 g, 4.94 mmol) was added. The orange solution was allowed to stir for 2 days. The reaction solution was reduced to dryness and liquid Me_2CHNCS (0.05 g, 4.8 mmol) was added to the residue and the solution was allowed to stir for 3 weeks. After removing the solvent/reagent under vacuum, the residue was chromatographed on alumina (1.2 x 45 cm). A red-orange band eluted first with CH_2Cl_2 , closely followed by a yellow band. A purple band, eluted very slowly with a 1:1 mixture of CH_2Cl_2 /ethanol and was collected. Each fraction was reduced to dryness and NMR spectra (CDCl_3) of the residues were recorded. The spectrum of the first band (red-orange) showed greater than 70% (by

integration) of the peaks were due to unreacted 42a and Me_2CHNCS . Three new Cp resonances were also observed. ^1H NMR of first fraction (CDCl_3): 5.67 (singlet, 5H, Cp), 5.66 (singlet, 5H, Cp), 5.64 (singlet, 5H, Cp) 5.56 (singlet, 5H, Cp, 50a), 5.49 (singlet, 5H, Cp, cis-42a), 5.04 (doublet, 5H, Cp, $J(\text{H-H})=2$ Hz, trans-42a), 4.72 (broad sextet), 4.02 (septet, 1H, Me_2CHNCS), 1.38 (broad doublet, 6H, $J(\text{H-H})=6.6$ Hz, $(\text{CH}_3)_2\text{CHNCS}$), 1.27 (broad doublet, $J(\text{H-H})=6$ Hz). The second band (yellow) was identified as trans-42a and the third fraction (purple) showed the presence of SPPH_3 , CH_2Cl_2 and ethanol.

I. Attempted Reaction of 42a and MeNCS

To an NMR sample of 42a in CDCl_3 , a small amount of MeNCS was added and spectra were recorded after 10 minutes and 24 hours. The spectrum remained unchanged from that of the starting materials except that two new Cp resonances (5.67 and 5.66 ppm) were observed. However, these new peaks comprised <20% of the total Cp resonances and the reaction was abandoned.

J. Attempted Reaction of 42a and $(\text{C}_6\text{H}_{11}\text{N})_2\text{C}$

To an NMR sample of 42a in CDCl_3 , a small amount of $\text{RN}=\text{C}=\text{NR}$ ($\text{R} = \text{C}_6\text{H}_{11}$) was added and spectra were recorded after 5 minutes, 3.5 hours, 24 hours and 5 days. No changes in the spectrum were observed other than some formation of the dimer, $[\text{CpW}(\text{CO})_2\text{SCHMe}_2]_2$, 50a.

References

1. a) Denise, B.; Sneed, R.P.A. *Chemtech* **1982**, *12*, 108.
b) Palmer, D.A.; van Eldik, R. *Chem. Rev.* **1983**, *83*, 651.
c) Eisenberg, R.; Hendricksen, D.E. *Adv. Catal.* **1979**, *28*, 79.
2. a) Bolton, J.R. *Science* **1978**, *202*, 705.
b) Williams, R.; Crandall, R.S.; Bloom, A. *Appl. Phys. Lett.* **1978**, *33*, 381.
3. a) Ito, T.; Yamamoto, A. in "Organic and Bio-organic Chemistry of Carbon Dioxide"; Inoue, S., Yamazake, N., Eds.; Wiley: New York, 1980.
b) Cramer, J.; Meyers, A.L. *Atmos. Environ.* **1972**, *6*, 563.
4. Kolomnikov, I.S.; Grigoryan, M. *Russ. Chem. Rev.* **1978**, *47*, 334.
5. Darensbourg, D.; Kudarski, R.A. *Adv. Organomet. Chem.* **1983**, *22*, 129 and references therein.
6. Darensbourg, D.J.; Pala, M.; Waller, J. *Organometallics*, **1983**, *2*, 1285.
7. Darensbourg, D.J.; Rokicki, A.; Darensbourg, M.Y. *J. Am. Chem. Soc.* **1981**, *103*, 3223.
8. Darensbourg, D.J.; Rokicki, A. *J. Am. Chem. Soc.* **1982**, *104*, 349.
9. Darensbourg, D.J.; Rokicki, A. *Organometallics*, **1982**, *1*, 1685.
10. Slater, S.G.; Lusk, R.; Schumann, B.F.; Darensbourg, M.Y. *Organometallics*, **1982**, *1*, 1662.
11. Roberts, D.R.; Geoffroy, G.L.; Bradley, M.G. *J. Organometal. Chem.* **1980**, *198*, C75.
12. Gambarotta, S.; Strologo, S.; Floriani, C.; Chiesi-Villa, A.; Guastini, C. *J. Am. Chem. Soc.* **1985**, *107*, 6278.

13. Sullivan, B.P.; Meyer, T.J. *Organometallics*, **1986**, *5*, 1500.
14. Kundel, P.; Berke, H. *J. Organomet. Chem.* **1988**, *339*, 297.
15. Bennett, M.A.; Robertson, G.B.; Rokicki, A.; Wickramasinghe, W.A. *J. Am. Chem. Soc.* **1988**, *110*, 7098.
16. Ito, T.; Matsubara, T. *J. Chem. Soc. Dalton Trans.* **1988**, 2241.
17. Darensbourg, D.J.; Darensbourg, M.Y.; Goh, L.Y.; Ludvig, M.; Wiegrefe, P. *J. Am. Chem. Soc.* **1987**, *109*, 7539.
18. Sneeden, R.P.A. in "Comprehensive Organometallic Chemistry"; Wilkinson, G., Stone, F.G.A., Abel, E.W., Eds.; Pergamon Press: Oxford, 1982; Vol. 8, Chapter 50.4, p 225.
19. Kolomnikov, I.S.; Lobeveva, T.S.; Gorbachevskaya, V.V.; Aleksandrov, G.G.; Struckhov, Y.T.; Vol'Pin, M.E. *J. Chem. Soc. Chem. Commun.* **1971**, 972.
20. Moloy, K.G.; Marks, T.J. *Inorg. Chim. Acta* **1985**, *110*, 127.
21. Johnston, R.F.; Cooper, J.C. *Organometallics*, **1987**, *6*, 2448.
22. Yasuda, H.; Okamoto, T.; Matsuoka, Y.; Nakamura, A.; Kai, Y.; Kanehisa, N.; Kasai, N. *Organometallics*, **1989**, *8*, 1139.
23. Darensbourg, D.J.; Grötsch, G.; Wiegrefe, P.; Rheingold, A.L. *Inorg. Chem.* **1987**, *26*, 3827.
24. Lee, G.R.; Maher, J.M.; Cooper, N.J. *J. Am. Chem. Soc.* **1987**, *109*, 2956.
25. Belmore, K.A.; Vanderpool, R.A.; Tsai, J.C.; Khan, M.A.; Nicholas, K.M. *J. Am. Chem. Soc.* **1988**, *110*, 2004.
26. Reinking, M.K.; Ni, J.; Fanwick, P.E.; Kubiak, C.P. *J. Am. Chem. Soc.* **1989**, *111*, 6459.
27. Newman, L.J.; Bergman, R.G. *J. Am. Chem. Soc.* **1985**, *107*, 5314.
28. Crutchley, R.J.; Powell, J.; Faggiani, R.; Lock, C.J.L. *Inorg. Chim. Acta*

- 1977, 24, L15.
29. Tsuda, T.; Sananda, S.; Ueda, K.; Saegusa, T. *Inorg. Chem.* **1976**, *15*, 2329.
30. Gattow, G.; Behrendt, W. in "Topics in Sulfur Chemistry"; Senning, A., Ed.; Georg Thieme: Stuttgart, West Germany, 1977; Vol. 2, pp 178-190 and references therein.
31. Coucouvanis, D. *Prog. Inorg. Chem.* **1979**, *26*, 301.
32. Burns, R.P.; McCullough, F.P.; McAuliffe, C.A. *Adv. Inorg. Chem. Radiochem.* **1980**, *23*, 211.
33. Bladon, P.; Bruce, R.; Knox, G.R. *J. Chem. Soc. Chem. Commun.* **1965**, 557.
34. Sato, F.; Iida, K.; Sato, M. *J. Organomet. Chem.* **1972**, *39*, 197.
35. Avdeef, A.; Facker, J.P., Jr. *J. Coord. Chem.* **1975**, *4*, 211.
36. Havlin, R.; Knox, G.R. *Z. Naturforsch.* **1966**, *21b*, 1108.
37. Gattow, G.; Behrendt, W. in "Topics in Sulfur Chemistry"; Senning, A., Ed.; Georg Thieme: Stuttgart, West Germany, 1977; Vol. 2, pp 119-154 and references therein.
38. Chadha, R.K.; Kumar, R.; Tuck, D.G. *Polyhedron*, **1988**, *7*, 1121.
39. Black, S.J.; Einstein, F.W.B.; Hayes, P.C.; Kumar, R.; Tuck, D.G. *Inorg. Chem.* **1986**, *25*, 4181.
40. Ansari, M.A.; Chandrasekaran, J.; Sarkar, S. *Inorg. Chem.* **1988**, *27*, 764.
41. Torres, M.R.; Perales, A.; Ros, J. *Organometallics*, **1988**, *7*, 1223.
42. Palazzi, A.; Busetto, L.; Grazini, M. *J. Organomet. Chem.* **1971**, *30*, 273.
43. Thiele, G.; Liehr, G.; Lindner, E. *J. Organomet. Chem.* **1974**, *70*, 427.
44. Cecconi, F.; Ghilardi, C.A.; Midollini, S.; Moneti, S.; Orlandini, A.; Scapacci, G. *J. Chem. Soc. Dalton Trans.* **1989**, 211.
45. Kim, Y.-J.; Osakada, K.; Sugita, K.; Yamamoto, T.; Yamamoto, A. *Organometallics*, **1988**, *7*, 2182.

46. Usón, R.; Fornies, J.; Espinet, P.; Lalinde, E. *J. Organomet. Chem.* **1987**, *334*, 399.
47. Cámpora, J.; Carmona, E.; Gutiérrez-Puebla, E.; Poveda, M.L.; Ruíz, C. *Organometallics*, **1988**, *7*, 2577.
48. Morandini, F.; Consiglio, G.; Sironi, A. *Gazz. Chim. Ital.* **1987**, *117*, 61.
49. Rosi, M.; Sgamellotti, A.; Tarantelli, F.; Floriani, C. *J. Organomet. Chem.* **1987**, *332*, 153.
50. a) Bruce, M.I.; Humphrey, M.G.; Swincer, A.G.; Wallis, R.C. *Aust. J. Chem.* **1984**, *37*, 1747.
b) Mishra, A.; Agarwala, U.C. *Inorg. Chim. Acta* **1988**, *145*, 191.
51. Cecconi, F.; Ghilardi, C.A.; Midollini, S.; Monetti, S.; Orlandini, A. *J. Organomet. Chem.* **1987**, *323*, C5.
52. Kullberg, M.L.; Kubiak, C.P. *Inorg. Chem.* **1986**, *25*, 26.
53. Fenster, A.E.; Butler, I.S. *Inorg. Chem.* **1974**, *13*, 915.
54. Le Bozec, H.; Dixneuf, P.H.; Carty, A.J.; Taylor, N.J. *Inorg. Chem.* **1978**, *17*, 2568.
55. Conway, P.; Grant, S.M.; Manning, A.R. *J. Chem. Soc. Dalton Trans.* **1979**, 1920.
56. Thewissen, D.H.M.W. *J. Organomet. Chem.* **1980**, *188*, 211.
57. Schenk, W.A.; Schwietzke, T.; Müller, H. *J. Organomet. Chem.* **1982**, *232*, C41.
58. Ibers, J.A. *Chem. Soc. Rev.* **1982**, *11*, 57.
59. Gaffney, T.R.; Ibers, J.A. *Inorg. Chem.* **1982**, *21*, 2062.
60. Gaffney, T.R.; Ibers, J.A. *Inorg. Chem.* **1982**, *21*, 2851.
61. Gaffney, T.R.; Ibers, J.A. *Inorg. Chem.* **1982**, *21*, 2854.
62. Gaffney, T.R.; Ibers, J.A. *Inorg. Chem.* **1982**, *21*, 2857.

63. Gaffney, T.R.; Ibers, J.A. *Inorg. Chem.* **1982**, *21*, 2860.
64. Lee, G.R.; Cooper, N.J. *Organometallics*, **1989**, *8*, 1538.
65. Darensbourg, D.J.; Sanchez, K.M.; Reibenspies, J. *Inorg. Chem.* **1988**, *27*, 3636.
66. Hadj-Bagheri, N.; Puddephatt, R.J. *J. Chem. Soc. Chem. Commun.* **1987**, 1269.
67. Fehlhammer, W.P.; Zinner, G.; Bakola-Christianopoulou, M. *J. Organomet. Chem.* **1987**, *331*, 193.
68. Seyferth, D.; Womack, G.B.; Archer, C.M.; Fackler, J.P. Jr.; Marler, D.O. *Organometallics*, **1989**, *8*, 443.
69. Rossi, R.; Marchi, A.; Duatti, A.; Magon, L.; Casellato, V.; Graziani, R. *J. Chem. Soc. Dalton Trans.* **1987**, 2299.
70. Herberich, G.E.; Mayer, H. *J. Organomet. Chem.* **1987**, *322*, C29.
71. a) Jernakoff, P.; Cooper, N.J. *J. Am. Chem. Soc.* **1987**, *109*, 2173.
b) Jernakoff, P.; Cooper, N.J. *Ibid* **1989**, *111*, 7424.
72. Leboeuf, J.-F.; Leblanc, J.-C.; Moïse, C. *J. Organomet. Chem.* **1987**, *335*, 331.
73. Abbott, R.G.; Cotton, F.A.; Shamshoun, E.S. *Gazz. Chim. Ital.* **1986**, *116*, 91.
74. Gambarotta, S.; Strologo, S.; Floriani, C.; Chiesi-Villa, A.; Guastini, C. *Inorg. Chem.* **1985**, *24*, 654.
75. Bruce, R.; Knox, G.R. *J. Organomet. Chem.* **1966**, *6*, 67.
76. Dean, W.K.; Heyl, B.L. *J. Organomet. Chem.* **1978**, *159*, 171.
77. Hunt, J.; Knox, S.A.R.; Oliphant, V. *J. Organomet. Chem.* **1974**, *80*, C50.
78. X-ray crystal structure analyses were determined in the laboratory of Dr. Peter Bird, Department of Chemistry, Concordia University, Montréal, Québec, Canada.
79. a) Chiesi Villa, A.; Gaetani Manfreditti, A.; Guastini, C.; Nardelli, M. *J. Chem. Soc. Chem. Commun.* **1970**, 1322.

- b) Chiesi Villa, A.; Gaetani Manfreditti, A.; Guastini, C.; Nardelli, M. *Acta Cryst. Sect B* **1972**, *28*, 2231.
- c) Chiesi Villa, A.; Gaetani Manfreditti, A.; Guastini, C.; Nardelli, M. *Acta Cryst. Sect B* **1974**, *30*, 2788.
- e) Lewis, D.F.; Lippard, S.J.; Zubieta, J.A. *Inorg. Chem.* **1972**, *11*, 823.
- f) Fackler, J.P. Jr.; Zegarski, W.J. *J. Am. Chem. Soc.* **1973**, *95*, 8566.
80. Darensbourg, D.J.; Sanchez, K.M.; Rheingold, A.L. *J. Am. Chem. Soc.* **1987**, *109*, 290.
81. Darensbourg, D.J.; Sanchez, K.M.; Reibenspies, J.H.; Rheingold, A.L. *J. Am. Chem. Soc.* **1989**, *111*, 7094.
82. Ashby, M.T.; Enemark, J.H. *J. Am. Chem. Soc.* **1986**, *108*, 730.
83. Millar, M.M.; O'Sullivan, R.; de Vries, N.; Koch, S.A. *J. Am. Chem. Soc.* **1985**, *107*, 3714.
84. Kamata, M.; Hirotsu, K.; Higuchi, J.; Tatsumi, K.; Yoshida, T.; Hoffmann, R.; Otsuka, S. *J. Am. Chem. Soc.* **1981**, *103*, 5772.
85. Baird, M.C.; Hartwell, G. Jr.; Wilkinson, G. *J. Chem. Soc. (A)* **1967**, 2037.
86. Grundy, K.R.; Harris, R.O.; Roper, W.R. *J. Organometal. Chem.* **1975**, *90*, C34.
87. Baird, M.C.; Wilkinson, G. *J. Chem. Soc. (A)* **1967**, 865.
88. a) Hartgerink, J. M.Sc. Thesis, McGill University, 1981, p 26.
- b) Beck, W.; Danzer, W.; Thiel, G. *Angew. Chem.* **1973**, *85*, 625.
- c) Beck, W.; Danzer, W.; Thiel, G. *Angew. Chem. Int. Ed.* **1973**, *12*, 582.
89. a) Abel, E.W. *J. Chem. Soc.* **1960**, 4406.
- b) Abel, E.W.; Armitage, D.A.; Brady, D.B. *J. Organomet. Chem.* **1966**, *5*, 130.
- c) Anderson, H.H. *J. Org. Chem.* **1956**, *21*, 869.

- d) McCombie, H.; Saunders, B.C. *Nature*, **1947**, *159*, 491.
- e) Sasin, R.; Sasin, G.S. *J. Org. Chem.* **1955**, *20*, 387.
90. Rakowski DuBois, M.; VanDerveer, M.C.; DuBois, D.L.; Haltiwanger, R.C.; Miller, W.K. *J. Am. Chem. Soc.* **1980**, *102*, 7456.

CHAPTER 5

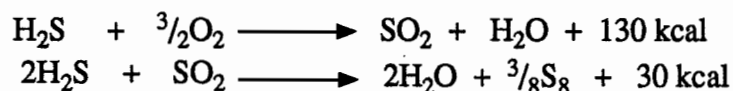
The Preparation and Characterization of $\text{CpW}(\text{CO})_2(\text{PPh}_3)(\text{S}(\text{SO}_2)\text{R})$

(R = CHMe_2 , CH_2Ph , 4- $\text{C}_6\text{H}_4\text{Me}$)

Introduction:

The presence of sulfur-containing compounds in petroleum feedstocks results in the emission of SO_2 into the atmosphere when these fuels are burned. These emissions result in the environmental hazard, "acid rain". Desulfurization of the feedstocks and/or treatment of the combustion products is now a political and an environmental priority.

Presently, fossil fuels undergo hydrodesulfurization via treatment with H_2 over metal-sulfide catalysts to give saturated hydrocarbons and H_2S . Highly toxic H_2S cannot be released to the atmosphere and must be converted to non-toxic products. In the Claus process (1), H_2S is first partially oxidized to SO_2 , which reacts with H_2S to give S_8 and H_2O (Scheme 5.1). Various heterogeneous catalysts have been used in both steps but like



Scheme 5.1 The Claus Process (1)

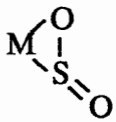
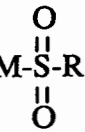
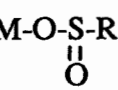
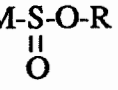
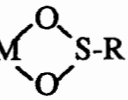
the hydrodesulfurization process, it is not clear what chemical reactions are taking place with these catalysts. Hence, reactions of organometallic complexes with SO_2 may reveal some insight into the reactivity of SO_2 and the kinds of processes that may be occurring.

Reactions of SO₂ with Metal-Alkyl Complexes

Sulfur dioxide reacts with transition metal complexes to give products with one of a number of possible linkages (2). Table 5.1 lists eight types of SO₂ linkages found in metal complexes and the regions where the $\nu(\text{SO})$ bands have been observed in the IR spectrum (2,3). Reports of simple SO₂ adducts (M-SO₂, I) are known, wherein the SO₂ molecule coordinated to the metal possesses a pyramidal (I) or coplanar (II) geometry (4-17). Adduct formation with a ligand such as M-L-SO₂ (III) has been reported (3,18-22). An η^2 -SO₂ bonding mode is also known (M- η^2 -SO₂, IV) (23-26) and the lower $\nu(\text{SO})$ frequencies reflect the S-O bond activation. A very common product is a S-sulfinate (M-S(O)₂R, V) complex (2,27-37) where the SO₂ molecule has inserted into a metal-carbon bond. Another possible SO₂ insertion linkage is the O-sulfinate (M-O-S(O)-R, VI) (2,38-41) where the metal is bound to an oxygen atom and the R group is coordinated to the S(O) moiety. These complexes have been observed as intermediates to the S-sulfinate complexes. The O-alkyl-S-sulfoxylate (M-S(O)-OR, VII) linkage where the S(O) moiety is coordinated to the metal centre and the R group bound to an oxygen atom, is also known (38-39). Lastly, the O'-O'-sulfinate (M-(O)(O)-S-R, VIII) (2,42,43) linkage is a bidentate ligand in which both oxygen atoms are bound to the metal.

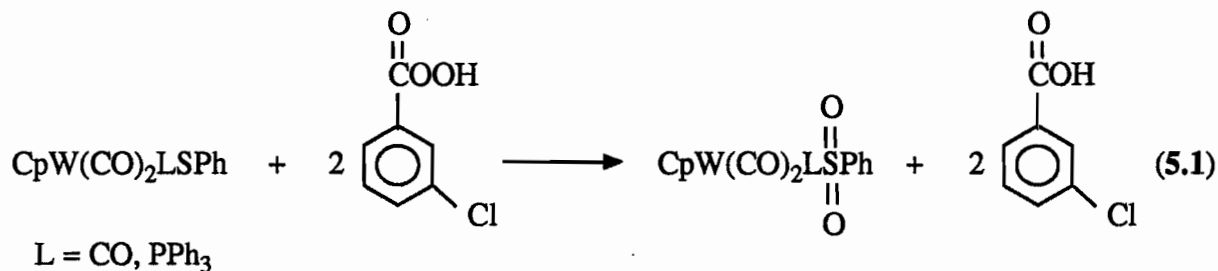
In the Group 6 triad, S-sulfinate complexes of Cr, Mo, and W are known. The complex, CpCr(CO)₃[S(O)₂Et] (37), was prepared via treatment of CpCr(CO)₃Et with SO₂. The complexes CpMo(CO)₃R (R = Me, Et, CH₂Ph) and CpMo(CO)₂(PPh₃)Me react readily in refluxing SO₂ to give the S-sulfates, CpMo(CO)₃[S(O)₂R] (R = Me, Et, CH₂Ph) and CpMo(CO)₂(PPh₃)[S(O)₂Me] (44), respectively. The tungsten analogues, CpW(CO)₃R (R = Me, CH₂Ph) (44) are much less reactive; CpW(CO)₃[S(O)₂CH₂Ph] was prepared by stirring CpW(CO)₃CH₂Ph in liquid SO₂ at 55°C for 3 days (31). The

Table 5.1 Diagnostic $\nu(\text{SO})$ frequencies of relevant SO_2 coordination geometries in metal complexes

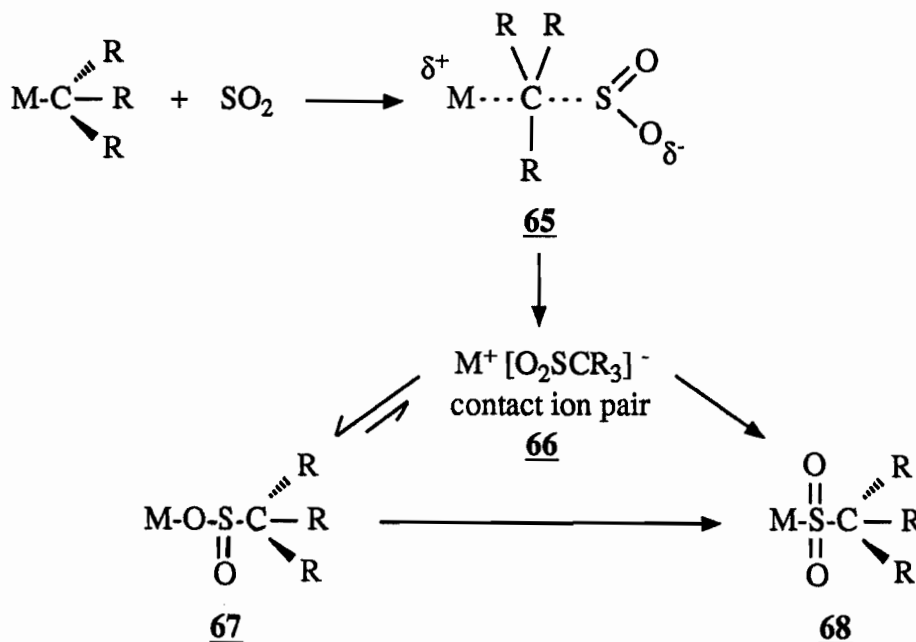
Coordination Geometry			Observed Ranges for $\nu(\text{SO}) \text{ cm}^{-1}$			
I	M-SO ₂ adduct	pyramidal	1237-1150	1065-990		
II	M-SO ₂ adduct	coplanar	1303-1250	1130-1087		
III	M-L-SO ₂	ligand adduct	1317-1210	1135-1051		
IV		η^2 - SO ₂	1200-1100	1000-850		
V		S-sulfinate	1250-1100	1100-1000		
VI		O-sulfinate	}	}		
VII		O-alkyl S-sulfinate			1085-1050	1000-820
VIII		O'-O'sulfinate				

1300 1200 1100 1000 900 800 cm^{-1}

complexes, $\text{CpW}(\text{CO})_2(\text{L})[\text{S}(\text{O})_2\text{Ph}]$ ($\text{L} = \text{CO}, \text{PPh}_3$) were not prepared by SO_2 insertion but by oxidation of $\text{CpW}(\text{CO})_2(\text{L})\text{SPh}$ with metachloroperbenzoic acid (Equation 5.1) (45).

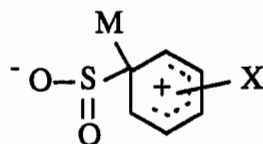


The mechanism of SO_2 insertion into metal-carbon bonds has been explored in detail (2,46-49) and is shown in Scheme 5.2. Electrophilic attack by SO_2 (65) gives a contact ion pair (66) that can form an O-sulfinate intermediate (67) or can give the S-sulfinate product (68) directly. The reaction proceeds with retention of configuration at the chiral metal center (50) and inversion of configuration at the α -carbon due to the backside attack by SO_2 (51,52). For aryl derivatives, the insertion proceeds via the



Scheme 5.2 The mechanism of SO_2 insertion into metal-carbon bonds (2,46-49).

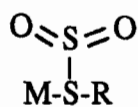
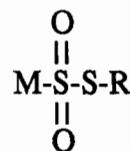
O-sulfinate intermediate (**67**) with stabilization of a proposed transition state (**69**) provided by substituents (X) on the aromatic ring.

**69**

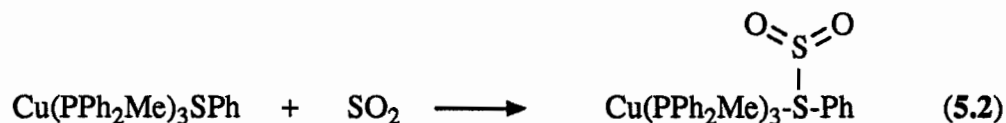
The rate of SO₂ insertion has been shown to be dependent upon the R group; decreasing as R becomes more electron-withdrawing (46,47,53) or larger in steric bulk (54). In fact, for some complexes with perfluoroalkyl groups, no reaction is observed (46,55-57). The rate of SO₂ insertion is also enhanced by increasing the base strength of the ancillary ligands (40,44,46,47,58,59). For instance, when CO is replaced with PPh₃, SO₂ insertion occurs more rapidly for CpMo(CO)₂(PPh₃)Me than for CpMo(CO)₃Me (44). These observations are consistent with electrophilic attack of SO₂ on these complexes.

Reactions of Metal-Oxygen and Metal-Sulfur Complexes with SO₂

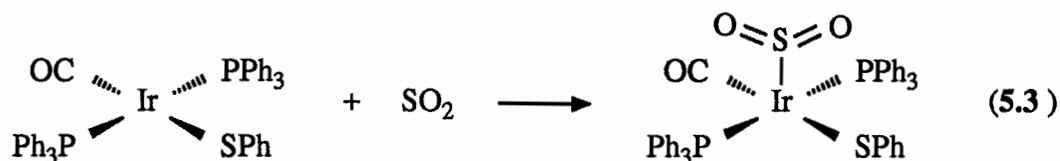
In comparison with metal-alkyl (or aryl) complexes, relatively few studies of reactions of metal-sulfur complexes with SO₂ have been reported (3,19-22). It appears that SO₂ can react with the metal-sulfur bond of thiolate complexes without insertion to give an adduct (**70**) with the thiolate sulfur. Species such as (**71**), an S-thiosulfinate have not been reported to date. An example of **70** was reported when a chloroform solution of

**70****71**

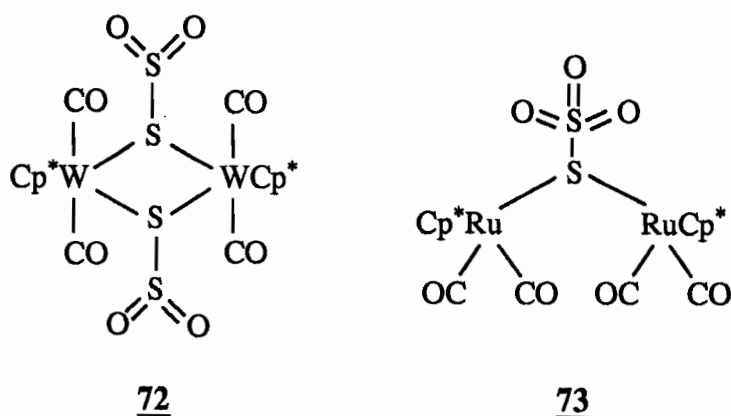
$\text{Cu}(\text{PPh}_2\text{Me})_3\text{SPh}$ treated with SO_2 , gave the thiolate-bound SO_2 adduct, $\text{Cu}(\text{PPh}_2\text{Me})_3(\text{S}(\text{SO}_2)\text{Ph})$, the structure of which was determined by x-ray crystallography



(Equation 5.2) (19). This complex is the only example reported thus far, where SO_2 is bound to a thiolato sulfur atom. On the other hand, $\text{Ir}(\text{SPh})(\text{CO})(\text{PPh}_3)_2$, reacted with SO_2 to give a metal-bound SO_2 adduct, $\text{Ir}(\text{SPh})(\text{CO})(\text{PPh}_3)_2(\text{SO}_2)$ (Equation 5.3) (3).

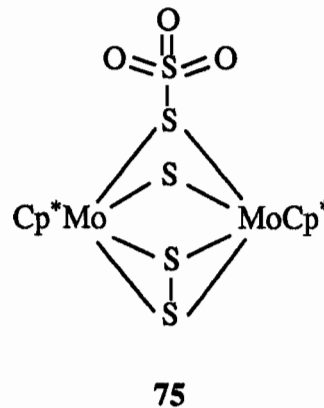
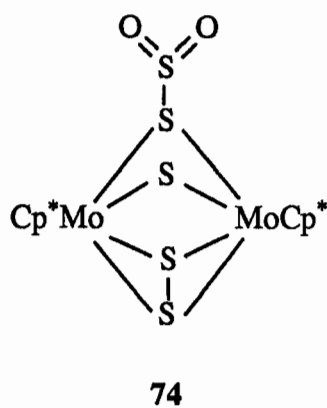


Other SO_2 adducts with metal sulfides have been reported. The dimers, $[\text{Cp}^*\text{W}(\text{CO})_2(\mu\text{-S}\cdot\text{SO}_2)]_2$ ($\text{Cp}^* = \eta^5\text{-C}_5\text{Me}_5$) (72) (20) and $[\text{Cp}^*\text{Ru}(\text{CO})_2]_2(\mu\text{-S}_2\text{O}_3)$ (73) (22) were formed when $\text{Cp}^*\text{W}(\text{CO})_3\text{H}$ and $\text{Cp}^*\text{Ru}(\text{CO})_2\text{H}$, respectively, were treated with SO_2 . In the case of 73, labelling studies with S^{18}O_2 determined that the third



oxygen atom in the $(\mu\text{-S}_2\text{O}_3)$ ligand was derived from an additional molecule of SO_2 . Likewise, SO_2 reacted with $\text{Cp}^*_2\text{Mo}_2(\mu\text{-S}_2)(\mu\text{-S})_2$ to give $\text{Cp}^*_2\text{Mo}_2(\mu\text{-S}_2)(\mu\text{-S})(\mu\text{-S}\cdot\text{SO}_2)$ (74) which in turn, can also react with a second molecule of SO_2 to give

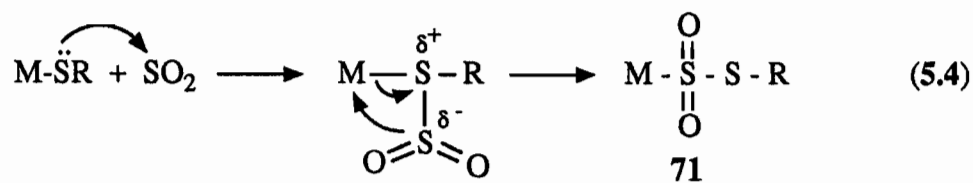
$\text{Cp}^*_2\text{Mo}_2(\mu\text{-S}_2)(\mu\text{-S})(\mu\text{-S}_2\text{O}_3)$ (**75**) (21). The related dimer, $[(\text{Me}_n\text{Cp})\text{Mo}(\mu\text{-S})(\mu\text{-SH})]_2$ ($n = 1, 5$), has been shown to catalytically reduce SO_2 to S_8 and H_2O (60,61).



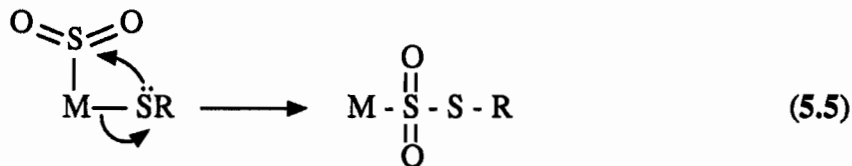
All the ligand- SO_2 adduct complexes (except **73** and **75**) reported showed a facile tendency to lose SO_2 (3,19-21). Preparation, workup and isolation of the products were performed under an atmosphere of SO_2 . Placing the complexes under vacuum or dissolving them in organic solvents resulted in loss of the coordinated sulfur dioxide. A long S-S bond distance ($\sim 2.6\text{\AA}$) was found in these complexes which is consistent with the observed lability of the SO_2 (19-22). Some S-sulfinate (32-36,42,44,62) and metal coordinated SO_2 adduct complexes (17,63-65) also eliminate SO_2 but require heating or UV irradiation. The aryl sulfinate of Hg and Bi (42) lose SO_2 at $\sim 150^\circ\text{C}$ as do $\text{CpFe}(\text{CO})_2[\text{S}(\text{O})_2\text{C}_6\text{F}_5]$ (62) and $\text{CpMo}(\text{CO})_3[\text{S}(\text{O})_2\text{CH}_2\text{Ph}]$ (44) upon irradiation.

Although, the thiosulfinate coordination mode, $\text{M-S}(\text{O})_2\text{SR}$ (**71**) is not yet known, its formation may be envisioned through at least four possible routes:

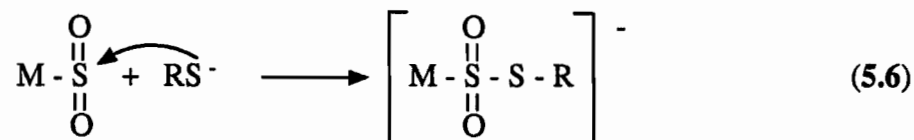
1) electrophilic attack by SO_2 on a thiolato sulfur atom, followed by rearrangement to give **71** (Equation 5.4),



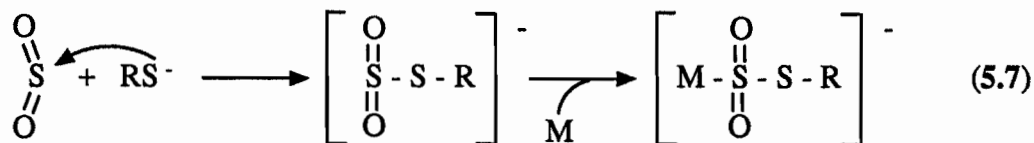
2) migration of a bound thiolato ligand on a metal-coordinated SO_2 moiety
(Equation 5.5)



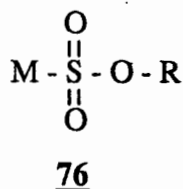
3) attack of a free thiolato anion, RS^- , on a metal-coordinated SO_2 molecule
(Equation 5.6) or



4) reaction of a free RS^- with SO_2 to give $[\text{S}(\text{O})_2\text{SR}]^-$ followed by coordination to the metal atom (Equation 5.7). Formation of $[\text{S}(\text{O})_2\text{SR}]^-$ by this route has been postulated (66) but to our knowledge no examples have been reported.

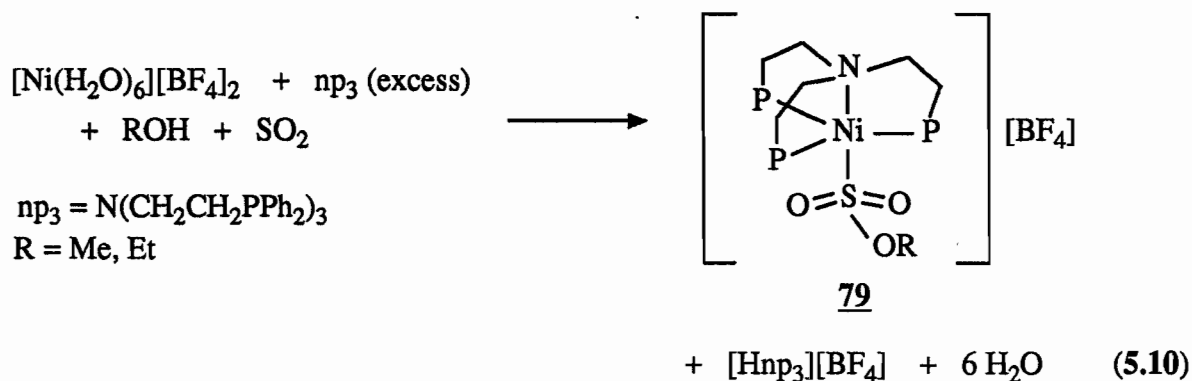


One or more of these pathways may be the routes to some of the known alkoxide analogues of **71**, the metal sulfonate compounds $\text{M}-\text{S}(\text{O})_2-\text{OR}$ (**76**). The complexes

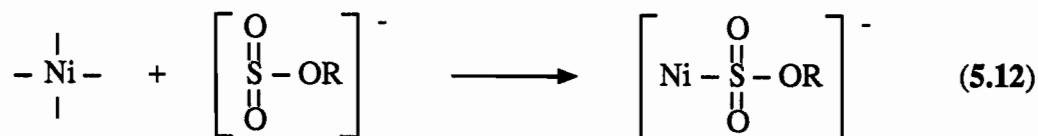
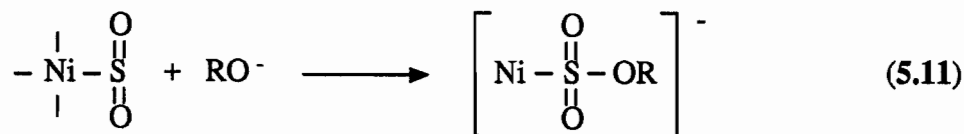


$\text{Pt}(\text{OMe})(\text{CF}_3)(\text{PPh}_2\text{CH}=\text{CHPh}_2)$ and $\text{M}(\text{OPh})(\text{tpp})$ ($\text{M} = \text{Rh}, \text{Ir}$; $\text{tpp} = \text{Ph}(\text{CH}_2\text{CH}_2\text{CH}_2\text{PPh}_2)_2$) have been reported to insert SO_2 into the $\text{M}-\text{OR}$ bond to give $\text{Pt}[\text{S}(\text{O})_2\text{OMe}](\text{CF}_3)(\text{PPh}_2\text{CH}=\text{CHPh}_2)$ (**77**) (Equation 5.8) (67,68) and

(70). This compound (**79**) was formed from the reaction of $[\text{Ni}(\text{H}_2\text{O})_6][\text{BF}_4]_2$ with excess np_3 in the appropriate alcohol (methanol or ethanol), followed by treatment with $\text{SO}_2(\text{g})$ (Equation 5.10). In this instance, the $\nu(\text{SO})$ region ($1300\text{-}1000\text{ cm}^{-1}$) in the IR spectrum

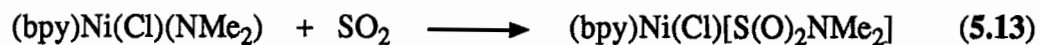


was extremely complex and only two strong bands at $\sim 1218\text{ cm}^{-1}$ and $\sim 634\text{ cm}^{-1}$ were tentatively assigned to the $\text{S}(\text{O})_2\text{OR}$ group; however, definitive evidence of the $\text{Ni-S}(\text{O})_2\text{OR}$ linkage was obtained in the x-ray crystal structure. In the preparation of **79**, the presence of excess amine (np_3) acts as a proton acceptor from ROH to give RO^- (**71**). The alkoxide ion might have attacked a pre-coordinated metal- SO_2 adduct to give $\text{Ni-S}(\text{O})_2\text{OR}$ (Equation 5.11) (route 3) or reacted with free SO_2 to form $[\text{S}(\text{O})_2\text{OR}]^-$ first (**66**) which then coordinated to the metal atom and yield **79** (Equation 5.12) (route 4) (**70**).



Insertion of SO_2 into the Ni-N bond of $(\text{bpy})\text{Ni}(\text{Cl})(\text{NMe}_2)$ (bpy = bipyridine) to

giving (bpy)Ni(Cl)[S(O)₂NMe₂] (Equation 5.13) (72) has been claimed; however, no characterization of any kind accompanied the report.



To date, the only reaction reported between SO₂ and metal-sulfur complexes has been adduct formation between the SO₂ and the coordinated sulfur ligand. In view of the ease of insertion of SO₂ into metal-carbon, metal-oxygen and perhaps metal-nitrogen bonds, there seems to be no obvious reason why insertion of SO₂ into a metal-sulfur bond might not also occur. Since the complexes CpW(CO)₂(PPh₃)SR insert CS₂ so easily, it was decided to study their reactions with SO₂.

Results and Discussion:

When an orange THF solution of $\text{CpW}(\text{CO})_2(\text{PPh}_3)\text{SR}$ (**42a-c**) was treated with $\text{SO}_2(\text{g})$ for 5 minutes, an immediate colour change to deep red occurred. Evolution of heat was noted but was also observed in the absence of **42a-c**. In the case of $\text{CpW}(\text{CO})_2(\text{PPh}_3)\text{SCHMe}_2$ (**42a**), the solution became slightly turbid. Recrystallizing the residue from THF/hexanes gave red-orange solids, $\text{CpW}(\text{CO})_2(\text{PPh}_3)\text{S}(\text{SO}_2)\text{R}$ (**80a-c**), which easily lost SO_2 when not kept under an atmosphere of SO_2 . Loss of SO_2 occurred upon dissolution in organic solvents such as CDCl_3 , resulting in an NMR spectrum identical to that of the starting thiolate (**42a-c**). Because of this, the NMR spectra of **80a-c** were recorded in CDCl_3 saturated with SO_2 . The solution IR spectra for **80a-c** were recorded under the same conditions but $\nu(\text{SO})$ bands due to coordinated SO_2 were not observed (3), due to the strong, broad $\nu(\text{SO})$ bands of free SO_2 ($1361, 1150 \text{ cm}^{-1}$) (73) which masked any other bands in this region. Grinding the sample in the preparation of Nujol mulls caused loss of SO_2 from **80a**. Thus, photoacoustic spectroscopy (PAS), which requires no sample preparation, was used to record the IR spectra for **80a-c**. The NMR and IR data of **80a-c** are listed in Table 5.2. A common feature in the NMR spectra of the SO_2 products was the appearance of a doublet due to coupling of the Cp ring protons with the phosphine atom; this indicated trans stereochemistry (74). Further evidence for a trans complex was detected in the methyl region of the spectrum of $\text{CpW}(\text{CO})_2(\text{PPh}_3)\text{S}(\text{SO}_2)\text{CHMe}_2$ (**80a**) wherein a doublet appeared at 1.40 ppm. In the methylene region of $\text{CpW}(\text{CO})_2(\text{PPh}_3)\text{S}(\text{SO}_2)\text{CH}_2\text{Ph}$ (**80b**), a singlet at 3.68 ppm was observed, also consistent with the trans geometry (74). In the solution IR spectrum, the carbonyl stretching bands for **80a-c** exhibited a weak symmetric $\nu(\text{CO})$ band between

Table 5.2 ^1H NMR and IR data of $\text{CpW}(\text{CO})_2(\text{PPh}_3)(\text{S}(\text{SO}_2)\text{R})$ (**80**)

		$\text{CpW}(\text{CO})_2(\text{PPh}_3)\text{S}(\text{SO}_2)_2\text{CHMe}_2$	$\text{CpW}(\text{CO})_2(\text{PPh}_3)\text{S}(\text{SO}_2)\text{CH}_2\text{Ph}$	$\text{CpW}(\text{CO})_2(\text{PPh}_3)\text{S}(\text{SO}_2)-4-\text{C}_6\text{H}_4\text{Me}$	
		80a	80b	80c	
isomer		trans	trans	cis	trans
^1H NMR ^{a,b} δ (ppm)	Cp	5.28 ^c	5.16 ^c	5.67	5.30 ^c
	CHMe_2	2.78 ^d			
	CH_2Ph		3.68		
	CH_3	1.40 ^e		2.28	2.31
	C_6H_x		7.30 ^f		7.26, 7.10 ^g
IR $\nu(\text{CO})$ (CHCl_3)		1946(m), 1871(s)	1951(m), 1873(s), 1862(s)		1967(m), 1870(s)
IR $\nu(\text{SO})$ (Nujol)			1249, 1089		1262, 1103
IR $\nu(\text{SO})$ (PAS)		1260, 1081	1248, 1090		1264, 1091

^a In CDCl_3 saturated with SO_2 .

^b PPh_3 resonances appear as a broad singlet between 7.35 - 7.50 ppm.

^c Doublet, $J(\text{H-H}) = 2$ Hz. ^d Septet, $J(\text{H-H}) = 6.6$ Hz. ^e Doublet, $J(\text{H-H}) = 6.6$ Hz.

^f $x = 5$, multiplet. ^g $x = 4$, AB quartet, $\Delta\nu = 32$ Hz, $J(\text{H-H}) = 8$ Hz.

1970-1940 cm^{-1} and a strong asymmetric $\nu(\text{CO})$ peak between 1860-1875 cm^{-1} , characteristic of trans-rich solutions (74,75). In the PAS IR spectra of **80a-c**, the $\nu(\text{SO})$ bands corresponding to coordinated SO_2 appeared in the range 1245-1265 cm^{-1} and 1080-1095 cm^{-1} . This correlated well with the regions associated with both metal-bound SO_2 adducts with a coplanar geometry as in II and ligand-bound SO_2 adducts as in III (Table 5.1). The observed $\nu(\text{SO})$ bands also overlap slightly with the regions associated with S-sulfinate complexes (V). A metal-bound SO_2 structure is not considered reasonable for **80a-c** since such a complex would exceed the 18 electron configuration. The elemental analysis for **80a** corresponded well with $\text{CpW}(\text{CO})_2(\text{PPh}_3)\text{SCHMe}_2 \cdot 2\text{SO}_2$ while for both **80b** and **80c**, the analytical data agreed with the formulation $\text{CpW}(\text{CO})_2(\text{PPh}_3)\text{SC}_7\text{H}_7 \cdot 1\text{SO}_2$. It is likely that the high sulfur content found for **80a** is due to free SO_2 in the lattice since the recrystallization solvents were saturated with SO_2 . The mass spectral data did not yield any useful information for **80a-c**. For **80a**, peaks corresponding $[\text{CpW}(\text{CO})\text{SCHMe}_2]_2^+$ and its related fragments were observed but the starting tungsten thiolate, **42a**, dimerizes easily (76) and a labile- SO_2 product might behave similarly. For **80b**, the molecular ion corresponding to **42b** appeared and for **80c**, no peaks in the FAB mass spectrum other than glycerol was observed.

The reaction of $\text{CpW}(\text{CO})_2(\text{PPh}_3)\text{SR}$ (**42a-c**) with SO_2 was monitored by NMR spectroscopy. Treatment of **42** with SO_2 for less than 5 minutes, gave a colour change from orange to dark red accompanied by heat evolution due to SO_2 dissolution. The NMR spectra of the treated samples, recorded at approximately 15 minute intervals, showed the same number of peaks as the starting thiolates, however, they were shifted downfield from those of the starting materials. For example, Figure 5.1 shows the spectrum of $\text{CpW}(\text{CO})_2(\text{PPh}_3)\text{SCH}_2\text{Ph}$ (**42b**) with increasing concentrations ($\text{A}_1\text{-E}_1$) of SO_2 in the solution. With no SO_2 treatment, the spectrum A_1 shows a singlet at 5.09 ppm and an AB quartet at 3.76, 3.42 ppm due to *cis*-**42b** and a doublet at 4.85 ppm and a

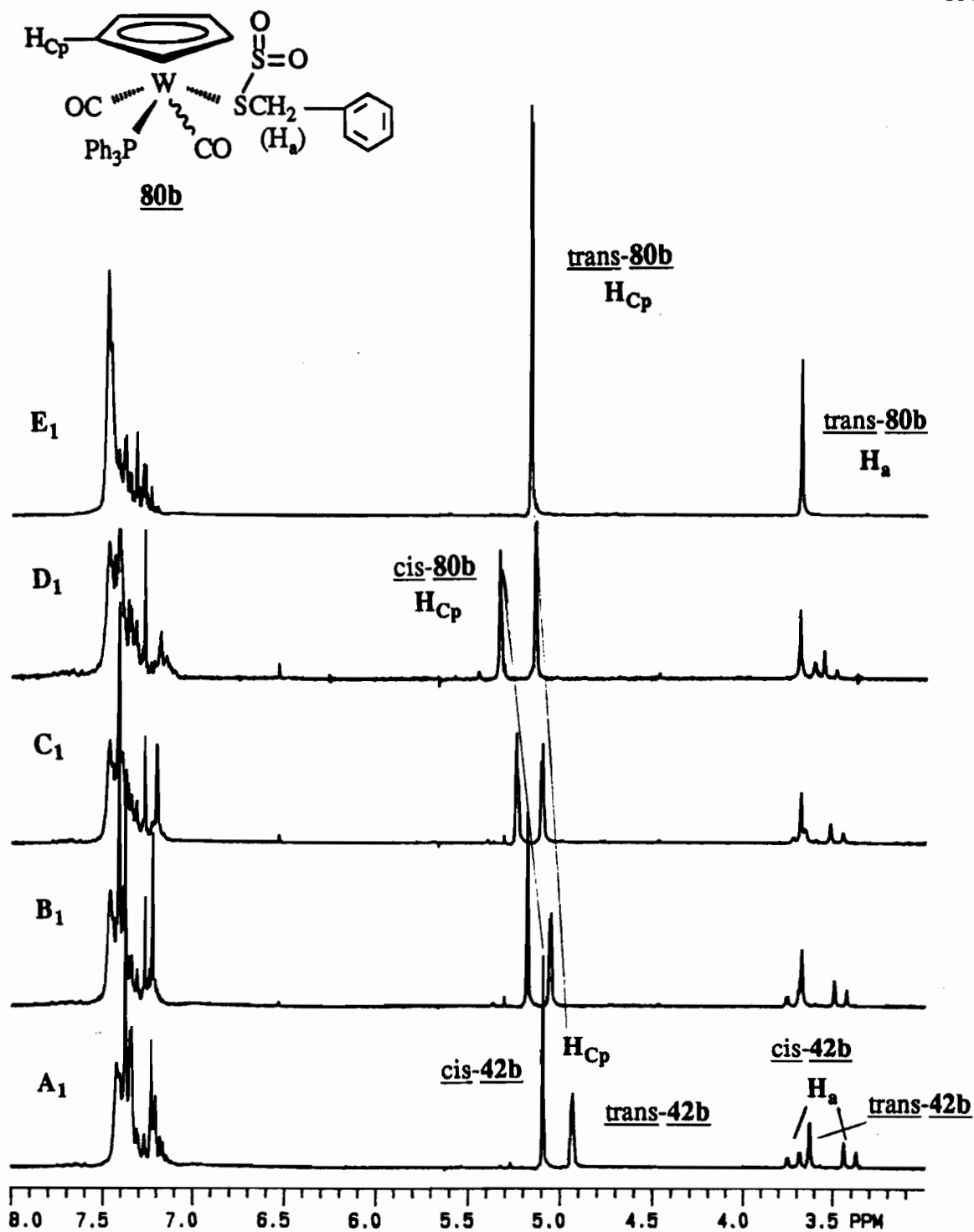


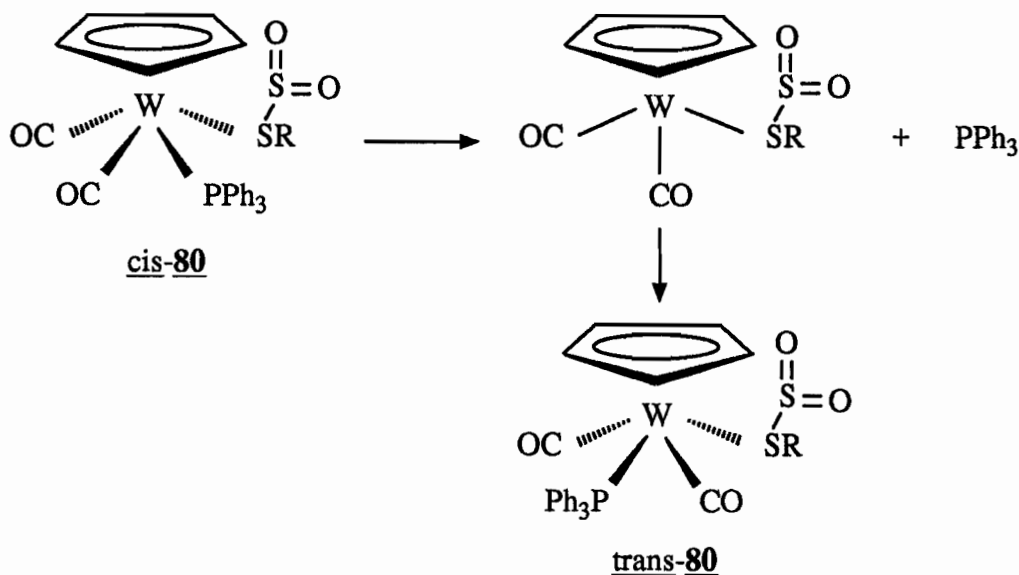
Figure 5.1 The reaction of $\text{CpW}(\text{CO})_2(\text{PPh}_3)\text{SCH}_2\text{Ph}$ (**42b**) with increasing volumes of added $\text{SO}_2(\text{g})$ to give $\text{CpW}(\text{CO})_2(\text{PPh}_3)\text{S}(\text{SO}_2)\text{CH}_2\text{Ph}$ (**80b**) monitored by ^1H NMR spectroscopy. Volume of $\text{SO}_2(\text{g})$ added : A_1) 0 mL; B_1) 3 mL; C_1) 6 mL; D_1) 15 mL; E_1) saturated with $\text{SO}_2(\text{g})$.

singlet at 3.64 ppm due to trans-42b. Slowly increasing the concentration of SO₂ (B₁-D₁) showed gradual shifting of the peaks, particularly the Cp resonances. Finally, in a solution saturated with SO₂ (E₁), the Cp region revealed only a doublet at 5.16 ppm and a singlet at 3.68 ppm, corresponding to trans-80b. From A₁-E₁ in Figure 5.1, peaks due to cis-80b decreased in intensity and those of trans-80b increased in intensity, suggesting the isomerization of the cis isomer to the trans isomer. Unlike the starting thiolate complexes 42a-c (75), the isomers of the SO₂ product do not equilibrate, but only the trans isomer was detected as shown in spectrum E₁. The rate of isomerization was inhibited by the addition of PPh₃. In Figure 5.2, NMR spectra shown are of a sample of CpW(CO)₂(PPh₃)SCHMe₂ (42a) immediately after SO₂ treatment (spectrum A₂) and 1 hour later (spectrum B₂) whereupon peaks due to cis-80a had disappeared and those of trans-80a had increased in intensity. The appearance of peaks corresponding to XPPH₃ where X = O or S and a new Cp peak at 5.81 ppm with a corresponding doublet and septet at 1.31 ppm and 3.14 ppm, respectively, were also observed accompanied by the formation of a small amount of a tan precipitate. In Figure 5.3, NMR spectra of 42a, with approximately 5 equivalents of free PPh₃, recorded directly after SO₂ treatment (spectrum A₃), 1.25 hours later (spectrum B₃) and 24 hours later (spectrum C₃) are shown. Spectrum B₃ is similar to B₂ except that only peaks corresponding to cis-80a and trans-80a appear. No precipitation appeared in the sample containing excess PPh₃. Comparison of A₂ and B₂ with A₃ and C₃ shows that the isomerization of cis-80a to trans-80a normally occurred within one hour, accompanied by some precipitation but the isomerization is slowed considerably in the presence of free PPh₃, which also seemed to inhibit further reaction. Similar results were observed for 80b and 80c.

From the data obtained, an SO₂ adduct of the coordinated thiolate sulfur atom is the probable structure for 80a-c. Such a complex would be expected to lose SO₂

concentrations of SO_2 appears to be consistent with very rapid exchange of the SO_2 coordinated to the thiolato sulfur. At low concentrations of SO_2 , **42** is probably still the major species, but rapid equilibrium with **80** (Equation 5.14) would shift the resonances and they would appear at chemical shifts between those of **42** and **80**. For spectrum B₁ the chemical shifts might represent a 10% contribution by **80** and a 90% contribution by **42**. As the concentration of SO_2 increases, so should the concentration of **80** and likewise its contribution to the chemical shifts of the peaks in the averaged spectrum. This would result in the gradual shift of the peaks shown in (C₁-E₁). The facile loss of SO_2 from known SO_2 adducts (3,19-21) supports the suggestion of rapid exchange of SO_2 in **80a-c**.

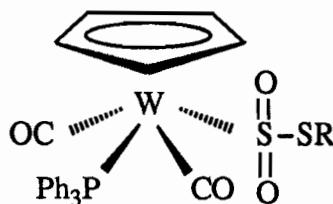
The isomerization of cis-80 to trans-80 is also consistent with the proposed structure. The averaged signals of cis-42 and cis-80 slowly disappeared while those of trans-42 and trans-80 increased in intensity. The addition of free PPh_3 slowed the isomerization. These observations suggest loss of PPh_3 from cis-80 gives an unsaturated species and followed by formation of trans-80 as presented in Scheme 5.3. The trans



Scheme 5.3 Isomerization of cis-CpW(CO)₂(PPh₃)(S(SO₂)R) (cis-80) to trans-CpW(CO)₂(PPh₃)(S(SO₂)R) (trans-80).

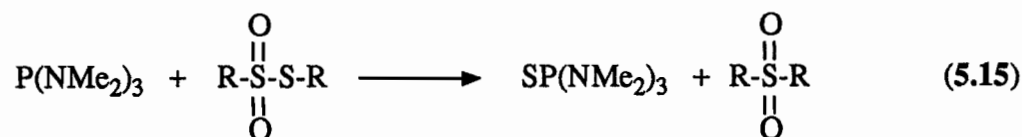
isomer is sterically less hindered within the inner coordination sphere. Examination of molecular models suggested that the interaction between the SO_2 molecule and the bulky PPh_3 ligand is also reduced. Loss of PPh_3 from *cis*- $\text{CpW}(\text{CO})_2(\text{PPh}_3)\text{SR}$ (**42a-c**) has been suggested to be the first step in the dimerization of **42a-c** to give $[\text{CpW}(\text{CO})_2\text{SCHMe}_2]_2$ (**50a**) (Chapter 3) (76) and in the production of the thioxanthates $\text{CpW}(\text{CO})_2\text{S}_2\text{CSR}$ (**62a-c**) via insertion of CS_2 (Chapter 4) (75).

An alternative structure, however, can be envisioned for **80** which contains an S-thiosulfinate ligand resulting from insertion of SO_2 in to the W-S bond. Presented as the *trans* isomer below, in accord with the IR data in the $\nu(\text{CO})$ region and with the observation of a doublet for the Cp protons in the NMR spectrum, this structure gives an equivalent environment for the R groups of the thiolate ligand which is consistent with the doublet observed for the methyl protons of **80a** and the singlet of the methylene protons of **80b**. The $\nu(\text{SO})$ bands detected for **80a-c** overlap slightly with the regions

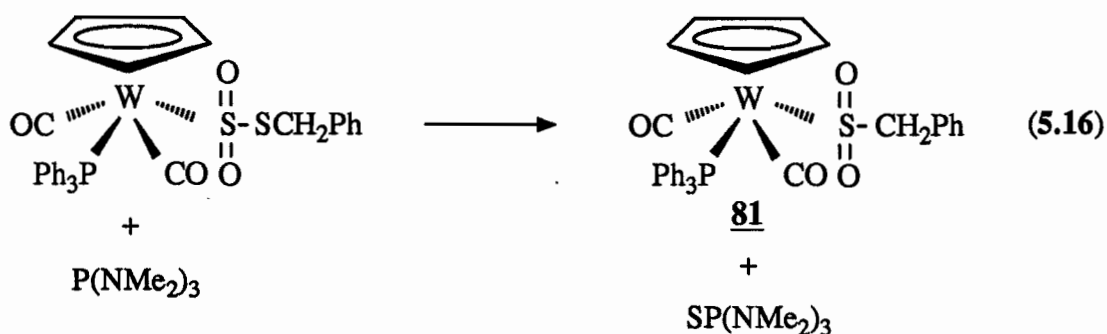


associated with S-sulfinate complexes (V). However, since S-thiosulfinate complexes are not known, the positions of the $\nu(\text{SO})$ bands for such complexes cannot be predicted with much certainty.

The facile loss of SO_2 from crystals of **80a-c** prevented the determination of the x-ray structure. Therefore, derivatization of $\text{CpW}(\text{CO})_2(\text{PPh}_3)(\text{S}(\text{SO}_2)\text{CH}_2\text{Ph})$ (**80b**) was attempted. The phosphine, $\text{P}(\text{NMe}_2)_3$, effectively desulfurizes organic thiosulfonates, $\text{RS}(\text{O})_2\text{SR}$, to give $\text{SP}(\text{NMe}_2)_3$ and $\text{RS}(\text{O})_2\text{R}$ (Equation 5.15) (77). Thus, treatment of

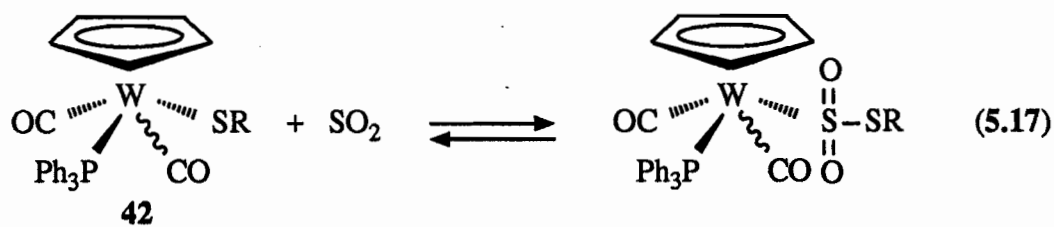


80b with $\text{P(NMe}_2)_3$ might be expected to give $\text{CpW(CO)}_2\text{PPh}_3[\text{S(O)}_2\text{CH}_2\text{Ph}]$ (**81**) and $\text{SP(NMe}_2)_3$ (Equation 5.16). An NMR sample of **80b** in CDCl_3 saturated with SO_2 was treated with an excess of $\text{P(NMe}_2)_3$, but after 30 hours the only peaks in the Cp region

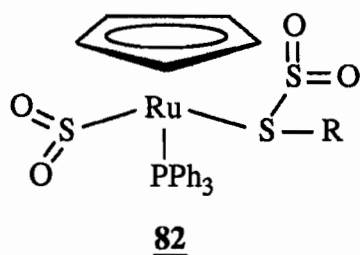


were due to **80b**. A new singlet at 3.60 ppm was assigned to the methylene proton resonance for $\text{PhH}_2\text{CS}_x\text{CH}_2\text{Ph}$ ($x = 1,2$) (**78**). Peaks corresponding to $\text{SP(NMe}_2)_3$ and XPPh_3 were also present. In the NMR spectrum of $\text{P(NMe}_2)_3$ with SO_2 in CDCl_3 peaks corresponding to XPPh_3 were observed. Therefore, it appears that desulfurization of **80b** with $\text{P(NMe}_2)_3$ does not occur according to Equation 5.16.

The *facile* loss of SO_2 exhibited by **80a-c** is not characteristic of S-sulfinate type complexes. Although loss of SO_2 can occur for such compounds it usually requires heating or UV irradiation (32-36,42,44,62). This also suggests that the NMR study of **42a-c** with increasing concentrations of SO_2 is not consistent with SO_2 insertion. The gradual shift of the peaks from spectra A₁-E₁ in Figure 5.1 would appear to require an exchange of SO_2 to give averaged spectra as shown in Equation 5.17. Such a phenomenon is unlikely; S-sulfinate complexes do not undergo insertion-elimination of SO_2 rapidly on the NMR time scale. Although, a structure containing an S-thiosulfinate



cannot be ruled out without definitive evidence such as x-ray crystal structure, it is more likely that 80a-c is an SO_2 adduct with a weak S-S interaction as has been observed in other systems (19-22). Only very recently, in this laboratory, another example of both metal- and thiolato-coordinated SO_2 has been found. The complex, $\text{CpRu(PPh}_3\text{)(SO}_2\text{)S(SO}_2\text{)R}$ ($\text{R} = \text{CHMe}_2, \text{CH}_2\text{CH}_2\text{Me}, 4\text{-C}_6\text{H}_4\text{Me}$) 82 was produced



when $\text{CpRu(PPh}_3\text{)}_2\text{SR}$ was treated with SO_2 (6). An x-ray crystal structure of 82 ($\text{R} = 4\text{-C}_6\text{H}_4\text{Me}$) confirmed the coordination of the two SO_2 molecules as shown above. Thus, the complex $\text{CpW(CO)}_2\text{(PPh}_3\text{)S(SO}_2\text{)R}$ (80a-c) and $\text{CpRu(PPh}_3\text{)(SO}_2\text{)S(SO}_2\text{)R}$ (82) are only the second and third systems, respectively, reported in which the SO_2 molecule has been found to coordinate as an adduct to a thiolato sulfur atom.

Experimental:A. Preparation of $\text{CpW}(\text{CO})_2(\text{PPh}_3)\text{S}(\text{SO}_2)\text{CHMe}_2$, **80a**

The tungsten thiolate complex, **42a** (0.078 g, 0.12 mmol) was dissolved in THF (5 mL). The red-orange solution was treated with $\text{SO}_2(\text{g})$ for 5 minutes and became dark red. Heat was evolved. The solution was then layered with hexanes (~15 mL) saturated with SO_2 and left at -16°C for 40 days. A red crystalline solid (0.077 g, 89%, m.p.=99-100°C), sensitive to loss of SO_2 , was isolated by removing the mother liquors with a disposable pipette. The crystals were dried by a gentle flow of SO_2 . Anal. Calc'd for $\text{C}_{28}\text{H}_{27}\text{O}_6\text{PS}_3\text{W}$ ($\text{CpW}(\text{CO})_2(\text{PPh}_3)\text{S}(\text{SO}_2)\text{CHMe}_2\cdot\text{SO}_2$): C, 43.65; H, 3.53; S, 12.48. Found: C, 42.76; H, 3.39; S, 12.27.

IR (Nujol): 1937 (s), 1853 (s), 1151 (w), 1123 (w), 1085 (w), 1063 (w), 1015 (w), 973 (w), 819 (w), 757 (w), 743 (w), 721 (w), 694 (m) cm^{-1} .

Mass spectrum, EI: 704 ($[\text{CpW}(\text{CO})\text{SCHMe}_2]_2^+$, 0.8); 661 ($[\text{Cp}_2\text{W}_2(\text{CO})_2\text{S}_2\text{CHMe}_2]^+$, 12.9); 594 ($\text{CpW}_2(\text{CO})_2\text{S}_2\text{CHMe}_2^+-2\text{H}^+$, 62.4); 562 ($\text{CpW}_2(\text{CO})_2\text{SCHMe}_2^+-2\text{H}^+$, 73.6); 534 ($\text{CpW}_2(\text{CO})\text{SCHMe}_2^+-2\text{H}^+$, 25.7); 337 ($\text{CpW}(\text{CO})\text{S}^+$, 15.8); 277 ($\text{CpW}(\text{CO})^+$, 25.4); 262 (PPh_3^+ , 70.1); 183 (W^+ , 100). Unidentified peaks: 503 (16.4), 483 (7.3); 457 (4.6).

B. Preparation of $\text{CpW}(\text{CO})_2(\text{PPh}_3)\text{S}(\text{SO}_2)\text{CH}_2\text{Ph}$, **80b**

A THF (10 mL) solution of **42b** (0.26 g, 0.37 mmol) was treated with SO_2 for 5-10 minutes. The orange-yellow solution became red-orange and heat was evolved. The

reaction solution was layered with hexanes (30 mL) saturated with SO₂ and left at -16°C for 4 days. A red-orange crystalline solid (0.21 g, 76.6%, m.p.=113-115°C) was isolated and dried under a flow of SO₂. Anal. Calc'd for C₃₂H₂₇O₄PS₂W (CpW(CO)₂(PPh₃)S(SO₂)CH₂Ph): C, 50.94; H, 3.61; S, 8.50. Found: C, 50.77; H, 3.57; S, 8.85.

IR (Nujol): 1965 (m), 1938 (w), 1862 (s), 1847 (s), 1249 (w), 1089 (s), 820 (w), 770 (w), 752 (w), 722 (w), 703 (w), 693 (w), 667 (w) cm⁻¹.

Mass spectrum, FAB in glycerol: 689 (M⁺-SO₂; 0.7); 567 (M⁺-SO₂-SCH₂Ph, 2.9). Unidentified peak: 510 (1.0).

C. Preparation of CpW(CO)₂(PPh₃)S(SO₂)₄-C₆H₄Me, **80c**

A THF (5 mL) solution of **42c** (0.19 g, 0.25 mmol) was treated with SO₂ for 5 minutes. Heat evolution and a change of colour from orange to dark-red was observed. The reaction solution was layered with hexanes (~15 mL) saturated with SO₂ and was kept at -16°C overnight. The mother liquors were removed from dark red crystals (0.18 g, 88.6%, m.p.=118-120°C) that were washed with hexanes saturated with SO₂ and dried under a flow of SO₂. Anal. Calc'd for C₃₂H₂₇O₄PS₂W (CpW(CO)₂(PPh₃)S(SO₂)₄-C₆H₄Me): C, 50.94; H, 3.61; S, 8.50. Found: C, 50.80; H, 3.51; S, 8.41.

IR (Nujol): 1953 (m), 1937 (m), 1867 (s, shoulder), 1856 (s), 1307 (w), **1262 (m)**, **1103 (m)**, 1089 (m), 1061 (w), 1014 (w), 870 (w), 843 (w), 821 (w), 802 (w), 753 (w), 744 (w), 722 (w), 694 (w) cm⁻¹.

Mass spectrum, FAB in glycerol: only peaks due to glycerol observed.

References

1. a) Grancher, P. *Hydrocarbon Process.* **1978**, 155.
b) Grancher, P. *Ibid* **1978**, 257.
2. a) Wojcicki, A. *Adv. Organomet. Chem.* **1974**, 12, 31.
b) Schenk, W.A. *Angew. Chem. Int. Ed.* **1987**, 26, 98.
3. Kubas, G.J. *Inorg. Chem.* **1979**, 18, 182.
4. Brown, C.K.; Georgiou, D.; Wilkinson, G. *J. Chem. Soc. (A)* **1971**, 3120.
5. Yagupsky, G.; Brown, C.K.; Wilkinson, G. *J. Chem. Soc. (A)* **1970**, 1392.
6. Shaver, A.; Plouffe, P.Y. unpublished results.
7. Burschka, V.C.; Baumann, F.E.; Schenk, W.A. *Z. Anorg. Allg. Chem.* **1983**, 502, 191.
8. Conway, P.; Grant, S.M.; Manning, A.R.; Stephens, F.S. *Inorg. Chem.* **1983**, 22, 3714.
9. Lorenz, I.P.; Hiller, W.; Conrad, M. *Z. Naturforsch.* **1985**, 40b, 1383.
10. Barbeau, C.; Dubey, R.J. *Can. J. Chem.* **1973**, 51, 3684.
11. Vaska, L.; Bath, S.S. *J. Am. Chem. Soc.* **1966**, 88, 1333.
12. La Placa, S.J.; Ibers, J.A. *Inorg. Chem.* **1966**, 5, 405.
13. Ritchey, J.M.; Moody, D.C.; Ryan, R.R. *Inorg. Chem.* **1983**, 22, 2276.
14. Dapporto, P.; Midollini, S.; Orlandini, A.; Sacconi, L. *Inorg. Chem.* **1976**, 15, 2768.
15. a) Moody, D.C.; Ryan, R.R. *Inorg. Chem.* **1979**, 18, 223.
b) Moody, D.C.; Ryan, R.R.; Larson, A.C. *Ibid* **1979**, 18, 227.
16. Mealli, C.; Orlandini, A.; Sacconi, L.; Stopppioni, P. *Inorg. Chem.* **1978**, 17,

3020.

17. Ryan, R.R.; Kubas, G.J. *Inorg. Chem.* **1978**, *17*, 637.
18. Snow, M.R.; McDonald, J.; Basolo, F.; Ibers, J.A. *J. Am. Chem. Soc.* **1972**, *94*, 2526.
19. Eller, P.G.; Kubas, G.J. *J. Am. Chem. Soc.* **1977**, *99*, 4346.
20. Kubas, G.J.; Wasserman, H.J.; Ryan, R.R. *Organometallics*, **1985**, *4*, 419.
21. Kubas, G.J.; Ryan, R.R.; Kubat-Martin, K.A. *J. Am. Chem. Soc.* **1989**, *111*, 7823.
22. Kubat-Martin, K.A.; Kubas, G.J.; Ryan, R.R. *Organometallics*, **1989**, *8*, 1910.
23. Kubas, G.J.; Jarvinen, G.D.; Ryan, R.R. *J. Am. Chem. Soc.* **1983**, *105*, 1883.
24. Hull, C.G.; Stiddard, M.H.B. *J. Chem. Soc (A)* **1968**, 710.
25. Kubas, G.J.; Ryan, R.R.; McCarty, V. *Inorg. Chem.* **1980**, *19*, 3003.
26. Moody, D.C.; Ryan, R.R. *J. Chem. Soc. Chem. Commun.* **1980**, 1230.
27. Ryan, R.R.; Kubas, G.J.; Moody, D.C.; Eller, P.G. *Struct. Bonding (Berlin)*, **1981**, *46*, 47.
28. Rausch, M.D.; Chang, Y.F.; Gordon, H.B. *Inorg. Chem.* **1969**, *8*, 1355.
29. Flood, T.C. *Top. Stereochem.* **1981**, *12*, 37.
30. Alexander, J.J. in "The Chemistry of the Metal-Carbon Bond"; Hartley, F.R., Patai, S., Eds.; Wiley: New York, 1985; Vol. 2, p 339.
31. Kroll, J.O.; Wojcicki, A. *J. Organomet. Chem.* **1974**, *66*, 95.
32. Collman, J.P.; Roper, W.R. *J. Am. Chem. Soc.* **1966**, *88*, 180.
33. Kubota, M.; Loeffler, B.M. *Inorg. Chem.* **1972**, *11*, 469.
34. Garves, K. *J. Org. Chem.* **1970**, *35*, 3273.
35. Chatt, J.; Mingos, D.M.P. *J. Chem. Soc. (A)* **1969**, 1770.
36. Cook, C.D.; Jauhal, G.S. *Can. J. Chem.* **1967**, *45*, 301.
37. Medina, R.M.; Masaguer, J.R. *J. Organomet. Chem.* **1986**, *299*, 341.

38. Jacobson, S.E.; Reich-Rohrwig, P.; Wojcicki, A. *J. Chem. Soc. Chem. Commun.* **1971**, 1526.
39. Jacobson, S.E.; Reich-Rohrwig, P.; Wojcicki, A. *Inorg. Chem.* **1973**, *12*, 717.
40. Wailes, P.C.; Weigold, H.; Bell, A.P. *J. Organomet. Chem.* **1971**, *33*, 181.
41. Dormond, A.; Dahchour, A.; Tirouflet, J. *J. Organomet. Chem.* **1981**, *216*, 49.
42. Deacon, G.B.; Felder, P.W. *Aust. J. Chem.* **1969**, *22*, 549.
43. Vitzthum, G.; Lindner, E. *Angew. Chem. Int. Ed.* **1971**, *10*, 315.
44. Graziani, M.; Bibler, J.P.; Montesano, R.M.; Wojcicki, A. *J. Organomet. Chem.* **1969**, *16*, 507.
45. Weinmann, D.J.; Abrahamson, H.B. *Inorg. Chem.* **1987**, *26*, 3034.
46. Jacobson, S.E. Ph.D Thesis, Ohio State University, 1972.
47. Jacobson, S.E.; Wojcicki, A. *J. Am. Chem. Soc.* **1973**, *95*, 6962.
48. Whitesides, G.M.; Boschetto, D.J. *J. Am. Chem. Soc.* **1971**, *93*, 1529.
49. Inagaki, S.; Fujimoto, H.; Fukui, K. *J. Am. Chem. Soc.* **1976**, *98*, 4693.
50. Flood, T.C.; Miles, D.L. *J. Am. Chem. Soc.* **1973**, *95*, 6460.
51. Alexander, J.J.; Wojcicki, A.; *Inorg. Chim. Acta* **1971**, *5*, 655.
52. Wojcicki, A.; Alexander, J.J.; Graziani, M.; Thomasson, J.E.; Hartman, F.A. *Proc. 1st Int. Symp. New Aspects Chem. Metal Carbonyl Derivatives* **1968**, 68.
53. Jacobson, S.E.; Wojcicki, A. *J. Am. Chem. Soc.* **1971**, *93*, 2535.
54. Hartman, F.A.; Wojcicki, A. *Inorg. Chem.* **1968**, *7*, 1504.
55. Bibler, J.P.; Wojcicki, A. *J. Am. Chem. Soc.* **1966**, *88*, 4862.
56. Bestian, H.; Clauss, K. *Angew. Chem. Int. Ed.* **1963**, *2*, 704.
57. Jensen, F.R.; Davis, D.D. *J. Am. Chem. Soc.* **1971**, *93*, 4047.
58. Graziani, M.; Wojcicki, A. *Inorg. Chim. Acta* **1970**, *4*, 347.
59. Bannister, W.D.; Booth, B.L.; Haszeldine, R.N.; Loader, P.L. *J. Chem. Soc (A)* **1971**, 930.

60. Kubas, G.J.; Ryan, R.R. *Polyhedron*, **1986**, *5*, 473.
61. Kubas, G.J.; Ryan, R.R. *J. Am. Chem. Soc.* **1985**, *107*, 6138.
62. Downs, R.L. Ph.D Thesis, Ohio State University, 1968.
63. Blum, J.; Scharf, G. *J. Org. Chem.* **1970**, *35*, 1895.
64. Deeming, A.J.; Shaw, B.L. *J. Chem. Soc. (A)* **1969**, 597.
65. Faraone, F.; Cusmano, F.; Piraino, P.; Peitropaolo, R. *J. Organomet. Chem.* **1972**, *44*, 391.
66. Sheldon, J.C.; Currie, G.J.; Lahnstein, J.; Hayes, R.N.; Bowie, J.H. *Nouv. J. Chim.* **1985**, *9*, 205.
67. Graziani, M.; Ros, R.; Carturan, G. *J. Organomet. Chem.* **1971**, *27*, C19.
68. Michelin, R.A.; Napoli, M.; Ros, R. *J. Organomet. Chem.* **1979**, *175*, 239.
69. Green, L.M.; Meek, D.W. *Organometallics*, **1989**, *8*, 659.
70. Ghilardi, C.A.; Midollini, S.; Sacconi, L. *Inorg. Chem.* **1977**, *16*, 2377.
71. a) Mealli, C.; Midollini, S.; Sacconi, L. *Inorg. Chem.* **1975**, *14*, 2513.
b) Sacconi, L.; Orlandini, A.; Midollini, S. *Ibid* **1974**, *13*, 2850.
c) Di Vaira, M.; Midollini, S.; Sacconi, L. *Ibid* **1977**, *16*, 1518.
72. Wenschuh, E.; Zimmering, R. *Z. Chem.* **1988**, 190.
73. Schenk, P.W.; Studel, R. in "Inorganic Sulfur Chemistry"; Nickless, G., Ed.; Elsevier: Amsterdam, 1968; p 373.
74. a) Manning, A.R. *J.Chem. Soc. (A)* **1967**, 1984.
b) Craig, P.J.; Green, M. *J.Chem. Soc. (A)* **1968**, 1978.
c) Faller, J.W.; Anderson, A.S. *J. Am. Chem. Soc.* **1970**, *92*, 5852.
d) Beach, D.L.; Datillo, M.; Barnett, K.W. *J. Organomet. Chem.* **1977**, *140*, 47.
75. Shaver, A.; Soo Lum, B.; Bird, P.; Arnold, K. *Inorg. Chem.* **1989**, *28*, 1900.
76. Shaver, A.; Soo Lum, B.; Bird, P.; Livingston, E.; Schweitzer, M. *Inorg. Chem.*

1990, in press.

77. Harpp, D.H.; Gleason, J.G.; Ash, D.K. *J. Org. Chem.* **1971**, *36*, 322.
78. a) Comparison of the NMR spectrum in CDCl_3 of an authentic sample of $\text{PhH}_2\text{CSCH}_2\text{Ph}$ from Aldrich.
- b) Comparison to the NMR spectrum in CDCl_3 of $\text{PhH}_2\text{CSSCH}_2\text{Ph}$: Pouchert, C.J. "The Aldrich Library of NMR Spectra", 2nd ed.; Aldrich: Milwaukee, 1983; Vol. 1, p 985.

Contributions to Original Knowledge:

1. The preparation of the tungsten thiolate complexes, cis/trans-CpW(CO)₂(PPh₃)SR, where R = CHMe₂, CH₂Ph, 4-C₆H₄Me, Ph, and phthalimido, reported here by the reaction of CpW(CO)₂(PPh₃)H with methyllithium and subsequently with RS-phth is new and is the most reliable route to these complexes.

2. A thiolate exchange reaction was discovered when treatment of CpW(CO)₂(PPh₃)SR with R'SH gave CpW(CO)₂(PPh₃)SR' and RSH for which R' = H was prepared. Thus, a series of CpW(CO)₂(PPh₃)SR' can be synthesized, particularly those with unusual R' groups where preparation of R'S-phth would be difficult.

3. The preparation and crystal structures of the dimers [CpW(CO)_xSCHMe₂]₂ (x = 1, 2) are the first tungsten analogues to be reported for these class of dimers and are unexpectedly different from those of analogous molybdenum complexes.

4. The insertion of CS₂ into the W-SR bond of CpW(CO)₂(PPh₃)SR, for R = CHMe₂, CH₂Ph, 4-C₆H₄Me, to give CpW(CO)₂S₂CSR is described with full supporting evidence, including a crystal structure of CpW(CO)₂S₂CSCH₂Ph. A mechanistic pathway involving the precoordination of CS₂ prior to insertion is proposed.

5. The reaction of CpW(CO)₂(PPh₃)SR, for R = CHMe₂, CH₂Ph, 4-C₆H₄Me, with SO₂ gave the previously unknown SO₂ adduct, CpW(CO)₂(PPh₃)S(SO₂)R. This complex is only the second system reported in which SO₂ is coordinated to a thiolato sulfur atom.

Appendix A

X-ray Structure Determinations

The x-ray crystal structures for $[\text{CpW}(\text{CO})_2\text{SCHMe}_2]_2$ (**50a**), $[\text{CpW}(\text{CO})\text{SCHMe}_2]_2$ (**51a**) and $\text{CpW}(\text{CO})_2\text{S}_2\text{CSCH}_2\text{Ph}$ (**62b**) were determined in the laboratory of Dr. Peter Bird, Department of Chemistry, Concordia University, Montréal, Québec. Tables A.1-A.9 lists the crystallographic data, final atomic coordinates and anisotropic thermal parameters for (**50a**), (**51a**) and (**62b**). Single crystals of **50a**, **51a** and **62b** suitable for x-ray crystallography were obtained by recrystallization from $\text{CH}_2\text{Cl}_2/\text{hexanes}$. The crystals of $[\text{CpW}(\text{CO})_2\text{SCHMe}_2]_2$ (**50a**) and $\text{CpW}(\text{CO})_2\text{S}_2\text{CSCH}_2\text{Ph}$ (**62b**) were mounted on a lithium borate fibre with 5-minute epoxy. The crystal of $[\text{CpW}(\text{CO})\text{SCHMe}_2]_2$ (**51a**) was placed in a lithium borate capillary and held in place with a trace of silicon grease, because the compound decomposes slowly in air. Preliminary Weissenberg and precession photographs were used to identify the possible space groups. Intensity data were collected after the unit cell data and orientation were obtained from 24 automatically aligned reflections. The data were corrected for Lorentz and polarization effects, and scaled using three reference reflections, whose intensities had been remeasured every 50 cycles. The structures were solved by conventional heavy atom methods. The tungsten coordinates were found from Patterson syntheses. Successive rounds of refinement, structure factor calculations, and Fourier syntheses revealed the positions of the sulfur atom and then the remaining carbon and oxygen atoms. After cycles of isotropic refinement using the block-diagonal method, a general Gaussian absorption correction was applied and refinement was continued for several more cycles. The structures were then refined anisotropically to

convergence: on the last cycle the positional parameter shifts were all less than $\frac{1}{20}$ of the corresponding standard deviation. Final difference syntheses showed only random noise.

Table A.1. Crystallographic Data for [CpW(CO)₂SCHMe₂]₂ (**50a**)

Crystal Parameters

Formula : C ₂₀ H ₂₄ O ₄ S ₂ W ₂	Formula weight = 760.13
Crystal system : orthorhombic	Space Group : Pnnm
a = 12.066(9) Å	α = 90°
b = 12.246(2) Å	β = 90°
c = 15.643(2) Å	γ = 90°
V = 2311.41 Å ³	Z = 8
d _{calcd} = 2.185 g cm ⁻³	μ(MoKα) = 103.56 cm ⁻¹
Colour = brown/black	Temp = 22°C
Crystal size = 0.08 x 0.11 x 0.60 mm	λ = 0.71069 Å
Transmission coeff. = 10-30%	

Data Collection and Structure Refinement

Diffractometer : Picker FACS-1	Radiation : Mo Ka
Monochromator : graphite	Scan method : θ / 2θ
Scan speed : 2°/min	Data limits : 3.5 < 2θ < 50°
Quadrant collected : +h+k+l	Friedel pairs collected: no
Reflections collected : 2148	Unique data F _o > 3σF _o : 1652
Least-squares method : block diagonal	Absorption correction : yes
Parameters refined : 134	Data/parameter ratio = 12.3
R = 0.075	R _w = 0.067
Goodness of fit = 1.21	

$$R = \Sigma [|F_o| - |F_c|] / \Sigma |F_o|$$

$$R_w = [\Sigma w (|F_o| - |F_c|)^2 / \Sigma F_o^2]^{1/2}, \text{ where } w = 1 / \sigma^2 (|F_o|)$$

$$\text{Goodness of fit} = [\Sigma w (|F_o| - |F_c|)^2 / (N_{\text{obs}} - N_{\text{parm}})]^{1/2}$$

Table A.2 Positional Parameters and Isotropic Thermal Parameters (\AA^2) for $[\text{CpW}(\text{CO})_2\text{SCHMe}_2]_2^{\text{a,b}}$ (**50a**).

	x	y	z	B_{iso}
W1	0.35517(13)	0.27022(9)	1/2	3.68(7)
W2	0.24006(12)	0.04221(9)	1/2	3.21(6)
S	0.3555 (5)	0.1375 (4)	0.3805 (5)	3.5 (3)
C11	0.2320 (22)	0.3041 (14)	0.3958 (20)	5.2 (14)
O11	0.1664 (15)	0.3272 (11)	0.3420 (16)	7.3 (12)
C22	0.1247 (20)	0.0843 (14)	0.4051 (18)	4.6 (13)
O22	0.0511 (15)	0.1060 (11)	0.3514 (15)	7.1 (12)
C1	0.2965 (19)	0.1549 (15)	0.2427 (19)	4.6 (13)
C2	0.3781 (22)	0.2141 (15)	0.1804 (20)	5.5 (15)
C3	0.2928 (21)	0.0665 (15)	0.1840 (20)	5.3 (15)
C15	0.439 (4)	0.3995 (24)	1/2	9.7 (32)
C16	0.4760 (20)	0.3577 (14)	0.3973 (23)	5.9 (16)
C17	0.0400 (19)	0.2135 (14)	0.0657 (24)	6.8 (17)
C25	0.318 (4)	0.4047 (20)	0	9.9 (32)
C26	0.2478 (18)	0.4139 (13)	0.1004 (20)	4.1 (12)
C27	0.1375 (21)	0.4307 (13)	0.064 (3)	7.3 (19)

^a Esd's given in parentheses refer to the last digit of the preceding number. ^b B_{iso} is the arithmetic mean of the principal axes of the thermal vibration ellipsoid.

Table A.3 Anisotropic Temperature Factors ($U_{ij} \times 100$)^{a,b} for $[\text{CpW}(\text{CO})_2\text{SCHMe}_2]_2$ (**50a**).

	U_{11}	U_{22}	U_{33}	U_{12}	U_{13}	U_{23}
W1	5.07(10)	4.21(8)	4.70(9)	-0.41(8)	0.00	0.00
W2	4.26(9)	4.14(8)	3.80(8)	0.00(8)	0.00	0.00
S	4.8 (4)	4.9 (4)	3.8 (4)	0.1 (3)	0.2 (3)	0.2 (3)
C11	10.3 (23)	5.4 (16)	3.9 (16)	-0.5 (16)	-1.0 (17)	1.3 (14)
O11	9.6 (16)	10.8 (15)	7.3 (14)	2.7 (13)	-2.4 (13)	2.5 (13)
C22	7.9 (19)	6.6 (16)	2.9 (14)	0.6 (15)	-0.6 (14)	0.7 (13)
O22	8.9 (15)	12.0 (16)	6.1 (13)	1.0 (13)	-2.2 (13)	2.2 (13)
C1	6.6 (18)	7.8 (17)	3.1 (14)	-1.2 (15)	-0.4 (15)	0.2 (15)
C2	9.5 (23)	7.1 (19)	4.1 (17)	-0.4 (17)	1.3 (17)	2.1 (15)
C3	8.0 (21)	7.9 (19)	4.3 (17)	-3.0 (16)	-0.1 (16)	-1.8 (15)
C15	7.9 (37)	4.9 (29)	23.9 (57)	-3.1 (27)	0.00	0.00
C16	5.6 (19)	6.1 (17)	10.7 (24)	-1.2 (15)	1.2 (18)	-0.8 (18)
C17	3.0 (16)	7.0 (18)	15.7 (32)	2.1 (14)	-0.4 (17)	-0.8 (19)
C25	13.9 (48)	0.8 (18)	22.8 (54)	-0.1 (24)	0.00	0.00
C26	4.4 (16)	5.0 (14)	6.0 (17)	-0.9 (13)	0.3 (15)	-1.1 (14)
C27	7.3 (19)	3.3 (13)	17.3 (39)	-0.5 (14)	3.6 (21)	-1.3 (17)

^a Figures in parentheses refer to last digit(s) of preceding number.

^b Thermal parameters are of the form:

$$-2\pi^2 [U_{11} \cdot h^2 \cdot (a^*)^2 + \dots + 2 \cdot U_{12} \cdot h \cdot k \cdot a^* \cdot b^* + \dots]$$

Table A.4. Crystallographic Data for [CpW(CO)SCHMe₂]₂ (51a)**Crystal Parameters**

Formula : C ₁₈ H ₂₄ O ₂ S ₂ W ₂	Formula weight = 704.11
Crystal system : monoclinic	Space Group : P2 ₁ /c
a = 9.441(4) Å	α = 90°
b = 11.727(3) Å	β = 65.56(3)°
c = 9.953(4) Å	γ = 90°
V = 1101.94 Å ³	Z = 4
d _{calcd} = 2.332 g cm ⁻³	μ(MoK _α) = 119.26 cm ⁻¹
Colour = brown/green	Temp = 22°C
Crystal size = 0.12 x 0.13 x 0.47 mm	λ = 0.71069 Å
Transmission coeff. = 23-45%	

Data Collection and Structure Refinement

Diffractometer : Picker FACS-1	Radiation : Mo Ka
Monochromator : graphite	Scan method : θ / 2θ
Scan speed : 2°/min	Data limits : 3.5 < 2θ < 45°
Quadrant collected : ±h+k+l	Friedel pairs collected: no
Reflections collected : 1736	Unique data F _o > 3σF _o : 1502
Least-squares method : block diagonal	Absorption correction : yes
Parameters refined : 110	Data/parameter ratio = 13.6
R = 0.054	R _w = 0.074
Goodness of fit = 1.31	

$$R = \Sigma [|F_o| - |F_c|] / \Sigma |F_o|$$

$$R_w = [\Sigma w (|F_o| - |F_c|)^2 / \Sigma F_o^2]^{1/2}, \text{ where } w = 1 / \sigma^2 (|F_o|)$$

$$\text{Goodness of fit} = [\Sigma w (|F_o| - |F_c|)^2 / (N_{\text{obs}} - N_{\text{parm}})]^{1/2}$$

Table A.5 Positional Parameters and Isotropic Thermal Parameters (\AA^2)
for $[\text{CpW}(\text{CO})\text{SCHMe}_2]_2$ ^{a,b} (**51a**)

	x	y	z	B_{iso}
W	0.03322(4)	0.02327(3)	0.86134(4)	2.03(3)
S	-0.1643 (3)	0.12639(21)	1.0644 (3)	2.33(11)
C1	0.1770 (11)	0.1355 (8)	0.8822 (10)	2.6 (5)
O1	0.2629 (9)	0.2021 (7)	0.8835 (10)	4.3 (5)
C2	0.0314 (17)	0.1181 (12)	0.6593 (13)	4.1 (7)
C3	-0.0960 (18)	0.0552 (19)	0.7104 (16)	5.7 (10)
C4	-0.0536 (22)	-0.0565 (13)	0.6943 (17)	5.0 (10)
C5	0.0856 (22)	-0.0739 (17)	0.6418 (19)	6.3 (12)
C6	0.1638 (24)	0.0371 (23)	0.6076 (18)	9.7 (17)
C7	-0.3660 (13)	0.0858 (9)	1.0905 (13)	3.0 (6)
C8	-0.4229 (15)	0.1866 (15)	1.0265 (17)	5.2 (9)
C9	-0.4679 (13)	0.0626 (15)	1.2503 (16)	4.4 (8)

^a Esd's given in parentheses refer to the last digit of the preceding number. ^b B_{iso} is the arithmetic mean of the principal axes of the thermal vibration ellipsoid.

Table A.6 Anisotropic Temperature Factors ($U_{ij} \times 100$)^{a,b} for [CpW(CO)SCHMe₂]₂ (**51a**).

	U_{11}	U_{22}	U_{33}	U_{12}	U_{13}	U_{23}
W	3.46(3)	3.10(3)	2.05(3)	-0.142(14)	-1.076(23)	0.128(12)
S	3.19(12)	3.38(11)	3.34(12)	-0.07(10)	-1.28(10)	-0.08(10)
C1	3.8(5)	3.3(5)	3.0(5)	1.7(4)	-0.3(4)	-0.1(4)
O1	5.5(5)	4.6(4)	7.9(7)	1.1(4)	-1.9(5)	0.7(5)
C2	9.4(9)	5.4(7)	4.4(7)	0.8(7)	-4.3(7)	-1.4(6)
C3	6.5(9)	13.9(14)	3.5(8)	0.2(10)	-2.9(7)	1.8(9)
C4	12.6(13)	6.0(7)	5.0(9)	-1.6(10)	-5.7(9)	-1.3(7)
C5	11.3(14)	11.1(14)	6.6(10)	5.6(12)	-6.2(10)	-5.5(10)
C6	6.8(11)	29.4(38)	1.8(8)	3.2(15)	-1.4(8)	-0.2(11)
C7	3.7(5)	3.7(5)	5.8(7)	-0.1(4)	-2.2(5)	-0.1(5)
C8	5.8(8)	7.9(10)	10.2(11)	0.4(7)	-5.1(8)	2.3(9)
C9	3.0(6)	9.0(10)	5.6(8)	0.5(7)	-0.9(6)	0.0(8)

^aFigures in parentheses refer to last digit(s) of preceding number.

^bThermal parameters are of the form:

$$-2\pi^2 [U_{11} \cdot h^2 \cdot (a^*)^2 \cdot + \dots + 2 \cdot U_{12} \cdot h \cdot k \cdot a^* \cdot b^* \cdot + \dots]$$

Table A.7 Crystallographic Data for CpW(CO)₂S₂CH₂Ph (62b).

Crystal Parameters

Formula : C ₁₅ H ₁₂ O ₂ S ₃ W	Formula weight = 504.29
Crystal system : monoclinic	Space Group : C2/c
a = 27.106(20) Å	α = 90°
b = 10.050(5) Å	β = 66.18(7)°
c = 13.108(13) Å	γ = 90°
V = 3570.8 Å ³	Z = 8
d _{calcd} = 2.051 g cm ⁻³	μ(MoKα) = 75.93 cm ⁻¹
Colour = red/brown	Temp = 22°C
Crystal size = 0.40 x 0.20 x 0.14 mm	λ = 0.71069 Å
Transmission coeff. = 22 - 34%	

Data Collection and Structure Refinement

Diffractometer : Picker FACS-1	Radiation : Mo Ka
Monochromator : graphite	Scan method : θ / 2θ
Scan speed : 2°/min	Data limits : 3.5 < 2θ < 50°
Quadrant collected : ±h+k+l	Friedel pairs collected: no
Reflections collected : 2875	Unique data F _o > 3σF _o : 2129
Least-squares method : block diagonal	Absorption correction : yes
Parameters refined : 190	Data/parameter ratio = 11.2
R = 0.032	R _w = 0.045
Goodness of fit = 0.91	

$$R = \Sigma [|F_o| - |F_c|] / \Sigma |F_o|$$

$$R_w = [\Sigma w (|F_o| - |F_c|)^2 / \Sigma F_o^2]^{1/2}, \text{ where } w = 1 / \sigma^2 (|F_o|)$$

$$\text{Goodness of fit} = [\Sigma w (|F_o| - |F_c|)^2 / (N_{\text{obs}} - N_{\text{parm}})]^{1/2}$$

Table A.8 Positional Parameters and Isotropic Thermal Parameters (\AA^2) for $\text{CpW}(\text{CO})_2\text{S}_2\text{CSCH}_2\text{Ph}^{\text{a,b}}$ (**62b**).

	x	y	z	B_{iso}
W	0.164357(8)	0.005526(20)	0.126042(17)	2.504(15)
S1	0.07378 (6)	-0.05959 (14)	0.63125 (12)	2.95 (8)
S2	0.12064 (6)	0.19324 (14)	0.58668 (12)	2.99 (8)
S3	0.00644 (6)	0.15652 (16)	0.59694 (14)	3.76 (9)
C1	0.1821 (3)	0.1651 (7)	0.0309 (5)	4.0 (4)
O1	0.19110 (22)	0.2623 (5)	-0.0212 (4)	6.2 (4)
C2	0.22399 (23)	-0.0605 (8)	-0.0088 (5)	3.9 (4)
O2	0.26158 (18)	-0.0972 (6)	-0.0861 (4)	6.0 (3)
C3	0.1476 (3)	-0.0931 (7)	0.3018 (5)	4.0 (4)
C4	0.2036 (3)	-0.0845 (7)	0.2354 (5)	4.4 (4)
C5	0.2171 (3)	0.0525 (8)	0.2187 (6)	4.7 (4)
C6	0.1685 (3)	0.1251 (6)	0.2730 (5)	4.2 (4)
C7	0.1265 (3)	0.0341 (7)	0.3248 (5)	4.2 (4)
C8	0.06538 (21)	0.1020 (5)	0.6055 (4)	2.6 (3)
C9	0.01792 (24)	0.3362 (6)	0.5766 (5)	3.8 (4)
C10	0.05234 (21)	0.3780 (5)	0.4598 (5)	2.8 (3)
C11	0.04118 (24)	0.3399 (6)	0.3672 (5)	3.4 (3)
C12	0.0715 (3)	0.3834 (6)	0.2618 (5)	3.9 (4)
C13	0.1138 (3)	0.4672 (7)	0.2405 (6)	4.0 (4)
C14	0.1262 (3)	0.5092 (6)	0.3300 (8)	4.3 (5)
C15	0.0958 (3)	0.4634 (7)	0.4381 (6)	3.7 (4)

^a Esd's given in parentheses refer to the last digit of the preceding number. ^b B_{iso} is the arithmetic mean of the principal axes of the thermal vibration ellipsoid.

Table A.9 Anisotropic Temperature Factors ($U_{ij} \times 100$)^{a,b}
for CpW(CO)₂S₂CSCH₂Ph (**62b**).

	U_{11}	U_{22}	U_{33}	U_{12}	U_{13}	U_{23}
W	3.694(16)	3.934(15)	3.440(16)	-0.603(9)	-1.923(13)	0.221(9)
S1	4.45 (8)	3.64 (7)	5.28 (9)	0.05 (6)	-2.66 (7)	0.36 (6)
S2	4.43 (8)	3.60 (7)	5.30 (9)	0.04 (4)	-2.45 (7)	0.59 (6)
S3	3.49 (8)	5.58 (9)	6.71 (11)	0.43 (7)	-1.85 (7)	1.93 (8)
C1	5.9 (4)	6.7 (4)	5.4 (4)	-2.5 (3)	-3.3 (3)	2.0 (3)
O1	11.7 (4)	7.3 (3)	9.5 (4)	-4.5 (3)	-6.1 (4)	4.5 (3)
C2	4.1 (3)	7.9 (5)	4.4 (4)	-0.2 (3)	-2.0 (3)	0.2 (3)
O2	5.9 (3)	12.1 (5)	6.0 (3)	0.6 (3)	-1.3 (3)	-0.7 (3)
C3	7.6 (4)	6.2 (4)	4.4 (3)	-1.1 (3)	-3.6 (3)	1.1 (3)
C4	7.4 (4)	7.2 (5)	4.8 (4)	1.6 (4)	-3.4 (4)	-0.0 (3)
C5	6.1 (4)	9.6 (5)	5.5 (4)	-2.0 (4)	-4.4 (4)	0.8 (4)
C6	8.2 (5)	5.8 (4)	5.6 (4)	-0.6 (3)	-4.4 (4)	-0.6 (3)
C7	6.6 (5)	7.6 (4)	4.0 (4)	1.1 (4)	-3.0 (3)	-1.4 (3)
C8	3.8 (3)	4.0 (3)	2.8 (3)	1.34(24)	-0.98(23)	0.13(22)
C9	5.1 (4)	5.0 (4)	6.4 (4)	1.4 (3)	-2.6 (3)	0.3 (3)
C10	4.3 (3)	2.9 (3)	5.7 (4)	0.79(22)	-2.6 (3)	0.50(24)
C11	5.3 (4)	3.7 (3)	6.5 (4)	-0.6 (3)	-3.3 (3)	0.2 (3)
C12	7.2 (4)	4.5 (4)	5.8 (4)	0.4 (3)	-3.6 (4)	-0.1 (3)
C13	6.1 (4)	4.9 (3)	6.4 (5)	0.2 (3)	-2.8 (4)	0.9 (3)
C14	5.1 (4)	5.7 (5)	8.6 (6)	-0.6 (3)	-3.6 (4)	1.0 (3)
C15	6.5 (4)	4.9 (3)	6.1 (4)	0.9 (3)	-4.3 (4)	-0.0 (3)

^aFigures in parentheses refer to the last digit(s) of the preceding number.

^bThe thermal parameters are of the form:
 $-2\pi^2 [U_{11} \cdot h^2 \cdot (a^*)^2 + \dots + 2 \cdot U_{12} \cdot h \cdot k \cdot a^* \cdot b^* + \dots]$

Appendix B

The data set for Figures 4.2 and 4.3 were plotted according to the first order equation below:

$$\begin{aligned} A &= \text{CpW(CO)}_2\text{(PPh}_3\text{)SR} & -\ln[A]_t + \ln[A]_0 &= kt & (4.7) \\ k &= \text{rate constant} \\ t &= \text{time} \end{aligned}$$

Figure 4.2 shows the plots of the reaction of $\text{CpW(CO)}_2\text{(PPh}_3\text{)SR}$ (**42**) with increasing volumes of CS_2 , monitored by ^1H NMR spectroscopy in CDCl_3 . Tables B.1 lists the data sets for curves A-C found in Figure 4.2. The initial concentrations and volumes (equivalents) of CS_2 added for each curve is listed with the appropriate table. The volume of CDCl_3 used is constant at 0.4 mL for all the experiments.

Figure 4.3 shows the plots of the reaction of $\text{CpW(CO)}_2\text{(PPh}_3\text{)SR}$ (**42**) with CS_2 and excess PPh_3 , monitored by ^1H NMR spectroscopy in CDCl_3 . Tables B.2 lists the data sets for curves A-C found in Figure 4.3. The initial concentrations and volumes (equivalents) of CS_2 and PPh_3 added for each curve is listed with the appropriate table.

Table B.1 Data set for Figure 4.2: First Order Plots of the Reaction of $\text{CpW}(\text{CO})_2(\text{PPh}_3)\text{SCHMe}_2$ (**42a**) with increasing volumes of CS_2 to give $\text{CpW}(\text{CO})_2\text{S}_2\text{CSCHMe}_2$ (**62a**).

$$[\text{A}] = [\text{CpW}(\text{CO})_2(\text{PPh}_3)\text{SCHMe}_2] = [\text{42a}]$$

Curve A

$[\text{A}]_0 = 3.046 \times 10^{-2} \text{ M}$
 volume of $\text{CS}_2 = 0.25 \text{ mL}$, 209 equivalents

Time ($\times 10^2 \text{ sec}$)	Fraction of integration area of Cp resonances due to 42a , a	$[\text{A}]_t = a \times [\text{A}]_0$ ($\times 10^{-2} \text{ M}$)	$-\ln [\text{A}]_t$
1.20	0.890	2.71	3.60
5.16	0.823	2.51	3.69
12.12	0.767	2.34	3.76
19.08	0.751	2.29	3.78
29.04	0.721	2.20	3.82
42.00	0.699	2.13	3.85
60.96	0.644	1.96	3.93
79.92	0.608	1.85	3.99
107.70	0.559	1.70	4.07

Curve B

$[\text{A}]_0 = 3.473 \times 10^{-2} \text{ M}$
 volume of $\text{CS}_2 = 0.15 \text{ mL}$, 130 equivalents

2.40	0.890	3.09	3.48
6.36	0.840	2.92	3.53
13.32	0.785	2.73	3.60
23.28	0.734	2.55	3.67
39.24	0.669	2.32	3.76
58.20	0.649	2.25	3.79
77.16	0.614	2.13	3.84
105.12	0.571	1.98	3.92
142.08	0.517	1.80	4.02

Curve C

$[\text{A}]_0 = 4.240 \times 10^{-2} \text{ M}$
 volume of $\text{CS}_2 = 0.05 \text{ mL}$, 43 equivalents

3.36	0.953	3.81	3.27
10.32	0.908	3.63	3.31
20.28	0.876	3.51	3.35
39.24	0.837	3.35	3.40
58.20	0.809	3.23	3.43
77.16	0.787	3.15	3.46
105.12	0.760	3.04	3.49
136.08	0.732	2.93	3.53
173.04	0.702	2.81	3.57

Table B.2 Data set for Figure 4.3: First Order Plots of the Reaction of $\text{CpW}(\text{CO})_2(\text{PPh}_3)\text{SCHMe}_2$ (**42a**) with CS_2 and excess PPh_3 to give $\text{CpW}(\text{CO})_2\text{S}_2\text{CSCHMe}_2$ (**62a**).

$$[\text{A}] = [\text{CpW}(\text{CO})_2(\text{PPh}_3)\text{SCHMe}_2] = [\text{42a}]$$

Curve A: control

volume of $\text{CS}_2 = 0.25$ mL, ~200 equivalents

$[\text{A}]_0 = 3.00 \times 10^{-2}$ M

wt of $\text{PPh}_3 = 0$ gms

Time ($\times 10^2$ sec)	Fraction of integration area of Cp resonances due to 42a , a	$[\text{A}]_t = a \times [\text{A}]_0$ ($\times 10^{-2}$ M)	$-\ln [\text{A}]_t$
6.72	0.849	2.55	3.67
10.92	0.817	2.45	3.71
17.88	0.777	2.33	3.76
27.84	0.740	2.22	3.81
43.80	0.705	2.11	3.86
62.76	0.641	1.92	3.95
81.72	0.597	1.79	4.02
100.68	0.559	1.68	4.09
128.64	0.501	1.50	4.20

Curve B

volume of $\text{CS}_2 = 0.25$ mL, ~200 equivalents

$[\text{A}]_0 = 2.94 \times 10^{-2}$ M

wt of $\text{PPh}_3 = 16.3 \times 10^{-3}$ gms, 3.25 equivalents

5.16	0.966	2.84	3.56
9.12	0.960	2.82	3.57
19.08	0.949	2.79	3.58
38.04	0.930	2.73	3.60
66.00	0.901	2.65	3.63
102.96	0.874	2.57	3.66
175.92	0.816	2.40	3.73

Curve C

volume of $\text{CS}_2 = 0.25$ mL, ~200 equivalents

$[\text{A}]_0 = 2.61 \times 10^{-2}$ M

wt of $\text{PPh}_3 = 31.2 \times 10^{-3}$ gms, 7.0 equivalents

3.96	0.922	2.41	3.727
7.92	0.910	2.38	3.739
17.88	0.904	2.36	3.746
36.84	0.897	2.34	3.754
64.80	0.886	2.31	3.766
101.76	0.881	2.30	3.772
174.72	0.862	2.25	3.795